University of Rhode Island

DigitalCommons@URI

2018

THE BIOLOGICAL FUNCTION OF HUMAN EPIDIDYMIS PROTEIN 4 IN EPITHELIAL OVARIAN CANCER

Nicole Elizabeth James
University of Rhode Island, neromano13@gmail.com

THE BIOLOGICAL FUNCTION OF HUMAN EPIDIDYMIS

PROTEIN 4 IN EPITHELIAL OVARIAN CANCER

BY

NICOLE ELIZABETH JAMES

A DISSERTATION SUBMITTED IN PARTIAL FULFILLMENT OF THE

REQUIREMENTS FOR THE DEGREE OF

DOCTOR OF PHILOSOPHY

IN

PHARMACEUTICAL SCIENCES

UNIVERSITY OF RHODE ISLAND

2018

DOCTOR OF PHILOSPHY DISSERTATION

OF

NICOLE ELIZABETH JAMES

APPROVED:

Dissertation Committee:

Major Professor   Clinton Chichester

                    Jennifer Ribeiro

                    Stephen Kogut

                    Joan Peckham

                    Nasser H. Zawia
            DEAN OF THE GRADUATE SCHOOL

UNIVERSITY OF RHODE ISLAND
2018

ABSTRACT

Epithelial ovarian cancer (EOC) is the most common gynecologic malignancy worldwide. EOC has a notably poor prognosis, owing to the fact that patients are frequently diagnosed at a late stage after the disease has significantly progressed. While many patients typically respond well to frontline platinum-based chemotherapy, the tumor becomes chemoresistant when a recurrence follows within five years. Therefore, there is an urgent need for the discovery of non-invasive early detection biomarkers and novel targeted therapies.

Human Epididymis Protein 4 (HE4) is a secretory protein that is encoded by the gene whey acidic protein (WAP)-four disulfide core domain protein 2. The WAP domain family is a conserved motif that is inherit of many antiproteases. HE4 was initially found to be a component of the innate immune defenses of multiple epithelia and to function in epithelial host defense, through the promotion of mucosal surfaces first line of defense. HE4 is highly overexpressed in EOC and has been identified as a novel clinical biomarker. Clinical and translational studies have established HE4 as a contributor to tumorigenesis and chemoresistance in EOC. However, the exact processes in which HE4 promotes pathogenesis is unclear. The driving hypothesis of this thesis is that HE4 represents a novel targeted therapy due to its established role EOC tumorigenesis and suggested function in innate immunity. This evidence underlies the goals of this dissertation which are to elucidate the precise mechanisms of HE4's contribution in EOC pathogenesis and establish HE4's role in tumor immune invasion. It is hoped that results from this investigation will ultimately aide in the

development of a novel targeted therapy against HE4 that can modulate tumor pathogenesis as well as the tumor immune response.

In manuscript I, subtractive hybridization revealed that HE4 significantly suppresses expression of osteopontin (OPN) in peripheral blood mononuclear cells (PBMCs) which ultimately compromised their cytotoxicity against ovarian cancer cells. Ovarian cancer cells exhibited enhanced proliferation in conditioned media from HE4-exposed PBMCs and this effect was attenuated by the addition of recombinant OPN and OPN - inducible cytokines (IL-12 and IFN-y). In addition, ovarian cancer cells and PBMCs with HE4 downregulation via short hairpin RNA (shRNA) were found to be increasingly more susceptible to cell death.

In manuscript II, subtractive hybridization identified dual specificity phosphatase 6 (DUSP6) as the most upregulated gene upon treatment with recombinant HE4 in PBMCs. Flow cytometry revealed that recombinant HE4 significantly upregulated DUSP6 levels specifically in CD8+ (cytotoxic T cell) and CD56+ (NK cell) populations. Exposure of these cells to HE4 led to an increase in ERK ½ phosphorylation, which was subsequently decreased upon DUSP6 inhibition. These results show that DUSP6 suppression of CD8+ and CD56+ lymphocyte toxicity is strongly enhanced by HE4. In co-culture of PBMCs and ovarian cancer cells, DUSP6 inhibition attenuated the enhanced proliferation noted upon stimulation with HE4. The effect of DUSP6 inhibition was obliterated in CD8+ and CD56+ devoid PBMCs.

In manuscript III, the role of DUSP6 and its relationship to HE4 in EOC was further elucidated. Increased DUSP6 levels were observed in ovarian cancer cells overexpressing HE4. siRNA-mediated downregulation of both HE4 and DUSP6

revealed a corresponding decrease of either factor. Treatment with an allosteric DUSP6 inhibitor in combination with chemotherapeutic agents produced synergistic effects on the reduction of cell viability. These effects correlated with alterations in expression of ERK pathway mediated genes. Finally, it was found that DUSP6 was significantly overexpressed in serous EOC patient tissue compared to normal adjacent tissue.

In manuscript IV it was determined from a small-scale proteomics study that 63 proteins were found to interact more strongly with HE4, in HE4 overexpressing clones compared to null vector control. The protein found to exhibit the highest interaction in the HE4 clones was Septin-2, a GTP binding protein. Immunohistochemical analysis of Septin-2 in EOC patient tissue revealed that levels were overexpressed in cancer compared to normal and benign controls. To identify Septin-2's role in EOC, stable knockdown cell lines were constructed using the ovarian cancer cell line SKOV3. Septin-2 knockdown cells demonstrated a significantly lowered proliferation rate compared wild-type (WT) and Plasmid C control cells. To better define the role of Septin-2 in EOC, proteomics was employed. Pathway analysis showed an enrichment in autophosphorylation, citric acid cycle, acetyl CoA/energy, and proteasomal/ubiquitin processes in Septin-2 knockout cells.

ACKNOWLEDGMENTS

PREFACE

This dissertation adopts manuscript format. It is comprised of an introduction, 4 manuscripts, and a conclusion. The format of each individual manuscript is in accordance with the journal that they were or will be submitted to.

TABLE OF CONTENTS

LIST OF TABLES

LIST OF FIGURES

CHAPTER 1

INTRODUCTION

1.1 Ovarian Cancer Incidence and Overall Survival

Worldwide ovarian cancer has an incidence of 240,000 cases per year and an annual

mortality rate of 152,000 [1]. This high mortality rate is largely due to that fact that in

many cases ovarian cancer is detected at an advanced disease state. In addition, while

the initial response rate to frontline chemotherapy is 60-80%, when the tumor recurs it

eventually becomes unresponsive to traditional platinum-based chemotherapeutics[2].

Unfortunately, only a minority of patients with advanced stage disease achieve long

term survival, as many patients will develop a recurrence within 12-18 months of

completion of their primary treatment regimen [3]. Currently, the five year survival

rate for ovarian cancer is only 35%[4] , and these dire statistics have not improved

significantly in the last 30 years[5].

1.2 Ovarian Cancer Subtypes

Ovarian Cancer is divided into two major subtypes that depend on the tissue of origin.

Non-epithelial ovarian cancer includes sex cord stromal, germ cell and non-specified

ovarian cancers. Non-epithelial ovarian cancers only represent 10% of all ovarian

cancer, [6]while the remaining 90% of cancer comprises epithelial ovarian cancer

(EOC). EOC encompasses serous, transitional cell, mucinous, endometrioid, and clear

cell ovarian cancer [7]. EOC is generally divided into two subtypes. Type 1 EOC are

considered more genetically stable, exhibit a slower tumor growth, and have disease contained within the ovary upon initial presentation. These cancers respond well to surgical intervention [7]. In contrast, type 2 EOC are characterized by an aggressive growth rate and are usually detected at an advanced stage of IIIC. High grade serous ovarian cancer (HGSOC) is the most common histological subtype of Type II EOC, representing nearly three quarters of all patients diagnosed with ovarian cancer [5]. Seventy percent of the time, HGSOC is diagnosed at an advanced stage, leading to a poor prognosis [5]. Therefore, efforts have been made to develop novel prognostic/diagnostic methods and treatments to combat chemoresistance and improve overall survival for HGSOC.

1.3 Current Ovarian Cancer Therapies

Many women who present with elevated tumor markers and abnormal imaging typically proceed with primary debulking surgery. Initial surgery has three goals: diagnosis, staging and cytoreduction. Diagnosis is important as needle biopsies are not indicated for larger ovarian masses to prevent inadvertent spreading of the disease [8]. If a patient presents with significant comorbidities, clinicians will favor neoadjuvant chemotherapy over surgery. This approach minimizes surgical side effects for patients, as the tumor will be reduced following chemotherapy [8].

For the past 20 years, standard of care for women diagnosed with EOC is a primary frontline regimen of carboplatin and paclitaxel [9]. Carboplatin binds to DNA forming a platinum adduct and causes cell death [10]. Paclitaxel's mechanism of action involves enhancing polymerization of tubulin, which stabilizes microtubules.

2

This stabilization results in the protection of the microtubule polymer from disassembly, and chromosomes are unable to achieve proper metaphase spindle organization. Ultimately, cells are halted in the G2/M phase of the cell cycle [11]. The overall response rate (ORR) for this combinational first line therapy is greater than 75%. However, the majority of patients experience a recurrence and progression of disease. Once a recurrence occurs post-frontline therapy, the chemotherapy chosen for the patient is based on the platinum-free interval (PFI), which represents the time between the completion of the last platinum-based treatment and the detection of relapse [12]. Patients that have a PFI of six months or less are considered to be platinum-resistant, while patients that have a PFI greater than six months mark are considered platinum-sensitive. This distinction determines the second-line chemotherapy regimen used for the patient. [13]For platinum-sensitive patients experiencing recurrence, doxil or gemcitabine is added to a platinum regimen [12]. Doxil, or pegalyated doxorubicin(PLD) is a polyethelyne-glycolate-coated liposomal nanoparticle version of doxorubicin that exhibits enhanced drug delivery [14]. Doxorubicin is an antitumor antibiotic that promotes cell death by intercalation into DNA, disrupting DNA repair mediated by topisomerase II, and generating free radicals [15], Gemcitabeine is a pyrimidine antimetabolite that is inhibits tumor cell progression through the G1/S phase, halting DNA synthesis [14]. While platinum-sensitive patients undoubtedly survive longer than patients who are initially platinum refractory, prognosis for these patients is still dismal. Platinum combinatorial therapies with doxil and gemcitabine exhibit a progression-free survival (PFS) of only 11.3 and 8.6, respectively[16].

3

For platinum-resistant ovarian cancer, a non-platinum monotherapy is used with a non-curative goal of toxicity management, as prognosis in this group is poor. Patients in this group are frequently enrolled in clinical trials as a last attempt to control disease [17]. Topotecan, which works through inhibition of topoisomerase I, is a typical example of a salvage chemotherapy that is used in platinum resistant ovarian cancer [18]. The response rate of patients to this treatment is only 12-18%, and PFS is around 3-4 months[19,20]. Other typical monotherapies for platinum-resistant second line EOC include doxil and bevacizumab [8]. Bevacizumab is a monoclonal antibody against vascular endothelial growth factor (VEGF), a major regulator of angiogenesis. Bevacizumab is approved in the recurrent setting, however it's overall efficacy continues to be studied clinically in different chemotherapy lines and in combination with various treatment regimens [21]. While many large phase III trials report an increase in PFS for patients, this response does not correlate with an increased overall survival [21]. Other approved therapies in the maintenance setting are PARP inhibitors. While these inhibitors are approved for all patients, within this setting it has shown the most substantial benefit for patients who harbor the BRCA mutation—about 20-25% of the patient population [22,23]. Current clinical trials for EOC have largely focused on the immune checkpoint inhibition of programmed death receptor (PD-1) and it's ligand PD-L1, however clinical trial results have suggested only a modest benefit [24]. Therefore, there is still a crucial treatment need for the non-BRCA patient population.

1.4 Detection Methods of EOC

Early detection for EOC is difficult as many symptoms reported by patients, such as bloating and pelvic pain, are common symptoms of benign disease [25]. In addition, the sensitivity and specificity of pelvic examinations for EOC screening purposes within an asymptomatic population are poor. Therefore, diagnosis relies heavily on tumor markers and radiologic imaging [25]. Currently, there has not been an official recommendation for routine screening of asymptomatic women who are not high risk for development of an ovarian malignancy [26].

Cancer antigen 125 (CA 125) is the most commonly used and validated tumor marker for the detection of EOC [27]. However, recently there has been sufficient research dedicated to an improvement of serum biomarkers for early detection of EOC. One biomarker that represents such improvement is Human Epididymis Protein 4 (HE4), which has been shown to have a higher specificity and comparable sensitivity to CA 125 [28]. From these results, the risk of ovarian malignancy algorithm (ROMA) was established, which takes into account a woman's menopausal status and incorporates preoperative serum levels of CA 125 and HE4. The ROMA score exhibits both a higher sensitivity and specificity than CA 125 alone [29]. As HE4 has been extensively studied clinically, its prognostic capabilities have also begun to be examined translationally.

1.5 Molecular Functions of HE4

HE4 is encoded by the Whey Acidic Protein (WAP) 4-disulphide core domain (WFDC2) gene. The WFDC2 transcript was thought to be exclusively expressed in

5

the epididymis and hence was originally proposed to be a specific marker for this tissue type [30]. WFDC2 is a member of the WAP domain, which is a conserved motif of 50 amino acids, including eight cysteine residues arranged as a 4-disulphide core [31]. While WAP proteins can display a variety of functions, the most comprehensively studied members of this family are the antiproteinases secretory leukocyte protease inhibitor (SLPI) and elafin. In addition to antiproteinase activities, both exhibit anti-inflammatory activities [32,33]. Due to the familial similarity of HE4, it has been proposed to function similarly to SLPI and elafin; however, this role has not been fully defined. In addition to HE4 overexpression in EOC tissue compared to normal and benign ovarian tissues [29,34], it is also readily expressed in the oral cavity, nasopharynx and respiratory tract [35]. It was suggested that HE4 functions in concert with other WAP domain family members to promote epithelial host defenses of the lung, nasal, and oral cavity; supporting the claim that HE4 plays a role in innate immune defenses [35]. HE4's known molecular functions in EOC pathogenesis, particularly its role in promotion of cell proliferation, chemoresistance, metastasis and steroid biosynthesis, are comprehensively discussed in Chapter 2.

1.6 Problem Statement

Challenges in both treatment and diagnosis of patients has led to strong efforts to elucidate new mechanisms of ovarian cancer pathology that can be used to develop novel targeted therapies, which are so desperately needed for this patient population. HE4 is a secretory protein that is overexpressed in EOC serum and tissue. Extensive studies have also shown that HE4 promotes EOC growth and chemoresistance.

6

However, the exact mechanisms of HE4 functions in EOC pathogenesis are not completely understood. In addition, while HE4 was initially found to play a role in innate immunity, its function in tumor immunity has yet to be defined. Therefore, further investigation of HE4's mechanistic promotion of tumorigenesis is an important step to determine potential efficacy of a targeted anti-HE4 therapy for the treatment of EOC.

The aim of this thesis research is to:

1. Determine genes most suppressed by HE4 in immune cell populations and determine their involvement in muting the cytotoxic ability of immune cells toward ovarian cancer cells.

2. Determine genes most induced by HE4 in immune cell populations and determine their involvement in muting the cytotoxic ability of immune cells toward ovarian cancer cells.

3. Establish the significance of HE4 regulated genes in EOC pathogenesis.

4. Define novel roles of proteins with an identified association with HE4 in EOC pathogenesis.

1.7 Hypothesis

The overall driving hypothesis of this investigation is that HE4 represents a novel therapeutic target due to its role in the promotion of EOC pathogenesis. While it is known that HE4 has a profound role in EOC diagnosis, its therapeutics capabilities have been largely undefined due to an incomplete identification of its signaling

7

network in EOC. Although the precise mechanism is unknown, it has been established that HE4 promotes tumorigenesis, chemoresistance, and metastasis in EOC. It has been previously proposed that HE4 plays a role in innate immunity; however, its immune functions in EOC have not been explored. The identification of novel genes and proteins at a global level in both EOC and immune cells could aide in the elucidation of a distinct HE4 signaling network. Thus, information obtained from these studies will ultimately contribute to a comprehensive understanding of the biological function of HE4 in EOC.

In manuscript I, subtractive hybridization revealed that *SPP1*, which encodes for the protein OPN, was the gene most suppressed by HE4 expression in peripheral blood mononuclear cells (PBMCs). Flow cytometry was employed to determine specific immune cell populations within the PBMCs best characterized this relationship. Downstream effectors of the suppressed gene responses were measured via ELISA after stimulation with recombinant HE4. Ovarian cancer cells and PBMCs were then co-cultured and treated with recombinant HE4 to determine how this treatment compared to the effect of untreated PBMCs on ovarian cancer cell viability, cell migration, and proliferation. Immunohistochemistry examined populations of OPN positive T cells in human serous EOC tissue. Finally, HE4 siRNA was employed to determine how its downregulation would affect apoptosis in ovarian cancer cells co-cultured with PBMCs. Results were visualized by propidium iodide (PI) and Annexin V staining.

8

In manuscript II, subtractive hybridization determined that the gene that was most induced by HE4 in peripheral blood mononuclear cells (PBMCs) was *MKP-3*, which encodes for the protein DUSP6. Flow cytometry allowed for identification of specific immune cell populations within the PBMCs that best characterize this relationship. Flow cytometry and western blot examined levels of ERK activation when cells were treated with recombinant HE4 and a small molecule DUSP6 inhibitor within specific immune cell populations. Cells were treated with recombinant HE4 alone and in combination with DUSP6 inhibition, and the following assessments were made: cell viability, cell proliferation using Ki67 staining, and apoptosis by flow cytometry detection of cells double positive for PI and annexin V. To verify effects the small molecule inhibitor on DUSP6, cell viability, proliferation, and apoptosis experiments were repeated in a co-culture devoid of the previously identified immune populations responsible for upregulation of DUSP6 via HE4.

In manuscript III, the relationship between HE4 and DUSP6 was further elucidated in ovarian cancer cells. To better define DUSP6's role in EOC, immunohistochemistry was performed to determine that levels of DUSP6 expression in patient tissue. Cell viability of ovarian cancer cells was assessed following treatment with a small molecule DUSP6 inhibitor alone and in combination with platinum-based chemotherapeutics to determine synergistic effects. qPCR was used to determine how DUSP6 inhibition alone and in combination with carboplatin or paclitaxel alters expression of extracellular signal-regulated protein kinases (p-ERK) response genes. HE4 and DUSP6 small interfering (si)RNA were employed to determine how decreases of either factor affects the other DUSP6 gene and protein levels were

9

assessed in HE4 overexpressing clones using qPCR and western blot.

In manuscript IV, Septin-2, a protein previously identified as strongly interacting with HE4, was characterized in ovarian cancer for the first time. Immunohistochemistry was employed to determine Septin-2 expression in EOC tissue. Two stable shRNA knockout Septin-2 ovarian cell lines were developed and proliferation of the control and knockout cell lines were compared by cell counting. Verification of the knockdown was confirmed by quantitative polymerase chain reaction (qPCR) and western blot. Finally, proteomics was utilized to determine global changes in protein levels in the stable Septin-2 knockout cells. Gene ontology pathway analysis was also performed to determine cellular proteins most affected by Septin-2 in EOC.

1.8 References

1. Evrick M, Liam F, Ferlay J, Mery L, Soerjomatara, I and BF. 2016 Cancer Today. Cancer Today. 2016;

2. Selvakumaran M, Pisarcik DA, Bao R, Yeung AT, Hamilton TC. Enhanced cisplatin cytotoxicity by disturbing the nucleotide excision repair pathway in ovarian cancer cell lines. Cancer Res. 2003;63:1311–6.

3. Morgan RD, Clamp AR, Evans DGR, Edmondson RJ, Jayson GC. PARP inhibitors in platinum-sensitive high-grade serous ovarian cancer. Cancer Chemother. Pharmacol. 2018. p. 647–58.

4. Ledermann JA. Front-line therapy of advanced ovarian cancer: new approaches. Ann Oncol [Internet]. 2017;28:viii46-viii50. Available from: http://academic.oup.com/annonc/article/28/suppl_8/viii46/4693818

5. Labidi-Galy SI, Papp E, Hallberg D, Niknafs N, Adleff V, Noe M, et al. High grade serous ovarian carcinomas originate in the fallopian tube. Nat Commun. 2017;8.

6. Ray-Coquard, I., Maurince, P., Lorusso D., Prat J. Oakin, A., Pautier, P., and, Colombo N. Non-epithelial ovarian cancer: ESMO Clinical Practice Guidelines for diagnosis, treatment and follow-up. Ann Oncol. 2018;0:1–18.

7. Zy,l B., Tang,D., and Bowden N. Biomarkers of platinum resistance in ovarian cancer: what can we use to improve treatment. Endocr Relat Cancer. 2018;25:R303–18.

8. Coleman RL, Monk BJ, Sood AK, Herzog TJ. Latest research and treatment of advanced-stage epithelial ovarian cancer. Nat. Rev. Clin. Oncol. 2013. p. 211–24.

9. Ledermann J. First-line treatment of ovarian cancer: questions and controversies to

address. Ther Adv Med Oncol. 2018;10:1–8.

10. De Sousa GF, Wlodarczyk SR, Monteiro G. Carboplatin: Molecular mechanisms of action associated with chemoresistance. Brazilian J. Pharm. Sci. 2014. p. 693–702.

11. Horwitz S. Taxol (paclitaxel): mechanisms of action. Ann Oncol. 1994;5:S3–6.

12. Luvero D, Milani A, Ledermann JA. Treatment options in recurrent ovarian cancer: Latest evidence and clinical potential. Ther. Adv. Med. Oncol. 2014. p. 229–39.

13. Foley OW, Rauh-Hain JA, del Carmen MG. Recurrent epithelial ovarian cancer: an update on treatment. Oncology (Williston Park) [Internet]. 2013;27:288–94, 298. Available from: http://www.ncbi.nlm.nih.gov/pubmed/23781692

14. Skarlos D V., Kalofonos HP, Fountzilas G, Dimopoulos MA, Pavlidis N, Razis E, et al. Gemcitabine plus pegylated liposomal doxorubicin in patients with advanced epithelial ovarian cancer resistant/refractory to platinum and/or taxanes. A HeCOG phase II study. Anticancer Res. 2005;25:3103–8.

15. Thorn CF, Oshiro C, Marsh S, Hernandez-Boussard T, McLeod H, Klein TE, et al. Doxorubicin pathways: Pharmacodynamics and adverse effects. Pharmacogenet Genomics. 2011;21:440–6.

16. Ferrandina G, Ludovisi M, Lorusso D, Pignata S, Breda E, Savarese A, et al. Phase III trial of gemcitabine compared with pegylated liposomal doxorubicin in progressive or recurrent ovarian cancer. J Clin Oncol. 2008;26:890–6.

17. Piancta, S, Cercere, SC, Dubois, A, Harter, P and HF. Treatment of recurrent ovarian cancer. Ann Oncol. 2017;28:viii51-viii56.

18. Herzog TJ. Update on the role of topotecan in the treatment of recurrent ovarian cancer. Oncologist [Internet]. 2002;7 Suppl 5:3–10. Available from: http://www.ncbi.nlm.nih.gov/pubmed/12324628

19. Gordon AN, Tonda M, Sun S, Rackoff W, Doxil Study I. Long-term survival advantage for women treated with pegylated liposomal doxorubicin compared with topotecan in a phase 3 randomized study of recurrent and refractory epithelial ovarian cancer. Gynecol Oncol [Internet]. 2004;95:1–8. Available from: http://www.ncbi.nlm.nih.gov/pubmed/15385103

20. ten Bokkel Huinink W, Gore M, Carmichael J, Gordon a, Malfetano J, Hudson I, et al. Topotecan versus paclitaxel for the treatment of recurrent epithelial ovarian cancer. J Clin Oncol [Internet]. 1997;15:2183–93. Available from: http://www.ncbi.nlm.nih.gov/pubmed/9196130

21. Rossi, Luigi1. Rossi L, Verrico M, Zaccarelli E, Papa A, Colonna M, Strudel M et al. B in ovarian cancer: A critical review of phase I studies. O [Internet]. 2017;8:12389–405. A from: http://www. ncbi. nlm. nih. gov/pubmed/27852039%0Ahttp://www. pubmedcentral. nih. gov/articlerender. fcgi?artid=PMC535535., Verrico M, Zaccarelli E, Papa A, Colonna M, Strudel M, et al. Bevacizumab in ovarian cancer: A critical review of phase III studies. Oncotarget [Internet]. 2017;8:12389–405. Available from: http://www.ncbi.nlm.nih.gov/pubmed/27852039%0Ahttp://www.pubmedcentral.nih.gov/articlerender.fcgi?artid=PMC5355353

22. Liu G, Yang D, Sun Y, Shmulevich I, Xue F, Sood AK, et al. Differing clinical impact of BRCA1 and BRCA2 mutations in serous ovarian cancer.

Pharmacogenomics [Internet]. 2012;13:1523–35. Available from:

http://www.ncbi.nlm.nih.gov/pubmed/23057551%5Cnhttp://www.pubmedcentral.

nih.gov/articlerender.fcgi?artid=PMC3603383

23. Earl H, Molica S, Rutkowski P. Spotlight on landmark oncology trials: The latest evidence and novel trial designs. BMC Med. 2017;15.

24. Gaillard SL, Secord AA, Monk B. The role of immune checkpoint inhibition in the treatment of ovarian cancer. Gynecol Oncol Res Pract [Internet]. 2016;3:11. Available from: http://gynoncrp.biomedcentral.com/articles/10.1186/s40661-016-0033-6

25. Eo, WK., Kim KH.,Park,EJ., Kim, HY., Kim, HB, Koh, SB.,and Nambung J. Diagnostic accuracy of inflammatory markers for distinguishing malignant and benign ovarian masses. J Cancer. 2018;9:1165–72.

26. Smith RA, Andrews KS, Brooks D, Fedewa SA, Manassaram-Baptiste D, Saslow D, Brawley OW WR. Cancer screening in the United States, 2017: A review of current American Cancer Society guidelines and current issues in cancer screening. CA Cancer J Clin. 2017;67:100–21.

27. Bozkurt M, Yumru AE, Aral I. Evaluation of the importance of the serum levels of CA-125, CA15-3, CA-19-9, carcinoembryonic antigen and alpha fetoprotein for distinguishing benign and malignant adnexal masses and contribution of different test combinations to diagnostic accuracy. Eur J Gynaecol Oncol. 2013;34:540–4.

28. Stiekema A, Korse CM, Aaronson NK, van Driel WJ, Kenter GG LC. New biomarkers in epithelial ovarian cancer: needed or redundant? Eur J Gynaecol Oncol. 2017;38:356–60.

29. Moore RG, McMeekin DS, Brown AK, DiSilvestro P, Miller MC, Allard WJ, et al. A novel multiple marker bioassay utilizing HE4 and CA125 for the prediction of ovarian cancer in patients with a pelvic mass. Gynecol Oncol. 2009;112:40–6.

30. Kirchhoff C, Habben I, Ivell R KN. A major human epididymis-specific cDNA encodes a protein with sequence homology to extracellular proteinase inhibitors. Biol Reprod. 1991;45:350–7.

31. Ranganathan S, SImpson KJ, Shaw DC NK. The whey acidic protein family: a new signature motif and three-dimensional structure by comparative modelling. J Mol Graph Model. 1999;17:106–13.

32. Jin FY, Nathan C, Radzioch D, Ding A. Secretory leukocyte protease inhibitor: A macrophage product induced by and antagonistic to bacterial lipopolysaccharide. Cell. 1997;88:417–26.

33. Vachon E, Bourbonnais Y, Bingle CD, Rowe SJ, Janelle MF, Tremblay GM. Anti-inflammatory effect of pre-elafin in lipopolysaccharide-induced acute lung inflammation. Biol Chem. 2002;383:1249–56.

34. Heliström I, Raycraft J, Hayden-Ledbetter M, Ledbetter JA, Schummer M, McIntosh M, et al. The HE4 (WFDC2) protein is a biomarker for ovarian carcinoma. Cancer Res. 2003;63:3695–700.

35. Bingle L, Cross SS, High AS, Wallace WA, Rassl D, Yuan G, et al. WFDC2 (HE4): a potential role in the innate immunity of the oral cavity and respiratory tract and the development of adenocarcinomas of the lung. Respir Res. 2006;7:61.

CHAPTER 2

REVIEW OF LITERATURE

Beyond the Biomarker: Understanding the Diverse Roles of Human Epididymis Protein 4 in the Pathogenesis of Epithelial Ovarian Cancer

Nicole E. James[1,2], Clinton Chichester[2], and Jennifer R. Ribeiro[1*]

_____

[1] Division of Gynecologic Oncology, Program in Women's Oncology, Department of Obstetrics and Gynecology, Women and Infants Hospital, Providence, RI, United States

[2] Department of Biomedical and Pharmaceutical Sciences, University of Rhode Island, Kingston, RI, United States

[*]Correspondence:
Jennifer R. Ribeiro
jrribeiro@wihri.org

2.1 Abstract

Human epididymis protein 4 (HE4) is an important clinical biomarker used for the detection of epithelial ovarian cancer (EOC). While much is known about the predictive power of HE4 clinically, less has been reported regarding its molecular role in the progression of EOC. A deeper understanding of HE4's mechanistic functions may help contribute to the development of novel targeted therapies. Thus far, it has been difficult to recommend HE4 as a therapeutic target owing to the fact that its role in the progression of EOC has not been extensively evaluated. This review summarizes what is collectively known about HE4 signaling and how it functions to promote tumorigenesis, chemoresistance, and metastasis in EOC, with the goal of providing valuable insights that will have the potential to aide in the development of new HE4-targeted therapies.

2.2 Introduction

Approximately 22,280 new cases of epithelial ovarian cancer (EOC) are diagnosed each year, resulting in 14,240 deaths annually in the United States (1). The 5-year survival rate for stage III ovarian cancer is only 39% (1). These dire statistics are due to the fact that the disease is frequently detected at an advanced stage, which drastically impacts overall patient survival. Initially, many patients respond well to first-line therapy that includes cytoreduction surgery and platinum-based treatment. However, many patients experience a chemoresistant recurrence within the first 2 years following treatment (2). Therefore, there is an urgent need for tools to aid in the early diagnosis of ovarian cancer when the disease is fundamentally curable, as well as

improved treatment options for later stage disease.

Human epididymis protein 4 (HE4) is a secretory protein that is member of the whey acidic protein domain family, bearing a conserved motif found in a number a protease inhibitors (3). HE4 was initially suggested to be involved in the innate immune defense of multiple epithelia and has also been found to function in epithelial host defense (4). In ovarian tissue, HE4 is highly overexpressed in EOC compared normal tissue (5, 6). Clinically, HE4 has been identified as a novel therapeutic biomarker for EOC and has also proven useful in detection of recurrent disease (7) Serum HE4 level predicts EOC with equal sensitivity to the established biomarker CA125 and is less likely to be elevated in benign disease (5). A multicenter study led by our institution established the FDA-approved Risk of Ovarian Malignancy Algorithm (ROMA), which combines menopausal status and serum levels of both HE4 and CA125 to detect and monitor EOC. ROMA demonstrates improved sensitivity and specificity over the Risk of Malignancy Index that uses CA125 alone as a serum based biomarker (6). Recently, it has been reported that HE4 can be detected in EOC patient urine, indicating the possibility that it may be utilized as a non-invasive biomarker (8).

While HE4 has been well studied in the clinical setting, less is known regarding its specific molecular and biological roles in EOC. Several studies have investigated its effect on gene expression in EOC cells, as well as on events associated with aggressive disease. This review will summarize HE4's effect on cell proliferation and tumor growth; invasion, migration, and adhesion; chemoresistance; and steroid biosynthesis (Figure 1). Each section will detail associated pathways and factors that are reported to be involved in these HE4-mediated effects, with the goal of revealing

common themes in signaling pathways affected by HE4 and exposing gaps in our knowledge of HE4 molecular and biological functions.

2.3 Review of Literature

Cell Proliferation and Tumor Growth

Within the past 5 years, a handful of *in vitro* and *in vivo* studies have begun to examine HE4's role in proliferation and tumor growth in EOC. A study by Wang et al. examined the role of HE4 in cell proliferation and found that cells treated with recombinant HE4 formed a statistically greater number of colonies compared with control treated cells (9). Furthermore, cells stimulated with recombinant HE4 exhibited greater cell viability compared with respective controls. In another study by Zhu et al. (10), proliferation rate in two different HE4-overexpressing cell lines was significantly higher than in the control cells. Likewise, Zhu et al. (11) and Lee et al. (12) determined that when HE4 was ablated via shRNA, cell proliferation decreased accordingly. Kong et al. report conflicting results, stating that HE4 inhibits proliferation in ovarian cells (13); however, no other studies support these claims, necessitating further explanation to understand the implications of their results. Several *in vitro* studies suggest that HE4 promotes proliferation through its involvement in cell cycle regulation (11). Silencing of HE4 causes G0/G1 cell cycle arrest and blocks the transition from the G1 to the S phase of the cell cycle. Conversely, when cells are stimulated with recombinant HE4, the number of cells in the G2/M phase is increased, while the number of cells in the G0/G1 phase is reduced (9). These results indicate that HE4 may mediate the cell cycle by promoting the G0/G1 transition. In addition, *in vivo* tumorigenicity studies using HE4 knockdown

19

clones revealed a marked inhibition in the growth of ovarian tumors in nude mice (14), while injection of HE4-overexpressing cells led to more aggressive tumor growth and an overall higher tumor volume compared with controls (10, 15). Taken together, results from numerous *in vitro* and *in vivo* studies provide compelling evidence that HE4 plays a role in cell proliferation and the promotion of tumorigenesis. A full list of factors associated with HE4-mediated cell proliferation and tumor growth can be found in Table 1A and is outlined in greater detail below.

Associated Pathways and Factors-Cell Proliferation and Tumor Growth

Human epididymis protein 4 has been connected to several oncogenic signaling cascades that play key roles in ovarian cancer progression, including the PI3K/AKT pathway, HIF1α, and ERK/mitogen-activated protein kinase (MAPK) signaling. Evidence of HE4's effect on activation of each of these pathways is discussed below.

Protein Kinase B Signaling

AKT has been established as a strong promoter of tumorigenesis, and the PI3K/AKT pathway is one of the most commonly hyperactivated pathways in many types of human cancers (16). Its diverse signaling regulates proliferation, growth, survival, motility, angiogenesis, and glucose metabolism (17). HE4-overexpressing OVCAR3 ovarian cancer cells were found to have a marked increase in activation of protein kinase B (AKT) compared with control cells, while HE4 knockdown in OVCAR3 cells reduced AKT activation (12). Moreover, it was found that HE4-overexpressing

20

SKOV3 clones had naturally higher gene levels of *AKT3* compared with the null-vector control (18), bolstering the claim that HE4 affects the PI3K/AKT pathway.

Hypoxia-Inducible Factor-1 Alpha (HIF1α)

Adaptation of malignant cells to hypoxic conditions is a key step in the promotion of tumorigenesis and angiogenesis (19–21), a process that is regulated by the transcription factor HIF1α. Co-immunoprecipitation revealed an interaction between HIF1α and HE4 in HE4-overexpressing SKOV3 xenografts. There was also strong colocalization of HE4 and HIF1α in SKOV3 ovarian xenograft tissue. In addition, when SKOV3 cells were treated with HIF1α siRNA or 2-methoxyestradiol (a HIF1α inhibitor), there was a marked decrease in HE4 protein levels (15). It is important to note that 2-methoxyestradiol is not a specific HIF1α inhibitor as it primarily causes the depolymerization of microtubules, which in turn prevents HIF1α expression (22). Thus, the specificity of the effect of HIF1α inhibition on HE4 levels may require further investigation. Although the exact mechanism and significance of the HE4-HIF1α interaction is not understood, this evidence suggests that HE4 could play a role in regulating HIF1α functions in angiogenesis.

MAPK Signaling

The MAPK pathway is composed of a family of conserved kinases that mediate essential cellular processes such as migration, growth, proliferation, differentiation, and apoptosis (23). The extracellular signal-regulated kinase (ERK) pathway is the best characterized of all MAPK pathways and is deregulated in approximately one-

21

third of all cancers. Several studies have shown activation of ERK in response to HE4 treatment or overexpression, or suppression of ERK phosphorylation in response to HE4 knockdown (11,12,18). Using microarray analysis, Zhu et al. determined that seven genes involved in the MAPK pathway (CHUK, GADD45A, IL1A, RPS6KA1, HSPA1B, DUSP1, and JUND) were differentially regulated in response to HE4 overexpression in ES-2 cells (10).

Activation of the MAPK/ERK pathway occurs through EGF binding of its membrane bound receptor, EGFR (24). Using co-immunoprecipitation studies in SKOV3 cells, Moore et al. found that HE4 interacts with EGFR, with a greater degree of immunoprecipitation seen in HE4-overexpressing clones than wild-type cells (15). Furthermore, ovarian xenograft tissue showed colocalization of HE4 and EGFR. In addition, when SKOV3 and OVCAR8 cells were stimulated with growth factors EGF, VEGF, and Insulin, nuclear localization of HE4 was significantly increased. Finally, when EGF was repressed by the small molecule inhibitor Iressa, relative intensity of HE4 staining was decreased in ovarian cancer cell lines. Collectively, these results provide several layers of evidence that HE4 is tied to growth factor signaling and the MAPK/ERK pathway, although further research is needed to elucidate the precise mechanisms involved.

HE4's Role in Proliferation in Other Cancers

Human epididymis protein 4 has been investigated as a putative biomarker in endometrial (25–39), lung (40–52), breast (53, 54), pancreatic (55, 56), and gastric cancer (57). While the majority of these studies examine the value of HE4 as a clinical

22

biomarker for detecting and monitoring disease, one study investigated the molecular mechanisms of HE4 in pancreatic and endometrial cancer. Lu et al. stimulated both pancreatic and endometrial cancer cell lines with recombinant HE4 and found that cell viability, cell growth, and DNA synthesis was increased prominently in both cancer types (56). They also report that HE4 upregulates gene expression of proliferating cell nuclear antigen (PCNA) and downregulates p21 in both cancer cell lines in a dose dependent manner. PCNA, which is expressed in the late G1/S phase of the cell cycle, is required for DNA repair, replication, cell proliferation, and cell cycle progression (58), while p21 is an important effector of tumor suppressor pathways by promoting cell cycle arrest. Specifically, p21 is able to facilitate p53-dependent G1 growth arrest (59). Therefore, results from this study highlight HE4's role in proliferation in both pancreatic and endometrial cancer and lend support to similar evidence from studies published on EOC.

Invasion, Migration, and Adhesion

Several studies have associated HE4 with metastatic properties, including invasion, migration, and adhesion of ovarian cancer cells. Lu et al. found that adhesion to a fibronectin substrate was twofold greater in SKOV3 cells overexpressing HE4 than in mock cells. In addition, a transwell migration assay demonstrated that the HE4-overexpressing clones had a 1.8-fold greater migration capacity than mock transfected cells. By contrast, immunofluorescence analysis showed that HE4 knockout clones displayed inhibited cell-spreading ability in a statistically significant fashion compared with respective controls. Furthermore, cell invasion, proliferation, and migration were

significantly decreased in these clones (14). In agreement with this study, Ribeiro et al. also found that OVCAR8 ovarian cells treated with recombinant HE4 exhibited 2.07-fold greater invasion capacity and 1.29-fold greater adhesion to a fibronectin matrix compared with untreated controls. Interestingly, there was no change in adhesion to collagen I, IV, laminin I, and fibrinogen matrices, suggesting that HE4 has a specific effect on fibronectin adhesion. Haptotaxis toward a fibronectin substrate also was increased in the ovarian cancer cells treated with recombinant HE4 by 1.72-fold (60).

Zhu et al. used wound healing and transwell invasion assays to show that HE4-overexpressing ES-2 and CaOV3 cells possess enhanced cell migration and invasion capacities. In addition, *in vivo* tail vein injection of HE4-overexpressing ES-2 cells into nude mice resulted in significantly more metastatic lung nodules than mock transfected cells (10). Using the same ovarian cancer cell lines, Zhuang et al. report the importance of HE4 interaction with annexin II (ANXA2) to promote invasion and migration *in vitro* and metastasis *in vivo* (61). Finally, Zou et al. found that knockdown of HE4 in SKOV3.ip1 cells inhibited migration and invasion (62). Taken together, these studies strongly suggest that HE4 plays a prominent role in the promotion of ovarian cancer metastasis. A full list of factors associated with HE4-mediated invasion, migration, and adhesion can be found in Table 1B and is outlined in greater detail below.

24

Associated Pathways and Factors—Invasion, Migration, and Adhesion

Human epididymis protein 4 appears to interact with numerous molecular pathways that promote metastasis in ovarian cancer. However, it is still not entirely known how HE4 affects signaling pathways and gene expression signatures to promote invasion, migration, and adhesion of ovarian cancer cells. Following is a summary of HE4-mediated molecular pathways that are involved in metastatic events in EOC.

Matrix Metalloproteinases (MMPs)

Human epididymis protein 4 has been associated with MMPs MMP-9 and MMP-2, and Cathepsin B. MMPs are a family of zinc-dependent endopeptidases that are vital for the remodeling of the extracellular matrix (63). They are expressed in almost all types of cancers and are responsible for stimulating angiogenesis, tumor growth, and metastasis (64, 65). Cathepsin B is a lysosomal cysteine protease that has been linked to cancer progression (66), specifically in signaling pathways related to angiogenesis (67). In addition, it can promote MMP activity by degrading MMP inhibitors (68). Interestingly, silencing of HE4 in ovarian cancer cells led to a decrease in protein levels of MMP-9, MMP-2, and Cathepsin B, suggesting these factors may be involved in HE4-mediated tumor promoting effects (11).

Interleukin-1 alpha (ILIA)

Interleukin-1 alpha is a pro-inflammatory cytokine that is involved in angiogenesis and metastasis. ILIA can directly stimulate the synthesis of VEGF (69) and fibroblastic pro matrix metallic proteinase I (70, 71). IL1A causes resistance to EGFR

inhibitors in both colon and head and neck cancers (72, 73). IL1A was also found to be differentially expressed in three separate microarray studies involving HE4. In two microarrays, IL1A levels positively associated with HE4 levels (10, 74), while in one study their levels were inversely associated (18). While there may be some ambiguity as to how HE4 and IL1A are mechanistically linked, the consistent connection between IL1A with HE4 merits further investigation.

Extracellular Matrix Proteins

Integrins are a family of transmembrane proteins that are vital to ECM adhesion and play important roles in wound healing as well as the pathogenesis of cancer (75–77). Integrin β5 (ITGβ5) gene expression was differentially regulated by HE4 in ES-2 and CaOV3 cells, which was confirmed by positive correlation of ITGB5 and HE4 staining in paraffin embedded ovarian tissue samples (10). This finding suggests that integrin signaling is one mechanism by which HE4 can promote increased adhesion of ovarian cancer cells. However, further research is needed to clarify the mechanisms involved.

In addition to ITGβ5, three other genes related to ECM modeling—syndecan 1 (SDC1), collagen type 1 alpha 1 (COL1A1), and dystroglycan 1 (DAG1)—were more highly expressed in cells overexpressing HE4 and were downregulated in cells with HE4 knockdown (10). SDC1, also known as CD138, is an essential cell surface adhesion molecule that is responsible for maintaining cell morphology and interactions within the surrounding microenvironment (78). Loss of SCD1 in cancer cells is associated with reduced ECM adhesion and enhanced invasion and cell

26

motility (79). Another ECM gene found to be affected by HE4 expression levels, COL1A1, is a crucial component of the ECM as it supports cartilage, bone, and tendon tissues in the body and also functions to maintain the rigidity and elasticity of tissues (80, 81). COL1A1 plays an important role in cancer, since tumor cells that express COL1A1 are able to dissociate from their surrounding stromal components, which is essential for tumor growth (81). The final ECM gene found to be affected by HE4 is DAG1, which is a cell adhesion molecule that plays a key role basement membrane assembly (82), muscle integrity (83), and the maintenance of basolateral cell adhesion in numerous epithelial tissues (84). Loss of DAG1 is associated with cancer progression (85). Taken together, these results show that HE4 is strongly interconnected with ECM related proteins, specifically those involved in the ITGβ5 signaling pathway.

Our lab has also determined that HE4 regulates several components of the extracellular matrix (60). We performed microarray analyses comparing untreated OVCAR8 wild-type cells to recombinant HE4 treated cells, and OVCAR8 cells overexpressing HE4 to null-vector control cells. Serpin peptidase inhibitor, member 2 (SERPINB2), gremlin 1 (GREM1), laminin-β3 (LAMB3), laminin-γ2 (LAMC2), fibroblast growth factor 5 (FGF5), and tenascin C (TNC) were all found to be significantly upregulated upon treatment with recombinant HE4. These genes encode for extracellular matrix proteins that promote cell migration and adhesion (60). Specifically, we found that HE4 upregulates LAMC2 and LAMB3 proteins in a time-dependent manner, and this increase of both factors in turn leads to an increase in laminin-332 levels (60). Laminin-332, a heterotrimer composed of LAMC2, LAMB3,

27

and LAMA2, is an important component of the basement membrane in epithelial

tissue. Abnormal increases in its levels have been shown to promote increased

invasion in cancers (86). Further evidence suggested involvement of the FAK pathway

in these events. In addition, activation of matriptase, a serine protease responsible for

cleaving laminin-332 in its β chain and regulating its effects on metastatic properties,

increased upon *in vitro* exposure to recombinant HE4 (60). This study provides

compelling evidence that HE4 is involved in basement membrane invasion and

adhesion.

Lewis y Antigen

Human epididymis protein 4 undergoes glycosylation before it is secreted by ovarian

cells (87), prompting Zhuang et al. to examine the relationship between HE4

glycosylation status and metastatic properties. Lewis y antigen is a glycosyl antigen

that is overexpressed in ovarian cancer and has been associated with chemoresistance

and poor prognosis (88–97). They determined that Lewis y antigen was present in

HE4 from benign and malignant ovarian tissues, *in vitro* cancer cells, and culture

medium. HE4 from ovarian cancer samples contained higher levels of Lewis y antigen

than HE4 from benign tissues, and their expression co-localized in ovarian cancer

tissue (98). Furthermore, when Lewis y antigen was over expressed, it promoted HE4-

mediated invasion and metastasis in ovarian cancer cell lines. Conversely, when Lewis

y antigen was blocked, the invasive and metastatic properties of HE4 were

significantly decreased (99). Interestingly, overexpression of Lewis y antigen

increased tyrosine phosphorylation of EGFR and HER/neu, which promoted cell

28

proliferation through the PI3K/Akt and Raf/MEK/MAPK pathways (100). Thus, it appears that Lewis y antigen and HE4 affect similar signaling pathways that promote tumor growth and malignancy (101). Taken together, these results show that Lewis y antigen could be a potential therapeutic target to decrease HE4 function in the treatment of EOC.

Heparin Cofactor II (HCII)

SERPIND1 encodes for the protein HCII, which is a serum glycoprotein and protease inhibitor (102). A study in non-small cell lung cancer (NSCLC) showed that HCII promotes cell motility, invasion, and filopodium dynamics through the PI3K/AKT pathway. High HCII expression in NSCLC tissue correlated to an increased recurrence rate and shorter overall survival (103). Furthermore, its levels were upregulated in metastatic brain cell lines compared with non-metastatic parental lines, suggesting an involvement of SERPIND1 in metastatic functions (104). Results from a microarray study by Zhu et al. showed that SERPIND1 was upregulated in HE4-overexpressing cells and conversely downregulated in HE4 knockdown cells. These results were validated *via* qPCR and immunohistochemistry. In addition, they found that 37/50 ovarian cancer samples showed positive expression of both SERPIND1 and HE4, and Spearman correlation analysis confirmed that HE4 and SERPIND1 were positively correlated. Finally, Kaplan–Meier analysis revealed that patients with high levels of HE4 and SERPIND1 had a worse prognosis (74). While these data strongly suggest a connection between HE4 and SERPIND1, which may be related to their roles in

29

promoting ovarian cancer metastasis, further study of the association between these two proteins is required.

Annexin II

Annexin II is a calcium-dependent, phospholipid-binding protein that is overexpressed in a variety of cancers and is involved in angiogenesis, proliferation, apoptosis, cell migration, invasion, and adhesion (105). High levels of Annexin II activate MAPK signaling, which in turn promotes tumor proliferation (106), invasion (107), and metastasis (108). Zhuang et al. employed mass spectrometry and co-immunoprecipitation to identify Annexin II (ANXA2) as a strong HE4 interacting partner (61). This binding promoted invasion and metastasis in ES-2 and CaOV3 ovarian cancer cells. *HE4* and *ANXA2* gene expression levels were found to be co-dependent, and examination of EOC tissue revealed that both HE4 and Annexin II levels were increased in malignant phenotypes compared with benign and normal ovarian tissues. Both proteins were also more highly expressed in tissues from patients with lymph node metastases than those without. Downregulation of HE4 was found to decrease expression of MKNK2 (MAP kinase-interacting serine/threonine-protein kinase 2) and LAMB2 (laminin, beta-2), two factors associated with MAPK and focal adhesion signaling pathways. When HE4 protein was supplemented, this effect was reversed. Collectively, these results show that HE4 interaction with Annexin II to activate MAPK and focal adhesion signaling is one mechanism by which HE4 may promote ovarian cancer metastasis.

30

Chemoresistance

Several studies show that HE4 is associated with chemoresistance clinically. The addition of HE4 serum levels in the ROMA score better predicts platinum resistance in patients than CA125 alone (15). Angioli et al. found that HE4 was able to predict chemotherapy response in EOC patients undergoing first-line therapy (109). In addition, higher levels of serum HE4 are reported in women who are resistant to first-line chemotherapy (110). Finally, higher HE4 levels inversely correlate with clinical outcome (111), optimal cytoreduction (112), progression free survival (113), and overall survival (15, 113). While the mechanism underlying HE4's contribution to chemoresistance has not been established fully, a few studies have begun to delineate HE4's role in this process. A full list of factors associated with HE4-mediated chemoresistance can be found in Table 1C and is outlined in detail below.

Associated Pathways and Factors—Chemoresistance

Antiapoptotic Gene Expression

A study performed in our lab by Ribeiro et al. determined that HE4 overexpression promotes collateral chemoresistance to both cisplatin and paclitaxel in SKOV3 and OVCAR8 cells (18). Conversely, CRISPR/Cas9 mediated knockdown of HE4 in SKOV3 cells overexpressing HE4 partially reversed their chemoresistance. Microarray analysis revealed suppression of cisplatin-induced early growth response 1 (*EGR1*) gene expression in HE4-overexpressing SKOV3 cells compared with null vector-transfected cells (18). *EGR1* is a transcription factor that regulates apoptosis, proliferation, and differentiation through regulating expression of genes such as p53,

31

BCL2, PTEN, IGF2, PDGF, VEGF, TGFB1, and TNF (114, 115). *EGR1* expression is influenced by MAPK signaling, including phospho-ERK and phospho-p38 (115). Ribeiro et al. found that p38 was strongly activated in SKOV3 null vector-transfected cells treated with cisplatin, while its activation was suppressed in HE4-overexpressing clones (18), suggesting that HE4-mediated chemoresistance may involve MAPK signaling.

Similarly, a study by Wang et al. showed that HE4 represses carboplatin-induced apoptosis *in vitro*. Recombinant HE4 caused an increase in expression of antiapoptotic protein B-cell lymphoma 2 (BCL-2) and a decrease in expression of pro-apoptotic Bax (Bcl-2 associated X protein) in SKOV3 cells treated with carboplatin (9). This decrease in the Bax/Bcl-2 ratio, in addition to the suppression of EGR1 when HE4 is overexpressed, may contribute to the overall decrease in pro-apoptotic factors that leads to chemoresistance in EOC.

Microtubule Stabilization

Microtubule-associated protein tau, which has been associated with paclitaxel resistance in ovarian (116), breast (117), and gastric cancer (118), was upregulated in SKOV3 cells overexpressing HE4 compared with null-vector cells (18). In addition, HE4-overexpressing cells were found to express significantly higher levels of SEPT3 (Septin 3) mRNA compared with null-vector controls (18). Septins are a family of conserved GTP binding proteins that are associated with microtubules and actin filaments and have an important role in cytoskeletal organization (119). Furthermore,

32

recombinant HE4 treatment of SKOV3 cells increased β-tubulin levels, indicating that HE4 might promote microtubule stability, leading to paclitaxel resistance.

Kinase Signaling Pathways

Human epididymis protein 4 knockdown has also been shown to lead to a reduction in cell growth and the resensitization of ovarian cancer cells to both cisplatin and paclitaxel (12). Lee et al. found that this effect was due to corresponding decreases of ERK and AKT in HE4 knockouts. Activation of these pathways suppresses apoptotic signaling in tumors, suggesting that HE4's regulation of these pathways may be an important mechanism of chemoresistance (120).

Steroid Biosynthesis

Evidence suggests an association between sex steroids and EOC pathogenesis, which is explained by processes that take place during the menstrual cycle. The ovarian surface epithelium (OSE) plays a critical role in ovulation and postovulatory wound repair. During the menstrual cycle, the OSE proliferates during the pro-estrus/estrus transition. After, ovulation the proliferation rate decreases (121). It is hypothesized that when the OSE is repeatedly exposed to high doses of luteinizing hormone and follicle stimulating hormone during the menstrual cycle, this can promote cell proliferation and increase the likelihood of tumor growth over time (121). Furthermore, epidemiological data have suggested that ovarian cancer progression, pathogenesis, and etiology are highly dependent on the activity of estrogens (121), and numerous experimental studies have demonstrated the promotive effect of estrogens

on ovarian tumors in mice and human EOC cell lines (122). However, activation of

diverse oncogenic pathways in EOC may lead to the eventual downregulation of ERα

levels and the overall decrease in ERα related signaling in ovarian cancers, rendering

them resistant to anti-estrogen therapies (122). Some evidence exists that HE4 may be

involved in this process by regulating steroid signaling in EOC. A full list of factors

associated with HE4-mediated steroid biosynthesis can be found in Table 1D and is

outlined in detail below.

Steroid Biosynthesis Gene Expression

Two separate microarray pathway analyses identified steroid biosynthesis as a

pathway affected by HE4 (10, 74). Important genes that were differentially expressed

between HE4-overexpressing and HE4 knockdown cell lines were Forkhead box

protein A2 (FOXA2) (74), squalene monooygenase (SQLE), 7-dehydrocholesterol

reductase (DHCR7), 24-dehydrocholesterol (DHCR24), and sterol-4-alpha-

carboxylate-3-dehydrogenase (NSDHL) (10). FOXA2, a transcription factor required

for normal metabolism (123), promotes cell proliferation, maintains cancer stem cells,

and is associated with a higher rate of relapse in triple-negative breast cancer (124).

Another gene differentially regulated by HE4, SQLE, is an enzyme required in the

later stages of cholesterol synthesis (125). Out of 22 cancer types, SQLE copy

number-driven gene expression was highest in breast, ovarian and colorectal cancer

(125). Also affected by HE4 levels was DHCR7, one of the terminal enzymes

involved in the production of cholesterol from 7-dehydrocholesterol (7DHC). DHCR7

was found to be an important regulatory determinate between cholesterol and vitamin

34

synthesis, as cholesterol is able to accelerate the proteasomal degradation of DHCR7, which can result in the accumulation of 7DHC and an increased production of vitamin D (126). DHCR24, which was also affected by modulation of HE4 levels, is another enzyme in the cholesterol biosynthesis pathway (127). It interacts physically and functionally with DHCR7 (128) and has a number of different cellular functions including anti-inflammatory and antiapoptotic functions, as well as regulation of oxidative stress and cell differentiation (129). DHCR24 has also been proposed to be involved in tumor progression, as its deregulation has been linked to prostate, ovarian, and urothelial carcinomas (127).

Finally, NSDHL is also involved in cholesterol biosynthesis and produces metabolites that are essential in the conversion of squalene to cholesterol (130). Interestingly, NSLD1 was found to have a role in the control of signaling, vesicular trafficking, and degradation of EGFR and its dimerization partners ERBB2 and ERBB3. A study by Sukhanova et al. showed that NSLD1 knockout *in vivo* leads to a reduction in EGFR activation (131). The results from these microarrays show that modulating HE4 levels results in differential expression of several genes involved in steroid biosynthesis—especially cholesterol—suggesting that HE4 may affect tumor metabolism and ultimately contribute to tumorigenesis.

Estrogen Signaling

In support of the above described pathway analyses, two other studies have shown that HE4 interacts with steroid signaling, specifically estrogen signaling. Lokich et al. showed that ERα expression was reduced in HE4-overexpressing SKOV3 cells,

35

resulting in increased resistance to tamoxifen and fulvestrant compared with wild-type cells (132). 5-Methylcytosine (5-MC), a methylated form of the DNA base cytosine, is one of the most prominently identified epigenetic modifications, and can cause suppression of ERα gene expression. Deregulation of DNA methylation can result in abnormal gene expression and tumorigenesis (133, 134). Lokich et al. found that 5-MC was readily detected in SKOV3 wild-type and null-vector cells but not in HE4-overexpressing clones, suggesting that HE4 overexpression may have an effect on epigenetic modifications (132). However, methylation of the ERα gene was not specifically examined in this study. It is unclear whether HE4 overexpression would promote increased methylation at the ERα promoter region (even with the presence of global demethylation), which would be expected given the reported suppression of ERα in this study.

Interestingly, Chen et al. reported that when HO8910 ovarian cancer cells were stimulated with estradiol (E2), there was an increase in the expression of HE4 at the mRNA and protein level. This effect was not observed in estrogen-insensitive SKOV3 cells; however, when HE4 was knocked down in SKOV3 cells, their proliferative response to estrogen was restored (135). Collectively with the results shown by Lokich et al, this study suggests that HE4 works to suppress estrogen signaling in ovarian cancer cells, which can contribute to resistance to anti-estrogen therapies. Conversely, it appears that estradiol promotes HE4 expression in estrogen-responsive cells, which could indicate a role for HE4 in the initial tumor promoting effects of estrogen. Further clarification of the effect of HE4 on estrogen signaling may be useful in improving implementation of anti-estrogen based therapies.

36

2.4 Conclusion

Ovarian cancer is an extremely deadly disease owing to the fact that patients are typically diagnosed at a late stage. Initially, patients respond well to frontline platinum therapy; however, a majority of tumors recur, and the initial chemosensitivity eventually gives way to a broad chemoresistance (136). Available detection methods have improved in recent years with the discovery of HE4 as a diagnostic and prognostic biomarker. However, there has yet to be a breakthrough targeted therapy to combat EOC. While PARP inhibitors are used in the maintenance setting for all patients, this therapy has most significantly benefited BRCA-positive patients, who comprise only 20–25% of patients (137, 138). In addition, inhibitors of immune checkpoints, such as programmed death ligand-1 have demonstrated modest benefit in clinical trials for ovarian cancer (139). Therefore, there is still a crucial need for novel targeted EOC treatments.

Although HE4 is well established as a clinical biomarker for ovarian cancer, it has been largely understudied for its therapeutic targeting potential. However, ongoing research continues to support that HE4 is profoundly involved in the pathogenesis of EOC. The individual studies mentioned in this review provide evidence that HE4 promotes EOC progression through pathways associated with cell proliferation, tumor growth, metastasis, chemoresistance, and steroid biosynthesis. These pathways, along with specific genes that have been shown to be associated with HE4, are summarized in Table 1. This compilation of HE4 regulated factors and pathways will serve as a starting point for scientists to further elucidate specific mechanisms by which HE4 ultimately drives tumorigenesis. In addition, a comprehensive summary of clinical, *in*

37

vivo, and *in vitro* studies related to each facet of EOC progression and HE4 can be seen in Figure 1. This diagram highlights the progress that has been made to establish HE4 as an attractive therapeutic target, while simultaneously denoting areas of research that are still lacking. The results discussed here suggest that inhibition of HE4 *via* a neutralizing antibody or small molecule inhibitor could provide viable treatment options for patients in dire need of more effective therapies.

38

2.5 References

1. Cancer facts fig. 2016. *Am Cancer Soc* (2016) 1:1–66.

2. Westin SN, Herzog TJ, Coleman RL. Investigational agents in development for the treatment of ovarian cancer. *Invest New Drugs* (2013) 31:213–29. doi:10.1007/s10637-012-9837-3

3. Bingle L, Singleton V, Bingle CD. The putative ovarian tumour marker gene HE4 (WFDC2), is expressed in normal tissues and undergoes complex alternative splicing to yield multiple protein isoforms. *Oncogene* (2002) 21:2768–73. doi:10.1038/sj.onc.1205363

4. Bingle L, Cross SS, High AS, Wallace WA, Rassl D, Yuan G, et al. WFDC2 (HE4): a potential role in the innate immunity of the oral cavity and respiratory tract and the development of adenocarcinomas of the lung. *Respir Res*(2006) 7:61. doi:10.1186/1465-9921-7-61

5. Heliström I, Raycraft J, Hayden-Ledbetter M, Ledbetter JA, Schummer M, McIntosh M, et al. The HE4 (WFDC2) protein is a biomarker for ovarian carcinoma. *Cancer Res* (2003) 63:3695–700.

6. Moore RG, McMeekin DS, Brown AK, DiSilvestro P, Miller MC, Allard WJ, et al. A novel multiple marker bioassay utilizing HE4 and CA125 for the prediction of ovarian cancer in patients with a pelvic mass. *Gynecol Oncol* (2009) 112:40–6. doi:10.1016/j.ygyno.2008.08.031

7. Piovano E, Attamante L, Macchi C, Cavallero C, Romagnolo C, Maggino T, et al. The role of HE4 in ovarian cancer follow-up: a review. *Int J Gynecol Cancer* (2014) 24:1359–65. doi:10.1097/IGC.0000000000000218

8. Sandow JJ, Rainczuk A, Infusini G, Makanji M, Bilandzic M, Wilson AL, et al. Discovery and validation of novel protein biomarkers in ovarian cancer patient urine. *Proteomics Clin Appl* (2018) 9:1700135. doi:10.1002/prca.201700135

9. Wang H, Zhu L, Gao J, Hu Z, Lin B. Promotive role of recombinant HE4 protein in proliferation and carboplatin resistance in ovarian cancer cells. *Oncol Rep* (2015) 33:403–12. doi:10.3892/or.2014.3549

10. Zhu L, Zhuang H, Wang H, Tan M, Schwab CL, Deng L, et al. Overexpression of HE4 (human epididymis protein 4) enhances proliferation, invasion and metastasis of ovarian cancer. *Oncotarget* (2015) 7:729–44. Available from: http://www.impactjournals.com/oncotarget/index.php?journal=oncotarget& page=article&op=view&path%5B%5D=6327&path%5B%5D=21088 (Accessed: December 14, 2017).

11. Zhu YF, Gao GL, Tang SB, Zhang ZD, Huang QS. Effect of WFDC 2 silencing on the proliferation, motility and invasion of human serous ovarian cancer cells in vitro. *Asian Pac J Trop Med* (2013) 6:265–72. doi:10.1016/S1995-7645(13)60055-3

12. Lee S, Choi S, Lee Y, Chung D, Hong S, Park N. Role of human epididymis protein 4 in chemoresistance and prognosis of epithelial ovarian cancer. *J Obstet Gynaecol Res* (2017) 43:220–7. doi:10.1111/jog.13181

13. Kong X, Chang X, Cheng H, Ma R, Ye X, Cui H. Human epididymis protein 4 inhibits proliferation of human ovarian cancer cells via the mitogen-activated protein kinase and phosphoinositide 3-kinase/AKT pathways. *Int J Gynecol Cancer* (2014) 24:427–36. doi:10.1097/IGC.0000000000000078

14. Lu R, Sun X, Xiao R, Zhou L, Gao X, Guo L. Human epididymis protein 4 (HE4) plays a key role in ovarian cancer cell adhesion and motility. *Biochem Biophys Res Commun* (2012) 419:274–80. doi:10.1016/j.bbrc.2012.02.008

15. Moore RG, Hill EK, Horan T, Yano N, Kim K, MacLaughlan S, et al. HE4 (WFDC2) gene overexpression promotes ovarian tumor growth. *Sci Rep* (2014) 4:3574. doi:10.1038/srep03574

16. Crowell JA, Steele VE, Fay JR. Targeting the AKT protein kinase for cancer chemoprevention. *Mol Cancer Ther*(2007) 6:2139–48. doi:10.1158/1535-7163.MCT-07-0120

17. Testa JR, Tsichlis PN. AKT signaling in normal and malignant cells. *Oncogene* (2005) 24:7391–3. doi:10.1038/sj.onc.1209100

18. Ribeiro JR, Schorl C, Yano N, Romano N, Kim KK, Singh RK, et al. HE4 promotes collateral resistance to cisplatin and paclitaxel in ovarian cancer cells. *J Ovarian Res* (2016) 9:28. doi:10.1186/s13048-016-0240-0

19. Maxwell PH, Wiesener MS, Chang GW, Clifford SC, Vaux EC, Cockman ME, et al. The tumour suppressor protein VHL targets hypoxia-inducible factors for oxygen-dependent proteolysis. *Nature* (1999) 399:271–5. doi:10.1038/20459

20. Dang CV, Semenza GL. Oncogenic alterations of metabolism. *Trends Biochem Sci* (1999) 24:68–72. doi:10.1016/S0968-0004(98)01344-9

21. Zhong H, De Marzo AM, Laughner E, Lim M, Hilton DA, Zagzag D, et al. Overexpression of hypoxia-inducible factor 1α in common human cancers and their metastases. *Cancer Res* (1999) 59:5830–5.

22. Diaz-Gonzalez JA, Russell J, Rouzaut A, Gil-Bazo I, Montuenga L. Targeting hypoxia and angiogenesis through HIF-1α inhibition. *Cancer Biol Ther* (2005) 4:1055–62. doi:10.4161/cbt.4.10.2195

23. Dhillon AS, Hagan S, Rath O, Kolch W. MAP kinase signalling pathways in cancer. *Oncogene* (2007) 26:3279–90. doi:10.1038/sj.onc.1210421

24. Schulze WX, Deng L, Mann M. Phosphotyrosine interactome of the ErbB-receptor kinase family. *Mol Syst Biol* (2005) 1:E1–13. doi:10.1038/msb4100012

25. Bian J, Sun X, Li B, Ming L. Clinical significance of serum HE4, CA125, CA724, and CA19-9 in patients with endometrial cancer. *Technol Cancer Res Treat* (2016) 16:435–9. doi:10.1177/1533034616666644

26. Gasiorowska E, Magnowska M, Izycka N, Warchol W, Nowak-Markwitz E. The role of HE4 in differentiating benign and malignant endometrial pathology. *Ginekol Pol* (2016) 87:260–4. doi:10.17772/gp/62356

27. Li J, Chen H, Mariani A, Chen D, Klatt E, Podratz K, et al. HE4 (WFDC2) promotes tumor growth in endometrial cancer cell lines. *Int J Mol Sci* (2013) 14:6026–43. doi:10.3390/ijms14036026

28. Angioli R, Capriglione S, Scaletta G, Aloisi A, Miranda A, De Cicco Nardone C, et al. The role of HE4 in endometrial cancer recurrence: how to choose the optimal follow-up program. *Tumour Biol* (2016) 37:4973–8. doi:10.1007/s13277-015-4324-z

29. Minář L, Klabenešová I, Jandáková E. [The importance of HE4 in differential diagnosis of endometrial cancer]. *Ces Gynekol* (2015) 80:256–63.

30. Brennan DJ, Hackethal A, Mann KP, Mutz-Dehbalaie I, Fiegl H, Marth C, et al. Serum HE4 detects recurrent endometrial cancer in patients undergoing routine clinical surveillance. *BMC Cancer* (2015) 15:33. doi:10.1186/s12885-015-1028-0

31. Capriglione S, Plotti F, Miranda A, Ricciardi R, Scaletta G, Alosi A, et al. Utility of tumor marker HE4 as prognostic factor in endometrial cancer: a single-center controlled study. *Tumour Biol* (2015) 36:4156. doi:10.1007/s13277-015-3049-3

32. Antonsen SL, Høgdall E, Christensen IJ, Lydolph M, Tabor A, Loft Jakobsen A, et al. HE4 and CA125 levels in the preoperative assessment of endometrial cancer patients: a prospective multicenter study (ENDOMET). *Acta Obstet Gynecol Scand* (2013) 92:1313–22. doi:10.1111/aogs.12235

33. Presl J, Novotny Z, Topolcan O, Vlasak P, Kucera R, Fushsova R, et al. CA125 and HE4 levels in a Czech female population diagnosed with endometrial cancer in preoperative management. *Anticancer Res* (2014) 34:327–31.

34. Brennan DJ, Hackethal A, Metcalf AM, Coward J, Ferguson K, Oehler MK, et al. Serum HE4 as a prognostic marker in endometrial cancer – a population based study. *Gynecol Oncol* (2014) 132:159–65. doi:10.1016/j.ygyno.2013.10.036

35. Saarelainen SK, Peltonen N, Lehtimäki T, Perheentupa A, Vuento MH, Mäenpää JU. Predictive value of serum human epididymis protein 4 and cancer antigen 125 concentrations in endometrial carcinoma. *Am J Obstet Gynecol* (2013) 209:142.e1–6. doi:10.1016/j.ajog.2013.04.014

36. Prueksaritanond N, Cheanpracha P, Yanaranop M. Association of serum HE4 with primary tumor diameter and depth of myometrial invasion in endometrial cancer patients at Rajavithi hospital. *Asian Pac J Cancer Prev* (2016) 17:1489–92. doi:10.7314/APJCP.2016.17.3.1489

37. Kalogera E, Scholler N, Powless C, Weaver A, Drapkin R, Li J, et al. Correlation of serum HE4 with tumor size and myometrial invasion in endometrial cancer. *Gynecol Oncol* (2012) 124:270–5. doi:10.1016/j.ygyno.2011.10.025

38. Zamani N, Modares Gilani M, Zamani F, Zamani MH. Utility of pelvic MRI and tumor markers HE4 and CA125 to predict depth of myometrial invasion and cervical involvement in endometrial cancer. *J Family Reprod Health* (2015) 9:177–83.

39. Bie Y, Zhang Z. Diagnostic value of serum HE4 in endometrial cancer: a meta-analysis. *World J Surg Oncol* (2014) 12:169. doi:10.1186/1477-7819-12-169

40. Yoon HI, Kwon OR, Kang KN, Shin YS, Shin HS, Yeon EH, et al. Diagnostic value combining tumor and inflammatory markers in lung cancer. *J Cancer Prev* (2016) 21:187–93. doi:10.15430/JCP.2016.21.4.302

41. Zeng Q, Liu M, Zhou N, Liu L, Song X. Serum human epididymis protein 4 (HE4) may be a better tumor marker in early lung cancer. *Clin Chim Acta* (2016) 455:102–6. doi:10.1016/j.cca.2016.02.002

42. Tang QF, Zhou ZW, Ji HB, Pan WH, Sun MZ. Value of serum marker HE4 in pulmonary carcinoma diagnosis. *Int J Clin Exp Med* (2015) 8:19014–21.

43. Li BT, Lou E, Hsu M, Yu HA, Naidoo J, Zauderer MG, et al. Serum biomarkers associated with clinical outcomes fail to predict brain metastases in patients with

stage IV non-small cell lung cancers. *PLoS One* (2016) 11(1):e0146063
doi:10.1371/journal.pcne.0146063

44. Lan WG, Hao YZ, Xu DH, Wang P, Zhou YL, Ma LB. Serum human epididymis
    protein 4 is associated with the treatment response of concurrent
    chemoradiotherapy and prognosis in patients with locally advanced non-small cell
    lung cancer. *Clin Transl Oncol* (2016) 18:375–80. doi:10.1007/s12094-015-1375-
    y

45. Lamy P-J, Plassot C, Pujol J-L. Serum HE4: an independent prognostic factor in
    non-small cell lung cancer. *PLoS One*(2015) 10:e0128836.
    doi:10.1371/journal.pone.0128836

46. Ma Q, Wang Q, Zhong DS. Advances of human epididymis protein 4 in lung
    cancer. *Chin J Lung Cancer* (2015) 18:184–6. doi:10.3779/j.issn.1009-
    3413.2015.03.10

47. Jiang Y, Wang C, Lv B, Ma G, Wang L. Expression level of serum human
    epididymis 4 and its prognostic significance in human non-small cell lung
    cancer. *Int J Clin Exp Med* (2014) 7:5568–72.

48. Lou E, Johnson M, Sima C, Gonzalez-Espinoza R, Fleisher M, Kris MG, et al.
    Serum biomarkers for assessing histology and outcomes in patients with metastatic
    lung cancer. *Cancer Biomark* (2014) 14:207–14. doi:10.3233/CBM-140399

49. Yamashita S, Tokuishi K, Moroga T, Yamamoto S, Ohbo K, Miyahara S, et al.
    Serum level of HE4 is closely associated with pulmonary adenocarcinoma
    progression. *Tumour Biol* (2012) 33:2365–70. doi:10.1007/s13277-012-0499-8

50. Yamashita SI, Tokuishi K, Hashimoto T, Moroga T, Kamei M, Ono K, et al.
    Prognostic significance of HE4 expression in pulmonary adenocarcinoma. *Tumour
    Biol* (2011) 32:265–71. doi:10.1007/s13277-010-0118-5

51. Iwahori K, Suzuki H, Kishi Y, Fujii Y, Uehara R, Okamoto N, et al. Serum HE4
    as a diagnostic and prognostic marker for lung cancer. *Tumour Biol* (2012)
    33:1141–9. doi:10.1007/s13277-012-0356-9

52. Tokuishi K, Yamashita SI, Ohbo K, Kawahara K. Splice variant HE4-V3 expression is associated with favorable prognosis in pulmonary adenocarcinoma. *Tumour Biol* (2012) 33:103–9. doi:10.1007/s13277-011-0252-8

53. Gündüz UR, Gunaldi M, Isiksacan N, Gündüz S, Okuturlar Y, Kocoglu H. A new marker for breast cancer diagnosis, human epididymis protein 4: a preliminary study. *Mol Clin Oncol* (2016) 5:355–60. doi:10.3892/mco.2016.919

54. Durur-Karakaya A, Durur-Subasi I, Karaman A, Akcay MN, Palabiyik SS, Erdemchi B, et al. The use of breast magnetic resonance imaging parameters to identify possible signaling pathways of a serum biomarker, HE4. *J Comput Assist Tomogr* (2016) 40:436–41. doi:10.1097/RCT.0000000000000390

55. Huang T, Jiang SW, Qin L, Senkowski C, Lyle C, Terry K, et al. Expression and diagnostic value of HE4 in pancreatic adenocarcinoma. *Int J Mol Sci* (2015) 16:2956–70. doi:10.3390/ijms16022956

56. Lu Q, Chen H, Senkowski C, Wang J, Wang X, Brower S, et al. Recombinant HE4 protein promotes proliferation of pancreatic and endometrial cancer cell lines. *Oncol Rep* (2015) 35. Available from: http://www.ncbi.nlm.nih.gov/pubmed/26497244 (Accessed: December 15, 2017).

57. Guo YD, Wang JH, Lu H, Li XN, Song WW, Zhang XD, et al. The human epididymis protein 4 acts as a prognostic factor and promotes progression of gastric cancer. *Tumour Biol* (2015) 36:2457–64. doi:10.1007/s13277-014-2858-0

58. Thomas H, Nasim MM, Sarraf CE, Alison MR, Love S, Lambert HE, et al. Proliferating cell nuclear antigen (PCNA) immunostaining – a prognostic factor in ovarian cancer? *Br J Cancer* (1995) 71:357–62. doi:10.1038/bjc.1995.72

59. Abbas T, Dutta A. P21 in cancer: intricate networks and multiple activities. *Nat Rev Cancer* (2009) 9:400–14. doi:10.1038/nrc2657

60. Ribeiro JR, Gaudet HM, Kahn M, Schorl C, James NE, Oliver MT, et al. Human epididymis protein 4 promotes events associated with metastatic ovarian cancer

via regulation of the extracelluar matrix. *Front Oncol* (2018) 7:332. doi:10.3389/fonc.2017.00332

61. Zhuang H, Tan M, Liu J, Hu Z, Liu D, Gao J, et al. Human epididymis protein 4 in association with Annexin II promotes invasion and metastasis of ovarian cancer cells. *Mol Cancer* (2014) 13:1–14. doi:10.1186/1476-4598-13-243

62. Zou S-L, Chang X-H, Ye X, Cheng H-Y, Cheng Y-X, Tang Z-J, et al. Effect of human epididymis protein 4 gene silencing on the malignant phenotype in ovarian cancer. *Chin Med J (Engl)* (2011) 124:3133–40.

63. Cathcart J, Pulkoski-Gross A, Cao J. Targeting matrix metalloproteinases in cancer: bringing new life to old ideas. *Genes Dis* (2015) 2:26–34. doi:10.1016/j.gendis.2014.12.002

64. Bhowmick NA, Neilson EG, Moses HL. Stromal fibroblasts in cancer initiation and progression. *Nature* (2004) 432:332–7. doi:10.1038/nature03096

65. Kalluri R, Zeisberg M. Fibroblasts in cancer. *Nat Rev Cancer* (2006) 6:392–401. doi:10.1038/nrc1877

66. Aggarwal N, Sloane BF. Cathepsin B: multiple roles in cancer. *Proteomics Clin Appl* (2014) 8:427–37. doi:10.1002/prca.201300105

67. Lakka SS, Gondi CS, Rao JS. Proteases and glioma angiogenesis. *Brain Pathol* (2005) 15:327–41. doi:10.1111/j.1750-3639.2005.tb00118.x

68. Gondi CS, Rao JS. Cathepsin B as a cancer target. *Expert Opin Ther Targets* (2013) 17:281–91. doi:10.1517/14728222.2013.740461

69. Dabkeviciene D, Sasnauskiene A, Leman E, Kvietkauskaite R, Daugelaviciene N, Stankevicius V, et al. MTHPC-mediated photodynamic treatment up-regulates the cytokines VEGF and IL-1alpha. *Photochem Photobiol* (2012) 88:432–9. doi:10.1111/j.1751-1097.2011.01062.x

70. Ma J, Sawai H, Matsuo Y, Ochi N, Yasuda A, Takahashi H, et al. Interleukin-1α enhances angiogenesis and is associated with liver metastatic potential in human

gastric cancer cell lines. *J Surg Res* (2008) 148:197–204.
doi:10.1016/j.jss.2007.08.014

71. Löffek S, Zigrino P, Angel P, Anwald B, Krieg T, Mauch C. High invasive
melanoma cells induce matrix metalloproteinase-1 synthesis in fibroblasts by
interleukin-1alpha and basic fibroblast growth factor-mediated mechanisms. *J
Invest Dermatol* (2005) 124:638–43. doi:10.1111/j.0022-202X.2005.23629.x

72. Gelfo V, Rodia MT, Pucci M, Dall'Ora M, Santi S, Solmi R, et al. A module of
inflammatory cytokines defines resistance of colorectal cancer to EGFR
inhibitors. *Oncotarget* (2016) 7. Available
from: http://www.ncbi.nlm.nih.gov/pubmed/27708224 (Accessed: January 3,
2018).

73. Stanam A, Gibson-Corley KN, Love-Homan L, Ihejirika N, Simons AL.
Interleukin-1 blockade overcomes erlotinib resistance in head and neck squamous
cell carcinoma. *Oncotarget* (2016) 7. Available
from: http://www.ncbi.nlm.nih.gov/pubmed/27738319 (Accessed: January 3,
2018).

74. Zhu L, Guo Q, Jin S, Feng H, Zhuang H, Liu C, et al. Analysis of the gene
expression profile in response to human epididymis protein 4 in epithelial ovarian
cancer cells. *Oncol Rep* (2016) 36:1592–604. doi:10.3892/or.2016.4926

75. Giancotti FG, Ruoslahti E. Integrin signaling. *Science* (1999) 285:1028–33.
doi:10.1126/science.285.5430.1028

76. Duperret EK, Dahal A, Ridky T. Focal-adhesion-independent integrin-αv
regulation of FAK and c-Myc is necessary for 3D skin formation and tumor
invasion. *J Cell Sci* (2015) 128:3997–4013. doi:10.1242/jcs.175539

77. Desgrosellier JS, Cheresh DA. Integrins in cancer: biological implications and
therapeutic opportunities. *Nat Rev Cancer* (2010) 10:9–22. doi:10.1038/nrc2748

78. Akl MR, Nagpal P, Ayoub N, Prabhu S, Gilksman M, Tai B, et al. Molecular and
clinical profiles of syndecan-1 in solid and hematological cancer for prognosis and

precision medicine. *Oncotarget* (2015) 6:28693–715.
doi:10.18632/oncotarget.4981

79. Teng YHF, Aquino RS, Park PW. Molecular functions of syndecan-1 in
disease. *Matrix Biol* (2012) 31:3–16. doi:10.1016/j.matbio.2011.10.001

80. Bou-Gharios G, Ponticos M, Rajkumar V, Abraham D. Extra-cellular matrix in
vascular networks. *Cell Prolif* (2004) 37:207–20. doi:10.1111/j.1365-
2184.2004.00306.x

81. Karsenty G, Park RW. Regulation of type I collagen genes expression. *Int Rev
Immunol* (1995) 12:177–85. doi:10.3109/08830189509056711

82. Matthew G, Mitchell A, Down JM, Jacobs LA, Hamdy FC, Eaton C, et al. Nuclear
targeting of dystroglycan promotes the expression of androgen regulated
transcription factors in prostate cancer. *Sci Rep* (2013) 3:2792.
doi:10.1038/srep02792

83. Ervasti JM, Ohlendieck K, Kahl SD, Gaver MG, Campbell KP. Deficiency of
glycoprotein component of the dystrophin complex in dystrophic muscle
deficiency of a glycoprotein component of the dystrophin complex in dystrophic
muscle. *Nature* (1990) 345:315–9. doi:10.1038/345315a0

84. Durbeej M, Larsson E, Ibraghimov-Beskrovnaya O, Roberds SL, Campbell KP,
Ekblom P. Non-muscle alpha-dystroglycan is involved in epithelial development. *J
Cell Biol* (1995) 130:79–91. doi:10.1083/jcb.130.1.79

85. Cross SS, Lippitt J, Mitchell A, Hollingsbury F, Balasubramanian SP, Reed
MWR, et al. Expression of beta-dystroglycan is reduced or absent in many human
carcinomas. *Histopathology* (2008) 53:561–6. doi:10.1111/j.1365-
2559.2008.03157.x

86. Tsuruta D, Kobayashi H, Imanishi H, Sugawara K, Ishii M, Jones JCR. Laminin-
332-integrin interaction: a target for cancer therapy? *Curr Med Chem* (2008)
15:1968–75. doi:10.2174/092986708785132834

48

87. Drapkin R, Von Horsten HH, Lin Y, Mok SC, Crum CP, Welch WR, et al. Human epididymis protein 4 (HE4) is a secreted glycoprotein that is overexpressed by serous and endometrioid ovarian carcinomas. *Cancer Res* (2005) 65:2162–9. doi:10.1158/0008-5472.CAN-04-3924

88. Yin BW, Finstad CL, Kitamura K, Federici MG, Welshinger M, Kudryashov V, et al. Serological and immunochemical analysis of Lewis y (Ley) blood group antigen expression in epithelial ovarian cancer. *Int J Cancer* (1996) 65:406–12. doi:10.1002/(SICI)1097-0215(19960208)65:4<406::AID-IJC2>3.0.CO;2-0

89. Li Q, Liu S, Lin B, Yan L, Wang Y. Expression and correlation of Lewis y antigen and integrins a5 and b1 in ovarian serous and mucinous carcinoma. *Int J Gynecol Cancer* (2010) 20:1482–9.

90. Sabbatini PJ, Kudryashiv V, Ragupath G, Danishefsky SJ, Livingston PO, Bornmann W, et al. Immunization of ovarian cancer patients with a synthetic Lewis(y)-protein conjugate vaccine: a phase 1 trial. *Int J Cancer* (2000) 87:79–85. doi:10.1002/1097-0215(20000701)87:1<79::AID-IJC12>3.0.CO;2-L

91. Smaletz O, Diz MD, do Carmo CC, Sabbaga J, Cunha-Junior GF, Azevedo S, et al. A phase II trial with anti-Lewis-Y monoclonal antibody (hu3S193) for the treatment of platinum resistant/refractory ovarian, fallopian tube and primary peritoneal carcinoma. *Gynecol Oncol* (2015) 138:272–7. doi:10.1016/j.ygyno.2015.05.023

92. Gao J, Hu Z, Liu J, Liu D, Wang Y, Cai M, et al. Expression of CD147 and Lewis y antigen in ovarian cancer and their relationship to drug resistance. *Med Oncol* (2014) 31:920. doi:10.1007/s12032-014-0920-9

93. Gao J, Hu Z, Liu D, Liu J, Liu C, Hou R, et al. Expression of Lewis y antigen and integrin αv, β3 in ovarian cancer and their relationship with chemotherapeutic drug resistance. *J Exp Clin Cancer Res* (2013) 32: 36. Available from: http://www.pubmedcentral.nih.gov/articlerender.fcgi?artid=3699420&tool=pmcentrez&rendertype=abstract(Accessed: January 6, 2018).

49

94. Zhang D, Gao J, Zhu L, Hu Z, Hou R, Liu S, et al. Chemoresistance is associated with MUC1 and lewis y antigen expression in ovarian epithelial cancers. *Int J Mol Sci* (2013) 14:11024–33. doi:10.3390/ijms140611024

95. Hu Z, Gao J, Zhang D, Liu Q, Yan L, Gao L, et al. High expression of Lewis y antigen and CD44 is correlated with resistance to chemotherapy in epithelial ovarian cancers. *PLoS One* (2013) 8:e57250. doi:10.1371/journal.pone.0057250

96. Hu Z, Gao S, Gao J, Hou R, Liu C, Liu J, et al. Elevated levels of Lewis Y and integrin α5β1 correlate with chemotherapeutic drug resistance in epithelial ovarian carcinoma. *Int J Mol Sci* (2012) 13:15588–600. doi:10.3390/ijms131215588

97. Zhang F, Liu J, Lin B, Liu Q, Zhao Y, Zhu L, et al. Increase in docetaxel-resistance of ovarian carcinoma-derived RMG-1 cells with enhanced expression of Lewis Y antigen. *Int J Mol Sci* (2011) 12:7323–34. doi:10.3390/ijms12117323

98. Zhuang H, Gao J, Hu Z, Liu J, Liu D, Lin B. Co-expression of Lewis y antigen with human epididymis protein 4 in ovarian epithelial carcinoma. *PLoS One* (2013) 8:e68994. doi:10.1371/journal.pone.0068994

99. Zhuang H, Hu Z, Tan M, Zhu L, Liu J, Liu D, et al. Overexpression of Lewis y antigen promotes human epididymis protein 4-mediated invasion and metastasis of ovarian cancer cells. *Biochimie* (2014) 105:91–8. doi:10.1016/j.biochi.2014.06.022

100. Liu J-J, Lin B, Hao Y-Y, Li F-F, Liu D-W, Qi Y, et al. Lewis(y) antigen stimulates the growth of ovarian cancer cells via regulation of the epidermal growth factor receptor pathway. *Oncol Rep* (2010) 23:833–41.

101. Burotto M, Chiou VL, Lee JM, Kohn EC. The MAPK pathway across different malignancies: a new perspective. *Cancer* (2014) 120:3446–56. doi:10.1002/cncr.28864

102. Tollefsen DM. Heparin cofactor II modulates the response to vascular injury. *Arterioscler Thromb Vasc Biol* (2007) 27:454–60. doi:10.1161/01.ATV.0000256471.22437.88

103. Liao W-Y, Ho C-C, Hou H-H, Hsu T-H, Tsai M-F, Chen K-Y, et al. Heparin co-factor II enhances cell motility and promotes metastasis in non-small cell lung cancer. *J Pathol* (2015) 235:50–64. doi:10.1002/path.4421

104. Valiente M, Obenauf AC, Jin X, Chen Q, Zhang XHF, Lee DJ, et al. Serpins promote cancer cell survival and vascular co-option in brain metastasis. *Cell* (2014) 156:1002–16. doi:10.1016/j.cell.2014.01.040

105. Lokman NA, Ween MP, Oehler MK, Ricciardelli C. The role of annexin A2 in tumorigenesis and cancer progression. *Cancer Microenviron* (2011) 4:199–208. doi:10.1007/s12307-011-0064-9

106. Ortiz-Zapater E, Peiró S, Roda O, Corominas JM, Aguilar S, Ampurdané C, et al. Tissue plasminogen activator induces pancreatic cancer cell proliferation by a non-catalytic mechanism that requires extracellular signal-regulated kinase 1/2 activation through epidermal growth factor receptor and annexin A2. *Am J Pathol* (2007) 170:1573–84. doi:10.2353/ajpath.2007.060850

107. Delys L, Detours V, Franc B, Thomas G, Bogdanova T, Tronko M, et al. Gene expression and the biological phenotype of papillary thyroid carcinomas. *Oncogene* (2007) 26:7894–903. doi:10.1038/sj.onc.1210588

108. Zhang Y, Zhou Z-H, Bugge TH, Wahl LM. Urokinase-type plasminogen activator stimulation of monocyte matrix metalloproteinase-1 production is mediated by plasmin-dependent signaling through annexin A2 and inhibited by inactive plasmin. *J Immunol* (2007) 179:3297–304. doi:10.4049/jimmunol.179.5.3297

109. Angioli R, Capriglione S, Aloisi A, Guzzo F, Luvero D, Miranda A, et al. Can HE4 predict platinum response during first-line chemotherapy in ovarian cancer? *Tumour Biol* (2014) 35:7009–15. doi:10.1007/s13277-014-1836-x

110. Chudecka-Głaz AM, Cymbaluk-Płoska AA, Menkiszak JL, Sompolska-Rzechuła AM, Tołoczko-Grabarek AI, Rzepka-Górska IA. Serum HE4, CA125, YKL-40, bcl-2, cathepsin-L and prediction optimal debulking surgery, response to
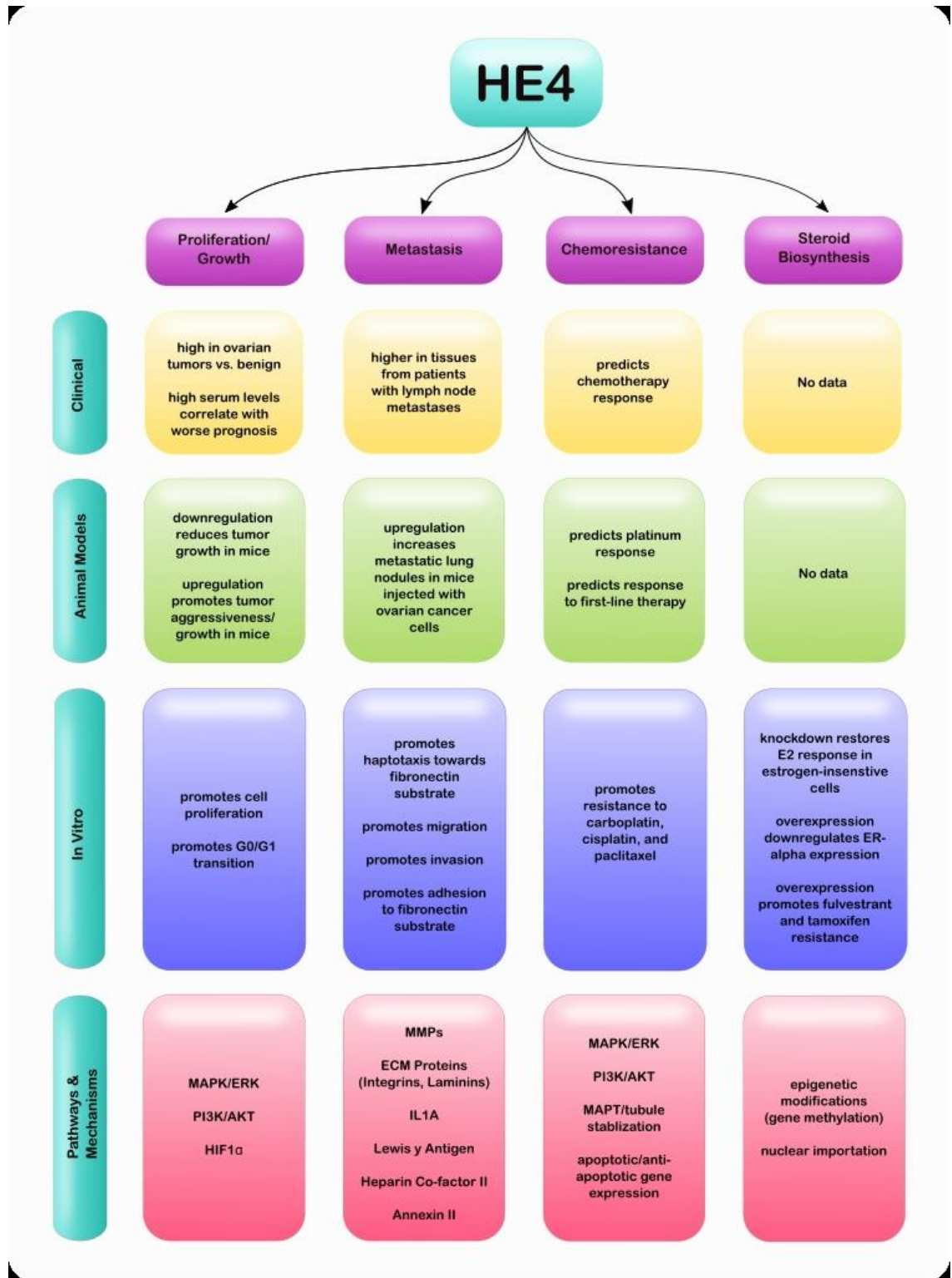
chemotherapy in ovarian cancer. *J Ovarian Res* (2014) 7:62. doi:10.1186/1757-2215-7-62

111. Gonzalez VD, Samusik N, Chen TJ, Savig ES, Aghaeepour N, Quigley DA, et al. Commonly occurring cell subsets in high-grade serous ovarian tumors identified by single-cell mass cytometry. *Cell Rep* (2018) 22:1875–88. doi:10.1016/j.celrep.2018.01.053

112. Angioli R, Plotti F, Capriglione S, Aloisi A, Montera R, Luvero D, et al. Can the preoperative HE4 level predict optimal cytoreduction in patients with advanced ovarian carcinoma? *Gynecol Oncol* (2013) 128:579–83. doi:10.1016/j.ygyno.2012.11.040

113. Yuan C, Li R, Yan S, Kong B. Prognostic value of HE4 in patients with ovarian cancer. *Clin Chem Lab Med* (2018). doi:10.1515/cclm-2017-1176

114. Zhao DY, Jacobs KM, Hallahan DE, Thotala D. Silencing Egr1 attenuates radiation-induced apoptosis in normal tissues while killing cancer cells and delaying tumor growth. *Mol Cancer Ther* (2015) 1535–7163. doi:10.1158/1535-7163.MCT-14-1051

115. Manente AG, Pinton G, Tavian D, Lopez-Rodas G, Brunelli E, Moro L. Coordinated sumoylation and ubiquitination modulate EGF induced EGR1 expression and stability. *PLoS One* (2011) 6:e25676. doi:10.1371/journal.pone.0025676

116. Gurler H, Yu Y, Choi J, Kajdacsy-Balla AA, Barbolina MV. Three-dimensional collagen type i matrix up-regulates nuclear isoforms of the microtubule associated protein tau implicated in resistance to paclitaxel therapy in ovarian carcinoma. *Int J Mol Sci* (2015) 16:3419–33. doi:10.3390/ijms16023419

117. Wang K, Deng QT, Liao N, Zhang GC, Liu YH, Xu FP, et al. Tau expression correlated with breast cancer sensitivity to taxanes-based neoadjuvant chemotherapy. *Tumour Biol* (2013) 34:33–8. doi:10.1007/s13277-012-0507-z

118. Wu H, Huang M, Lu M, Zhu W, Shu Y, Cao P, et al. Regulation of microtubule-associated protein tau (MAPT) by miR-34c-5p determines the chemosensitivity of gastric cancer to paclitaxel. *Cancer Chemother Pharmacol* (2013) 71:1159–71. doi:10.1007/s00280-013-2108-y

119. Russell SEH, Hall PA. Do septins have a role in cancer? *Br J Cancer* (2005) 93:499–503. doi:10.1038/sj.bjc.6602753

120. Cantley LC. The phosphoinositide 3-kinase pathway. *Science* (2002) 296:1655–7. doi:10.1126/science.296.5573.1655

121. Mungenast F, Thalhammer T. Estrogen biosynthesis and action in ovarian cancer. *Front Endocrinol* (2014) 5. doi:10.3389/fendo.2014.00192

122. Ribeiro JR, Freiman RN. Estrogen signaling crosstalk: implications for endocrine resistance in ovarian cancer. *J Steroid Biochem Mol Biol* (2014) 143:160–73. doi:10.1016/j.jsbmb.2014.02.010

123. Wolfrum C, Shih DQ, Kuwajima S, Norris AW, Kahn CR, Stoffel M. Role of Foxa-2 in adipocyte metabolism and differentiation. *J Clin Invest* (2003) 112:345–56. doi:10.1172/JCI18698

124. Perez-Balaguer A, Ortiz-Martinez F, Garcia-Martinez A, Pomares-Navarro C, Lerma E, Peiró G. FOXA2 mRNA expression is associated with relapse in patients with triple-negative/basal-like breast carcinoma. *Breast Cancer Res Treat* (2015) 153:465–74. doi:10.1007/s10549-015-3553-6

125. Brown DF, Caffa I, Cirmena G, Piras D, Garuti A, Gallo M, et al. Squalene epoxidase is a bona fide oncogene by amplification with clinical relevance in breast cancer. *Sci Rep* (2016) 6:19435. doi:10.1038/srep19435

126. Prabhu AV, Luu W, Sharpe LJ, Brown AJ. Cholesterol-mediated degradation of 7-dehydrocholesterol reductase switches the balance from cholesterol to vitamin D synthesis. *J Biol Chem* (2016) 291:8363–76. doi:10.1074/jbc.M115.699546

127. Dai M, Zhu XL, Liu F, Xu QY, Jiang SH, Yang XM, et al. Cholesterol synthetase DHCR24 induced by insulin aggravates cancer invasion and progesterone resistance in endometrial carcinoma. *Sci Rep* (2017) 7:41404. doi:10.1038/srep41404

128. Luu W, Hart-Smith G, Sharpe LJ, Brown AJ. The terminal enzymes of cholesterol synthesis, DHCR24 and DHCR7, interact physically and functionally. *J Lipid Res* (2015) 56:888–97. doi:10.1194/jlr.M056986

129. Zerenturk EJ, Sharpe LJ, Ikonen E, Brown AJ. Desmosterol and DHCR24: unexpected new directions for a terminal step in cholesterol synthesis. *Prog Lipid Res* (2013) 52:666–80. doi:10.1016/j.plipres.2013.09.002

130. Gabitiva L, Restifo D, Gorin A, Manocha K, Handorf E, Yang DH, et al. Endogenous sterol metabolites regulate growth of EGFR/KRAS-dependent tumors via LXR. *Cell Rep* (2015) 12:1927–38. doi:10.1016/j.celrep.2015.08.023

131. Sukhanova A, Gorin A, Serebriiskii IG, Gabitova L, Zheng H, Restifo D, et al. Targeting C4-demethylating genes in the cholesterol pathway sensitizes cancer cells to EGF receptor inhibitors via increased EGF receptor degradation. *Cancer Discov* (2013) 3:96–112. doi:10.1158/2159-8290.CD-12-0031

132. Lokich E, Singh RK, Han A, Romano N, Yano N, Kim K, et al. HE4 expression is associated with hormonal elements and mediated by importin-dependent nuclear translocation. *Sci Rep* (2014) 4:5500. doi:10.1038/srep05500

133. Robertson KD. DNA methylation and human disease. *Nat Rev Genet* (2005) 6:597–610. doi:10.1038/nrg1655

134. Bird A. DNA methylation patterns and epigenetic memory. *Genes Dev* (2002) 16:6–21. doi:10.1101/gad.947102

135. Chen Y, Wang S, Liu T, Wu Y, Li J, Li M. WAP four-disulfide core domain protein 2 gene(WFDC2) is a target of estrogen in ovarian cancer cells. *J Ovarian Res* (2016) 9:10. doi:10.1186/s13048-015-0210-y

136. Cottrill H, Cason S, Caroen S, Oronsky B, Donaldson E. A recurrent platinum refractory ovarian cancer patient with a partial response after RRx-001 resensitization to platinum doublet. *J Investig Med High Impact Case Rep* (2018) 6:2324709618760080. doi:10.1177/2324709618760080

137. Liu G, Yang D, Sun Y, Shmulevich I, Xue F, Sood AK, et al. Differing clinical impact of BRCA1 and BRCA2 mutations in serous ovarian cancer. *Pharmacogenomics* (2012) 13:1523–35. doi:10.2217/pgs.12.137

138. Earl H, Molica S, Rutkowski P. Spotlight on landmark oncology trials: the latest evidence and novel trial designs. *BMC Med* (2017) 15:111. doi:10.1186/s12916-017-0884-7

139. Gaillard SL, Secord AA, Monk B. The role of immune checkpoint inhibition in the treatment of ovarian cancer. *Gynecol Oncol Res Pract* (2016) 3:11. doi:10.1186/s40661-016-0033-6

Figure 2.1 Graphical Representation of clinical, in vivo and in vitro studies completed relating to HE4 and EOC.

Table 2.1 Summary of factors associated with HE4 in EOC

Gene symbol	Description	Association
(A) Cell proliferation and tumor growth		
AKT	Protein kinase B	• Upregulated in overexpressing OVCAR3 HE4 cell lines (10) • Decreased in response to HE4 knockdown in OVCAR3 cells (10) • Upregulated in HE4 SKOV3 clones compared with vector control (16)
HIF1α	Hypoxia-inducible factor-1 alpha	• Co-immunoprecipitation with HE4 SKOV3 xenograft tissue (13) • Colocalization with HE4 in SKOV3 xenograft tissue (13) • Treatment with 2-methoxyestradiol leads to marked decrease in HE4 (13)
ERK	Extracellular signal-regulated kinase	• Decrease in p-ERK when HE4 was silenced in SKOV3 cells (9) • Corresponding decrease and increase in ERK when HE4 was downregulated and overexpressed in OVCAR3 cells (10) • Increase in p-ERK in SKOV3 and OVCAR8 cells with recombinant HE4 treatment (16)
CHUK GADD45A IL1A RPS6KA1 HSPA1B DUSP1 JUND	Conserved helix–loop–helix ubiquitous kinase Growth arrest and DNA-damage-inducible protein GADD45 alpha Interleukin-1 alpha Ribosomal protein S6 kinase alpha 1 Heat shock 70 kDa protein 1B, Dual specificity protein phosphatase 1 Transcription factor JunD	• Upregulation when HE4 was induced in ES-2 cells (8)
EGF/EGFR	Epidermal growth factor/epidermal growth factor receptor	• Co-immunoprecipitation with HE4 SKOV3 xenograft tissue (13) • Colocalization with HE4 in SKOV3 xenograft tissue (13) • HE4 overexpressed in OVCAR8 cells when stimulated with recombinant protein (13) • HE4 increased when inhibited by IRESSA (13)
VEGF INS	Vascular endothelial growth factor Insulin	• HE4 overexpressed in OVCAR8 cells when stimulated with recombinant protein (13)
(B) Invasion, migration, and adhesion		
MMP-9 MMP-2 CTSB	Matrix metallopeptidase 9 Matrix metallopeptidase 9 Cathepsin B	• Downregulated when HE4 is silenced in ovarian cell lines (9)
IL1A	Interleukin-1 alpha	• Microarray results reveal correlation with HE4 levels (8, 71) • One microarray reports an inverse correlation with HE4 (16)
ITGβ5	Integrin β5	• Differentially regulated by HE4 in ES-2 and CaOV3 cells (8) • Correlation with HE4 in paraffin embedded ovarian human tissue (8)
SDC1 COL1A1 DAG1	Syndecan 1 Collagen type 1 alpha 1 Dystroglycan 1	• Differentially regulated in response to HE4 (71)
LAMB3 LAMC2 GREM1 TNC SERPIND2	Laminin-β3 Laminin-γ2 Gremlin 1 Tenascin C Serine peptidase inhibitor member 2	• Increased expression when stimulated with recombinant HE4 in OVCAR8 cells (57)
LAMA3	Laminin 332 Lewis y antigen	• Increased in response to HE4 stimulation of LAMB3 and LAMC2 (57) • Colocalized with HE4 in human ovarian tissue (98) • Immunohistochemistry stained found correlative staining with HE4 (98) • Overexpression promoted HE4-mediated invasion and metastasis in in vitro cell lines (99) • Knockdown promoted a decrease in invasion and metastatic properties of HE4 (99)
SERPIN D1	Heparin cofactor II	• Upregulated in HE4-overexpressing clones and downregulated in knockout in in vitro lines (71) • Spearman analysis revealed positive correlation with HE4 in human EOC tissue immunohistochemistry staining (71) • Poor patient prognosis when levels upregulated in combination with HE4 (71)
ANXA2	Annexin II	• Mass spectrometry and co-immunoprecipitation identify as strong interacting partner of HE4 (58) • Gene levels co-dependent with HE4 (58) • Higher along with HE4 in EOC patients with lymph node metastasis than those without (58)
LAMB2 MKN2	Laminin subunit beta-2 MAP kinase-interacting serine/threonine-protein kinase 2	• Gene levels decreased in presence of HE4 knockdown cell line (58)
(C) Chemoresistance		
EGR1	Early growth response protein 1	• Suppressed in overexpressing HE4 clones (16)
p38	p38 mitogen-activated protein kinase	• Activated in NV cells treated with cisplatin and suppressed in overexpressing HE4 clones (16)
BCL2	B-cell lymphoma 2	• Increased in response to recombinant HE4 in vitro (7)
BAX	bcl-2-like protein 4	• Decreased in response to recombinant HE4 in vitro (7)
MAPT SEPT3	Microtubule-associated protein tau Septin 3	• Upregulated in HE4-overexpressing clones (16)
TUBB	β-Tubulin	• Increased in response to recombinant HE4 in vitro (16)
ERK AKT	Extracellular signal-regulated kinase Protein kinase B	• Knockdown with HE4 lead to a reduction in cell growth and resensitization to cisplatin and paclitaxel (10)
(D) Steroid biosynthesis		
FOXA2	Forkhead box protein A2	• Differentially expressed in -overexpressing clones and knockouts (71)
SQLE DHCR7 NSDHL	Squalene monooygenase Dehydrocholesterol reductase Sterol-4-alpha-carboxylate-3 dehydrogenase	• Differentially expressed in HE4-overexpressing clones and knockouts (71)
5-MC	5-Methylcytosine	• Downregulated in HE4-overexpressing clones compared with wild-type SKOV3 cells and null vector (131)
ESR1	Estrogen/estrogen receptor	• Abolished in HE4-overexpressing clones (131) • When stimulated in H08910 cells HE4 increased in gene and protein levels. Effect not observed in SKOV3 cells (131) • Increase expression in HE4 SKOV3 knockdown (131)

CHAPTER 3

MANUSCRIPT I

HE4 Suppresses the Expression of Osteopontin in Mononuclear Cells and

Comprises Their Cytotoxicity Against Ovarian Cancer Cells

James NE[1,2], Cantillo E[1], Oliver MT[1], Rowswell-Turner RB[3], Ribeiro JR[1], Kim KK[3],

Chichester CO 3rd[2], DiSilvestro PA [1], Moore RG[3], Singh RK[1,3], Yano N[1*], Zhao TC[4]

_____

[1] Division of Gynecologic Oncology, Program in Women's Oncology, Department of Obstetrics and Gynecology, Women and Infants Hospital, Providence, RI, United States

[2] Department of Biomedical and Pharmaceutical Sciences, University of Rhode Island, Kingston, RI, United States

[3] Division of Gynecologic Oncology, Department of Obstetrics and Gynecology, Wilmot Cancer Institute, University of Rochester Medical Center, Rochester, NY 14642, United States

[4] Department of Surgery, Roger Williams Medical Center, Boston University Medical School, Providence RI, United States

[*]Correspondence:
Naohiro Yano
naohiro.yano@CharterCARE.org

I.1 Abstract

Ovarian tumors are known to suppress immunosurveillance and promote immune escape. Here, we examine the role of the secretory glycoprotein HE4 in ovarian cancer immune evasion. Through modified subtractive hybridization analyses of human peripheral blood mononuclear cells (PBMCs), we have characterized gene targets of HE4 and established a preliminary mechanism of HE4-mediated immune failure in ovarian tumors. Upon exposure of PBMCs to recombinant human HE4 *in vitro,* osteopontin (OPN) emerged as the most suppressed gene, while DUSP6 was the most upregulated gene. SKOV3, a human ovarian carcinoma cell line, exhibited enhanced proliferation in conditioned media from HE4-exposed PBMCs, and this effect was attenuated by the addition of recombinant OPN or OPN-inducible cytokines (IL-12 and IFN-γ). Additionally, upon co-culture with PBMCs, HE4-silenced SKOV3 cells were more susceptible to cytotoxic cell death. The relationship between HE4 and OPN was further reinforced through analysis of serous ovarian cancer patient samples. In these biopsy specimens, the number of OPN^{+} T cells correlates positively with progression free survival (PFS) and inversely with serum HE4 level. Taken together, these findings show that HE4 enhances ovarian cancer tumorigenesis by compromising OPN-mediated T cell activation.

I.2 Introduction

Human epididymis protein 4 (HE4) is a member of the whey acidic domain family of proteins (WAP), which are generally regarded as protease inhibitors (1-3). HE4 was first identified in the male reproductive tract but has since been found in select other tissues, such as the kidney, female reproductive tract, breast, and lungs (4,5). In addition, it is highly overexpressed in several human malignancies, including ovarian and endometrial cancer (5-8). HE4's role in normal and malignant tissue is still unclear; however, as a known negative prognostic factor in women with epithelial ovarian cancer, its serum levels correlate with chemoresistance and reduced survival (9-11). Our previous work with HE4 has led to the development of a USFDA approved biomarker tool for evaluation of pelvic masses, coined the Risk of Ovarian Malignancy Algorithm (ROMA) (12-15). The ROMA score incorporates HE4, CA-125, and menopausal status into a calculation to estimate ovarian cancer risk. As a biomarker, HE4 detection and monitoring is already improving patient care. However, it is imperative that we learn more about its function in order to better understand ovarian tumorigenesis and ultimately develop effective therapies for this fatal cancer.

In this present study, we begin to elucidate HE4's role in the interplay between tumor cells and the immune system. We generated cDNA-subtracted libraries of HE4 treated peripheral blood mononuclear cells (PBMCs) and employed a modified subtractive hybridization method to identify differentially expressed genes. This strategy identified osteopontin (OPN) as one of the most prominently suppressed targets in PBMCs following HE4 treatment. OPN is a secretory glycosylated phosphoprotein encoded by the gene *SPP1*. OPN contains an arginine-glycine-aspartate (RGD)

60

sequence that—via interactions with integrin family members or CD44—triggers downstream signaling events and relays early cell-mediated immune responses (16-18). We observed that HE4-induced OPN suppression mitigated the cytotoxicity of PBMCs against cultured human ovarian cancer cells *in vitro*. Further, the expression levels of OPN in stromal infiltrating T cells in biopsy samples from serous ovarian cancer patients showed direct association with patient progression free survival (PFS). Together, our data demonstrates that HE4 inhibits the immune function of PBMCs, most prominently T cells, via suppression of OPN production.

I.3 Materials and methods

Subtractive hybridization and TA-cloning**.**

Primary human PBMCs were obtained under the auspices of Women & Infants Hospital IRB approval from a single volunteer. Approximately 5×10^7 of PBMCs were obtained from 40 mL of heparinized total blood. The cells were suspended in 5 mL of serum free RPMI1640 medium (#31800022; Invitrogen, Carlsbad, CA, USA) and incubated with or without 0.01 μg / mL (approximately 270 pM) of rHE4 (MBS717359; MyBiosource, San Diego, CA, USA) for 6 hours, and total RNA was isolated using TRIzol reagent (Invitrogen). The dose of HE4 (0.01 μg / mL, 270 pM) was chosen as a comparable concentration to serum levels in patients with various types of ovarian tumors (19). Around 300 μg of total RNA was isolated in this scale of preparation. The RNA was stored at -80 degrees until messenger RNA (mRNA) isolation. Blood draws were repeated at a minimum of 7-day intervals until the amount of total RNA collected reached 1 mg. Next, mRNA was purified using oligo dT coated

61

magnetic beads (Takara-Clontech, Mountain View, CA, USA). Approximately 10 μg of mRNA was isolated from the 1 mg of total RNA, from which subtractive cDNA libraries were constructed using PCR-Select™ cDNA Subtraction Kit (Takara-Clontech, Mountain View, CA, USA), following the manufacturer's instructions. Briefly, the tester and driver cDNAs are synthesized from poly A+ RNA generated from control and HE4 treated PBMCs. The tester and driver cDNAs are each digested with a restriction enzyme, Rsa I, to yield shorter, blunt-ended molecules. The tester cDNA is then subdivided into two portions, and each is ligated with a different cDNA adaptor. The ends of the adaptor do not contain a phosphate group, so only one strand of each adaptor attaches to the 5' ends of the cDNA. The two adaptors have stretches of identical sequence to allow annealing of the PCR primer once the recessed ends have been filled in. The differentially expressed genes were identified through two steps of hybridizations followed by two steps of PCR. The PCR products of the differentially expressed genes were cloned into a pUC19-TA vector. The clones containing the inserts were selected by blue/white selection and were amplified by colony PCR using M13 primers.

Cell culture

The human ovarian cancer cell lines SKOV3 and OVCAR8 were obtained from ATCC (Manassas, VA, USA). RPMI1640 (#31800022; Invitrogen) and DMEM supplemented with 1.0 mM of sodium pyruvate (#31600034; Invitrogen) were used for culturing PBMC and SKOV3, respectively. Conditioned media was obtained from 24-hour PBMC culture with or without 0.01 μg / mL (270 pM) of rHE4. Residual

62

rHE4 in the conditioned media was deprived as follows. Five mLs of media was incubated with 10 μg (100 μL) of anti-human HE4 antibody (sc-293473; Santa Cruz Biotechnology, Santa Cruz, CA, USA) for 1 hour at 4 degrees. Then, 100 μL packed volume of protein G coated sepharose beads (GE Healthcare Life Science, Pittsburg, PA, USA) was added and incubated for 4 hours at 4 degrees. After the incubation, the sepharose beads were removed by centrifugation and the supernatants were processed through a sterile 0.2 μm pore syringe filter. The conditioned media were used without any dilution. For the cell-mediated cytotoxicity assay, 2×10^5 target cells (SO or shHE4 transfected SKOV3) were seeded in each well of 6-well plates, and then were incubated overnight with complete media. The next day, cells were placed in serum free media for another overnight incubation to induce quiescence, and then 1×10^7 of the effector cells (PBMC) mixed with propidium iodide (Invitrogen) were added to each well. Some of the wells contained 5 pg / mL of rIL-12 (219-IL-005; R&D Systems, Minneapolis, MN, USA), 20 pg / mL of rIFN-γ (SRP3058; Sigma-Aldrich, St. Louis, MO, USA) or 0.05 μg / mL of rHE4 (ab132299; Abcam) in combinations as indicated in Figure 4 (lower panel). The ovarian cancer cell lines were morphologically normal and kept growing up to 72 hours in serum deprived DMEM. In order to avoid unexpected effects of unknown constituents in the serum, all experiments were performed under serum free condition. shRNA for human HE4 (TR318721; Origene, Minneapolis, MN, USA) were transfected into SKOV3 using Lipofectamine 2000^{TM} (Invitrogen) following the manufacturer's instructions. In other cases, cells were treated with 20 pg / mL recombinant OPN (ab92964; Abcam) or 0.01 μg / mL rHE4.

63

Quantitative Real-Time PCR

RNA was isolated from PBMCs of healthy donors using TRIzol (Invitrogen) according to the manufacturer's instructions. cDNA was synthesized using SuperScript III reverse transcriptase (Invitrogen). qPCR was performed using Premix Ex-Taq[TM] II (Clontech-Takara) probes for OPN, IL-12B and IFN-γ. All reactions were normalized using GAPDH as an endogenous control. Amplification data were analyzed using the ΔΔ Ct method.

Flow cytometry

FITC-labeled anti CD3 (HIT3a), CD14 (M5E2), CD19 (HIB19) and CD56 (B159) antibodies were obtained from BD Biosciences (Billerica, MA, USA). Alexa Fluoro® 647-labeled anti OPN antibody (EPR3688) was obtained from Abcam. After staining for cell surface markers (CD3, CD14, CD19 and CD56), the cell membrane was permeabilized by 0.2 % Triton X-100 and 0.2 % digitonin, and then stained for OPN. Flow cytometric analysis was performed with FACSCanto system and FACSDiva software (BD Biosciences).

ELISA

ELISA kits for OPN, IL-12AB, IFN-γ and HE4 were obtained from R&D Systems. The assays were performed following the manufacturer's instructions.

Viability and migration assays

1×10^3 / well SKOV3 cells were seeded in a 96-well culture plate. After overnight incubation with serum free medium, conditioned media was added to the quiescent cells that were cultured for 24, 48 and 72 hours. The cell viabilities at each time point were evaluated using CellTiter-Blue® (Promega, Madison, WI, USA). Cell migration assays were performed using InnoCyte™ Cell Migration Assay (EMD Millipore, Taunton, MA, USA). 5×10^4 SKOV3 cells were seeded in the upper chamber of a 96-well plate with the lower chamber containing the PBMC-conditioned media. Migration activities were accessed after incubating the cells for 24 hours in a CO_2 incubator at 37 °C.

Immunohistochemistry

SKOV3 cells were seeded at 0.5×10^4 / chamber in a 4-chamber slide. After overnight incubation with serum free medium, conditioned media was added to the quiescent cells and the cells were cultured for 48 hr. The cells were fixed with 2 % formaldehyde and permealized by 0.2 % TritonX-100. The slides were then incubated with a mouse monoclonal anti-Ki67 antibody (clone B56; PD Pharmingen, Franklin Lakes, NJ, USA) overnight at 4°C in a humidified chamber. The slides were then incubated with an ALP conjugated anti-mouse IgG (H+L) secondary antibody (Bio-Rad, Hercules, CA, USA) for 30 minutes at room temperature. Bound antibody was detected using the ALP substrate kit (Vector Laboratories, Burlingame, CA, USA) and lightly counterstained with veronal acetate buffered 1% methyl green solution, pH 4.0 (Vector laboratories). Permount™ (Fisher Scientific, Ottawa, Ontario, Canada) was

65

used as the mounting media and sections were cover slipped. The immunohistochemical studies were repeated four times on samples prepared from different cultures. The proportion of Ki67 positive cells was calculated according to the following formula: $100 \times$ (the number of Ki67-positive nuclei/total number of nuclei). Each image was analyzed at least four times to obtain an average labeling index.

Western blotting

Cellular contents of HE4 in SKOV3 cell lines transfected with shRNA against HE4 were assessed by western blotting. Antibodies against HE4 were obtained from Origene (TA326648). Anti-actin antibody (clone 2G2; EMD Millipore) was used for detection of the internal loading control. The results were visualized with SuperSignal™ West Pico chemiluminescent substrate (ThermoFisher Scientifics) and analyzed with the UN-SCAN-IT gel software for Windows (Version 6.1; Silk Scientific Inc.).

Confocal immunofluorescent microscopy

Formalin-fixed, paraffin-embedded tissue sections were cut to a thickness of 4 μm. For heat-induced epitope retrieval, deparaffinized sections in 0.01 M citrate buffer were treated three times at 90 °C for 5 minutes using a microwave oven. After blocking with 10% normal horse serum, sections were incubated with rabbit anti-OPN antibody (FL-314; Santa Cruz Biotechnology) or mouse anti-CD3 (PS-1; Abcam) overnight at 4 °C, washed with PBS and incubated with DyLight 488 goat anti-rabbit

66

IgG (DL1488; Vector Laboratories) or DyLight 594 horse anti-mouse IgG (DL2594; Vector Laboratories) secondary antibodies for 1 hour at room temperature in the dark. Slides were washed again with PBS and cover-slipped with DAPI-containing mounting medium (Vector Laboratories). Confocal images were acquired with a Nikon C1si confocal (Nikon Inc. Mellville, NY, USA) using diode lasers 402, 488 and 561. Ten fields/sample were randomly selected based on DAPI staining and counts were performed for CD3 and OPN using a 40x objective. Counts are expressed as # of positive cells/mm^2. All donors of the biopsies and the PBMCs provided written informed consent. The study was approved by the Women & Infants Hospital ethics committee.

Statistics

Data ware expressed as average ± SEM of at least three independent experiments. An unpaired, two-tailed Student t-test was used to determine significance. Multiple treatments were analyzed by using one-way ANOVA followed by Ryan's multiple comparison test. Spearman's rank correlation test was used to assess the immunofluorescent staining on biopsy specimens. Differences between groups were considered statistically significant when $p < 0.05$.

I.4 Results

Differential expression of PBMC genes after HE4 exposure

To identify differentially expressed genes after HE4 exposure, modified subtractive hybridization was performed. PCR products of the differentially expressed genes were

67

cloned into pUC19-TA vectors to create a differential cDNA library. PCR products from 252 HE4-induced and 253-HE4 suppressed gene colonies were sequenced resulting in the identification of 211 induced genes and 208 suppressed genes. Among the identified genes, 23 induced and 15 suppressed sequences showed no significant similarity (NSS) to known genes in available nucleotide databases. Among the 208 suppressed genes, OPN emerged as the most frequently identified gene (6 times out of 253 sequences, 2.4%; Table 1).

HE4 reduces OPN expression in PBMCs

HE4-induced suppression of osteopontin in PBMCs was then confirmed via three modalities: flow cytometry, quantitative PCR (qPCR), and ELISA using PBMCs from four individual donors. First, PBMCs were cultured with recombinant human HE4 (rHE4; 0.01 μg / mL) for 24 hours and collected for flow cytometry analysis. Protein expression of OPN in CD3^{+} PBMCs (T cells) was found to be significantly reduced with HE4 exposure (48.8 ± 1.0 % vs 37.4 ± 1.0 %; $p < 0.05$; Figure 1A). PBMCs were harvested after a 6-hour incubation with rHE4 (0.01 μg / mL), revealing a 0.70 ± 0.03-fold reduction in OPN mRNA production (Fig 1B). PBMCs were then exposed to rHE4 (0.01 μg / mL) for 24 hours and concentrations of OPN in the cell lysates and the culture supernatants were measured by ELISA. The concentrations of OPN in lysates (159.82 ± 3.14 vs 103.61 ± 3.23 pg / mL, $p < 0.01$) and culture supernatants (53.37 ± 3.14 vs 30.08 ± 3.48 pg / mL, $p < 0.01$) were also decreased with HE4 exposure (Figure 1C).

68

HE4-mediated IL-12 and IFN-γ reduction in PBMCs is reversible with supplementation of OPN

In lipopolysaccharide-stimulated macrophages, OPN has been shown to enhance IL-12 production and suppress IL-10 production, thereby promoting Th1 activity (17, 18). In order to estimate the impact of HE4 on PBMCs, transcriptional expression and protein levels of Th1 related cytokines IFN-γ and IL-12 were evaluated. Cells were incubated with either: (a) vehicle control, (b) 0.01 μg / mL rHE4 or (c) 0.01 μg / mL of rHE4 and 20 pg / mL rOPN for 6 hours and cell lysates and/or culture supernatants were taken for qPCR and ELISA. As shown in Figure 2A, relative expressions of IL-12B and IFN-γ mRNA were decreased (61% and 69% respectively) upon treatment with rHE4. This suppression was partially reversed by the addition of recombinant OPN (rOPN) to culture conditions. Protein expression, as determined by ELISA, is shown in Figure 2B. IL-12 concentrations, both in lysates and culture supernatants, were reduced after HE4 exposure (4.81 ± 0.17 to 2.05 ± 0.08 pg / mL in cell lysate and 7.17 ± 0.26 to 3.56 ± 0.20 pg / mL in supernatant). The addition of rOPN resulted in a nearly complete reversal of HE4-mediated IL-12 suppression. Similarly, IFN-γ concentrations in the cell lysates and supernatant decreased significantly with rHE4 treatment (from 35.55 ± 1.03 to 14.41 ± 1.10 pg / mL and from 19.92 ± 0.82 to 11.10 ± 0.59 pg / mL, respectively) and the addition of rOPN again caused recovery of the cytokine levels.

Conditioned media from HE4-treated PBMCs enhanced the viability, proliferation, and invasiveness of ovarian cancer cells

69

In order to assess the effects of PBMC-produced soluble factors on cancer cell activity, SKOV3, an immortalized ovarian cancer cell line, was incubated with the conditioned media from PBMC cultures (2×10^6 / mL density) with or without rHE4. SKOV3 cells cultured with HE4-treated PBMC media showed significantly higher viability than cells cultured with the HE4-depleted PBMC conditioned media at 48 hours (1773.84 ± 436.38 vs. 3081.17 ± 348.03, $p < 0.01$) and 72 hours (3146.67 ± 494.87 vs. 4568.84 ± 407.74, $p < 0.01$; Figure 3A). Next, a cell migration assay was employed to determine whether conditioned media from rHE4-exposed PBMCs affects ovarian cancer migration as a surrogate of metastatic capability. The SKOV3 cells that were incubated with HE4-exposed PBMC media showed more extensive migration than control cells (RFU of 1147.21 ± 365.09 vs. 3138.14 ± 419.66, $p < 0.01$, Figure 3B). Immunohistochemistry using anti-Ki67 was performed to evaluate the proliferation of SKOV3 cells in the presence of rHE4-exposed PBMC media or vehicle-exposed conditioned media. The proliferation rate of tumor cells in HE4-exposed PBMC conditioned media was higher than control media (63.8 ± 18.1 vs 39.9 ± 7.6 %, $p < 0.01$, Figure 3C). These findings suggest that PBMCs alter their soluble factor release under the influence of rHE4, thus enhancing the viability, proliferation and migration capabilities of the cultured ovarian cancer cells.

HE4 inhibition increases ovarian cancer susceptibility to PBMC-mediated cytotoxicity
In order to evaluate the impact of native (tumor-cell produced) HE4 on PBMCs, SKOV3 cells were co-cultured with PBMCs after stable transfection with HE4 specific shRNA (shHE4) or a scrambled oligonucleotide control plasmid (SO). Clones

70

of shRNA transfected cells were tested for their phenotype by western blotting and ELISA (Figure S5). After a 2-hour incubation at 37 °C, the effector cells were washed away and the target cells were analyzed by flow cytometry. The silencing of HE4 in SKOV3/PBMC co-cultures led to a significant increase in IL-12 and IFNγ concentrations (Table 2). As shown in Figure 4, HE4 silencing also increased tumor cell susceptibility to PBMC cytotoxicity, an effect that was reversed by the addition of rHE4. Furthermore, this "rescue" by rHE4 was at least partially abrogated by the addition of recombinant IL12 (rIL-12) or recombinant IFN-γ (rIFN-γ) to the culture conditions. These findings suggest that the native HE4 production by ovarian cancer cells is critical to cell-mediated cytotoxicity resistance.

Ovarian cancer patient prognosis correlates to the number of intra- and peri-tumoral CD3$^+$ T cells and stromal OPN-producing cells

Twenty biopsies from high-grade serous ovarian cancer patients were evaluated by dual fluorescent stain with antibodies against CD3 and OPN (Table 3). In the tumor segments of the biopsy specimen, some CD3$^-$ tumor cells showed high OPN expression, while in the stromal area of the biopsy the principal OPN$^+$ cells were CD3$^+$ T cells (Figure 5A). A significant portion of the stromal CD3$^+$OPN$^+$ cells was accompanied by strong OPN staining in their cytosols or the surrounding areas (Figure 5B). In order to investigate the clinical relationship of HE4, OPN and CD3, numbers of T cells (CD3$^+$) and total OPN$^+$ cells were correlated with pre-operative serum HE4 level (available for 13 patients) or PFS duration (available for 16 patients). The numbers of CD3$^+$ infiltrating T cells, both in the tumor and stroma, were directly

71

proportional (tumor, r = 0.541, p = 0.03; stroma, r = 0.512, p = 0.02) to the patients' PFS duration (Figure 5C). Additionally, the number of OPN^{+} cells, both in tumor and stroma, were in inversely proportional (tumor; r = -0.635, p = 0.019, stroma; r = -0.582, p = 0.037) to serum levels of HE4. Moreover, the number of OPN^{+} cells in the stroma (but not in the tumor) were directly proportional to the patients' PFS duration (r = 0.711, p = 0.002; Figure 5D). These findings suggest that tissue infiltrating T cells play a critical role in the suppression of ovarian cancer progression.

I.5 Discussion

HE4 is known to be highly overexpressed in ovarian cancer, but its causal relationship to ovarian tumorigenesis has not been firmly established. Emerging studies suggest that HE4 overexpression promotes ovarian tumor growth and imparts strong resistance against the most commonly used chemotherapeutics (20-24). Accordingly, serum HE4 level is an early predictor of platinum resistance (9, 23), and ovarian cancer patients that experienced greater HE4 reduction during neoadjuvant chemotherapy exhibited improved overall survival (24). Our study has shown a novel role for HE4 in the inhibition of immune cell activity through OPN suppression. We identified the gene for OPN, *SPP1*, as the most prominently suppressed gene in PBMCs in response to HE4 exposure *in vitro*. Additionally, HE4 was found to downregulate OPN production in CD3^{+} T cells. It is important to note that the changes in OPN expression in T cells after HE4 exposure are quite modest according to the flow cytometric analysis, and this raises the question of whether these small differences translate into functional consequences. However, the changes in OPN levels determined by qPCR and ELISA

72

(Figure 1B and C) appear much more robust. These findings suggest that the secretion of OPN is an important factor to include in the assessment of the biological response to HE4. In accordance with this hypothesis, we confirmed suppressed secretion of OPN-induced cytokines IL-12 and IFN-γ in the rHE4 exposed PBMCs. HE4's inhibition of immune cell function was further clarified by our co-culture experiments showing reduced antitumoral cytotoxicity.

OPN is primarily considered a pro-tumorigenic protein. In various types of cancers, serum OPN levels are directly proportional to degree of malignancy and inversely proportional to patient survival (25-27). OPN also plays a critical role in tumor formation and growth by promoting cancer cell survival, proliferation, metastasis, and angiogenesis (28, 29). On the other hand, some studies describe anti-tumor effects of OPN (30-33). Among them, Crawford et al., with elegantly designed cancer cell inoculation experiments using OPN null mice, demonstrated that host-derived OPN acted as a chemoattractant to enhance the host defense activity of macrophages, whereas tumor-derived OPN inhibited macrophage function to enhance the growth or survival of cancers (30). In our study, the number of OPN$^+$ cells in stroma (mainly CD3$^+$ T cells), but not in tumor (mainly CD3$^-$ tumor cells), correlated positively to patients' PFS durations. The dichotomic function of OPN presented by Crawford et al. may serve as an explanation of the findings in the present study.

In summary, this study is the first to implicate HE4 in ovarian cancer immune escape and provide the rationale for targeting HE4 to restore normal tumor immune editing. We are currently working to identify small molecules and/or neutralizing antibodies to further validate the utility of HE4 inhibition as a novel immunotherapeutic in the

treatment of ovarian cancer. However, several barriers remain in the achievement of this objective. For example, PBMCs in ovarian cancer patients may already be exposed to a chronically high level of HE4, which may have differing effects than the acute exposure performed in our study. Secondly, due to multiple complicated steps in the subtractive hybridization procedure, this study stands on the data from a single donor. The benefit of this experimental strategy lies in perspicuous outcomes; however, it also introduces inherent limitations in interpretation of the results. To begin to circumvent this pitfall, we validated the HE4-mediated downregulation of OPN using flow cytometry, qPCR, and ELISA in PBMCs from four healthy donors. This issue will be further addressed in subsequent studies on HE4. Lastly, it is important to note that OPN is known to play a role in humoral immunity (34-36). Further studies are required to fully understand the role of HE4 and OPN in humoral immunity in relation to ovarian cancer. Additionally, as we showed in Table 1 that PBMCs modulated a variety of genes in response to HE4 exposure. It is therefore very likely that other factors, besides osteopontin, are also contributing to in the inhibitory effect of HE4 on the immune system. Further analysis of the functions of these genes, and how they are associated with HE4, is warranted.

I.6 References

1. Kirchhoff C, Habben I, Ivell, R, Krull, N. A major human epididymis-specific cDNA encodes a protein with sequence homology to extracellular proteinase inhibitors. Biol Reprod 1991; 45:350-7.

2. Ranganathan S, Simpson KJ, Shaw DC, Nicholas KR. The whey acidic protein family: a new signature motif and three-dimensional structure by comparative modeling. J Mol Graph Model 1999; 17:106-13.

3. Schalkwijk J, Wiedow O, Hirose S. The trappin gene family: proteins defined by an N-terminal transglutaminase substrate domain and a C-terminal four-disulphide core. Biochem. J. 1999; 340(Pt3):569-77.

4. Bingle L, Singleton V, Bingle CD. The putative ovarian tumour marker gene HE4 (WFDC2), is expressed in normal tissues and undergoes complex alternative splicing to yield multiple protein isoforms. Oncogene 2002; 21:2768-73.

5. Galgano MT, Hampton GM, Frierson HF Jr. Comprehensive analysis of HE4 expression in normal and malignant human tissues. Mod Pathol 2006; 19:847-53.

6. Drapkin R, von Horsten HH, Lin Y, Mok SC, Crum CP, Welch WR, Hecht JL. Human epididymis protein 4 (HE4) is a secreted glycoprotein that is overexpressed by serous and endometrioid ovarian carcinomas. Cancer Res 2005; 65:2162-9.

7. Schaner ME, Ross DT, Ciaravino G *et al.* Gene expression patterns in ovarian carcinomas. *Mol.* Biol Cell 2003; 14:4376-86.

8. Hellström I, Raycraft J, Hayden-Ledbetter M *et al.* The HE4 (WFDC2) protein is a biomarker for ovarian carcinoma. Cancer Res 2003; 63:3695-700.

9. Angioli R, Capriglione S, Aloisi A *et al.* Can HE4 predict platinum response during first-line chemotherapy in ovarian cancer? Tumour Biol. 2014; 35:7009-15.

10. Chudecka-Głaz AM, Cymbaluk-Płoska AA, Menkiszak JL, Sompolska-Rzechuła AM, Tołoczko-Grabarek, AI, Rzepka-Górska IA. Serum HE4, CA125, YKL-40, bcl-2, cathepsin-L and prediction optimal debulking surgery, response to chemotherapy in ovarian cancer. J. Ovarian. Res. 2014; 7:62.

11. Vallius T, Hynninen J, Auranen A *et al.* Serum HE4 and CA125 as predictors of response and outcome during neoadjuvant chemotherapy of advanced high-grade serous ovarian cancer. Tumour Biol 2014; 35:12389-95.

12. Moore RG, Brown, AK, Miller MC *et al*. The use of multiple novel tumor biomarkers for the detection of ovarian carcinoma in patients with a pelvic mass. Gynecol Oncol 2008; 108: 402-8.

13. Moore RG, Brown AK, Miller MC *et al.* Utility of a novel serum tumor biomarker HE4 in patients with endometrioid adenocarcinoma of the uterus. Gynecol Oncol 2008; 110: 196-201.

14. Moore RG, McMeekin DS, Brown AK *et al*. A novel multiple marker bioassay utilizing HE4 and CA125 for the prediction of ovarian cancer in patients with a pelvic mass. Gynecol Oncol 2009; 112: 40-6.

15. Moore RG, Jabre-Raughley M, Brown AK *et al*. Comparison of a novel multiple marker assay vs the Risk of Malignancy Index for the prediction of epithelial ovarian cancer in patients with a pelvic mass. Am J Obstet Gynecol 2010; 203: 228.e1-6.

16. Denhardt DT, Lopez CA, Rollo EE, Hwang SM, An XR, Walther SE. Osteopontin-induced modifications of cellular functions. Ann NY Acad Sci 1995; 760:127-42.

17. O'Regan AW, Chupp GL, Lowry JA, Goetschkes M, Mulligan N, Berman Osteopontin is associated with T cells in sarcoid granulomas and has T cell adhesive and cytokine-like properties in vitro. J Immunol 1999; 162:1024-31.

18. Ashkar S, Weber GF, Panoutsakopoulou V *et al*. Eta-1 (Osteopontin): An early component of type-1 (cell-mediated) immunity. Science 2000; 287:860-4.

19. Huhtinen K, Suvitie P, Hiissa J *et al*. Serum HE4 concentration differentiates malignant ovarian tumours from ovarian endometriotic cysts. Br J Cancer 2009; 100: 1315-9.

20. Moore RG, Hill EK, Horan T *et al*. HE4 (WFDC2) gene overexpression promotes ovarian tumor growth. Sci Rep 2014; 4:3574.

21. Ribeiro JR, Schorl C, Yano N, Romano N, Kim KK, Singh RK, Moore RG. HE4 promotes collateral resistance to cisplatin and paclitaxel in ovarian cancer cells. J Ovarian Res 2016; 9:28.

22. Pelissier A, Roulot A, Guéry B, Bonneau C, Bellet D, Rouzier R. Serum CA125 and HE4 levels as predictors for optimal interval surgery and platinum sensitivity after neoadjuvant platinum-based chemotherapy in patients with advanced epithelial ovarian cancer. J Ovarian Res 2016; 9: 61.

23. Lee S, Choi,S, Lee Y, Chung D, Hong S, Park N. Role of human epididymis protein 4 in chemoresistance and prognosis of epithelial ovarian cancer. J Obstet Gynecol Res 2017; 43: 220-7.

24. Plotti F, Scaletta G, Capriglione S *et al.* The Role of HE4, a novel biomarker, in predicting optimal cytoreduction after neoadjuvant chemotherapy in advanced ovarian cancer. Int J Gynecol Cancer 2017; 27: 696-702.

25. Singhal H, Bautista DS, Tonkin KS, O'Malley FP, Tuck AB, Chambers AF, Harris JF. Elevated plasma osteopontin in metastatic breast cancer associated with increased tumor burden and decreased survival. Clin Cancer Res 1997; 3:605-11.

26. Chiodoni C, Colombo MP, Sangaletti S. Matricellular proteins: from homeostasis to inflammation, cancer, and metastasis. Cancer Metastasis Rev 2010; 29:295-307.

27. Kluger HM, Hoyt K, Bacchiocchi A *et al*. Plasma markers for identifying patients with metastatic melanoma. Clin Cancer Res 2011; 17:2417-25.28. Bellahcène A, Castronovo V, Ogbureke KU, Fisher LW, Fedarko NS. Small integrin-binding ligand N-linked glycoproteins (SIBLINGs): multifunctional proteins in cancer. Nat Rev Cancer 2008; 8:212-26.

29. Chong HC, Tan CK, Huang RL, Tan NS. Matricellular proteins: a sticky affair with cancers. J Oncol 2012;2012:351089.

30. Crawford HC, Matrisian LM, Liaw L. Distinct roles of osteopontin in host defense activity and tumor survival during squamous cell carcinoma progression in vivo. Cancer Res 1998; 58:5206-15.

31. Bourassa B, Monaghan S, Rittling SR. Impaired anti-tumor cytotoxicity of macrophages from osteopontin-deficient mice. Cell Immunol 2004; 227:1-11.

32. Hsieh YH, Margaret Juliana M, Ho KJ, Kuo HC, van der Heyde H, Elmets C, Chang PL. Host-derived osteopontin maintains an acute inflammatory response to suppress early progression of extrinsic cancer cells. Int J Cancer 2012; 131:322-33.

33. Danzaki K, Kanayama M, Alcazar O, Shinohara ML. Osteopontin has a protective role in prostate tumor development in mice. Eur J Immunol 2016; 46: 2669-78.

34. Take Y, Nakata K, Hashimoto J, Tsuboi H, Nishimoto N, Ochi T, Yoshikawa H. Specifically modified osteopontin in rheumatoid arthritis fibroblast-like synoviocytes supports interaction with B cells and enhances production of interleukin-6. Arthritis Rheum 2009; 60: 3591-601.

35. Guo B, Tumang JR, Rothstein TL. B cell receptor crosstalk: B cells express osteopontin through the combined action of the alternate and classical BCR signaling pathways. Moll Immunol 2009; 46: 587-91.

36. Kon S, Nakayama Y, Matsumoto N *et al*. A novel cryptic binding motif, LRSKSRSFQVSDEQY, in the C-terminal fragment of MMP-3/7-cleaved osteopontin as a novel ligand for α9β1 integrin is involved in the anti-type II collagen antibody-induced arthritis. PLoS One 2014; 9: e116210.

Figure I.1 HE4 downregulates expression of OPN in PBMCs.

(A) Two-color flow cytometric analysis of PBMC following a 24-hour incubation with 0.01 μg / mL of rHE4 (HE4) or vehicle (CTR). 2D-scatterplots of OPN (Alexa Fluor 647) and CD3 (FITC) are shown. The numbers on the scatterplots represent mean ± SEM % of each quadrant. (B) OPN transcription in response to a 6-hour incubation with 0.01 μg / mL rHE4 (HE4) or vehicle (CTR) were evaluated by real time PCR. A bar graph represents relative expression levels against control. (C) OPN concentrations of PBMC lysates and culture supernatants after a 24-hour incubation with 0.01 μg / mL of rHE4 (HE4) or vehicle (CTR) were evaluated by ELISA. All the experiments were done with PBMCs from four individual donors and repeated 3 (A), 9 (B) and 10 (C) times. The mean is shown in the bar graphs; error bars represent SEM (n > 10). * $p < 0.05$, **$p < 0.01$.

Figure I.1
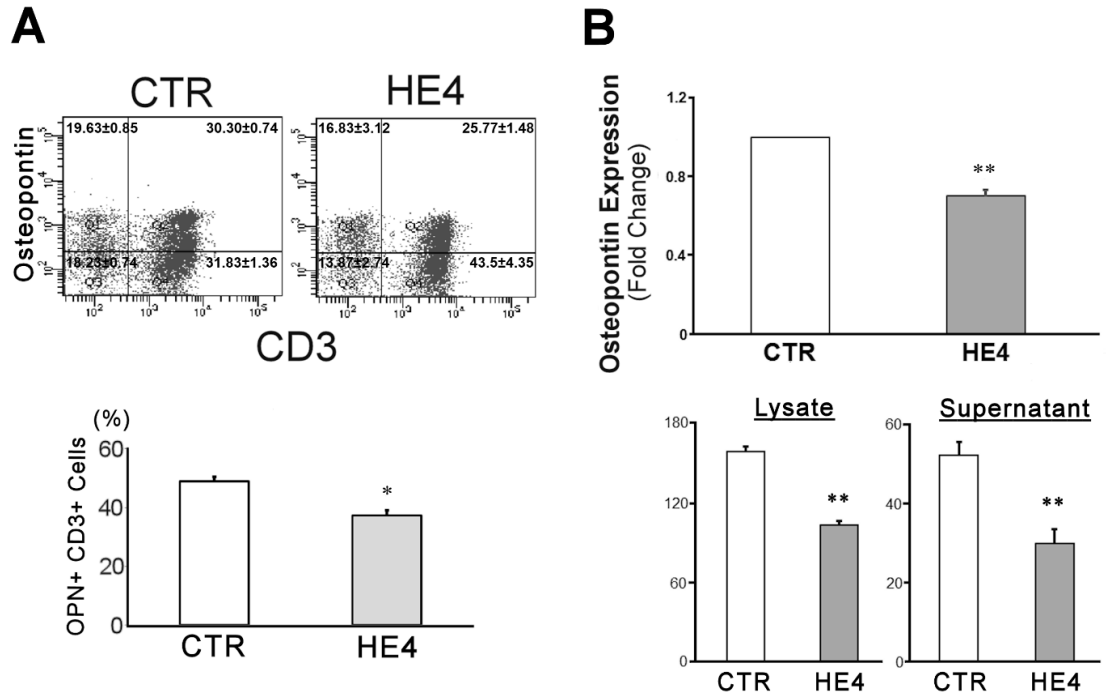
Figure I.2 HE4 suppresses expression and secretion of IL-12 and IFN-γ by PBMCs.
(A) PBMCs were incubated for 6 hours in serum free media under the indicated
conditions (vehicle, 0.01 μg / mL rHE4 and rHE4 + 20 pg / mL of rOPN). After a
6- hour incubation, transcription levels of IL-12B (p40) and IFN-γ were evaluated by
real time PCR. A bar graph represents relative expression levels against control. (B)
The concentrations of IL-12AB (p70) and IFN-γ in the cell lysates and the culture
supernatants from 24-h incubation under the same conditions were measured by
ELISA. All the qPCRs and ELISAs were done with PBMCs from four individual
donors. Each assay was repeated 4 times (qPCR) or 10 times (ELISA). The mean is
shown; error bars represent SEM. * $p < 0.01$.

Figure I.2
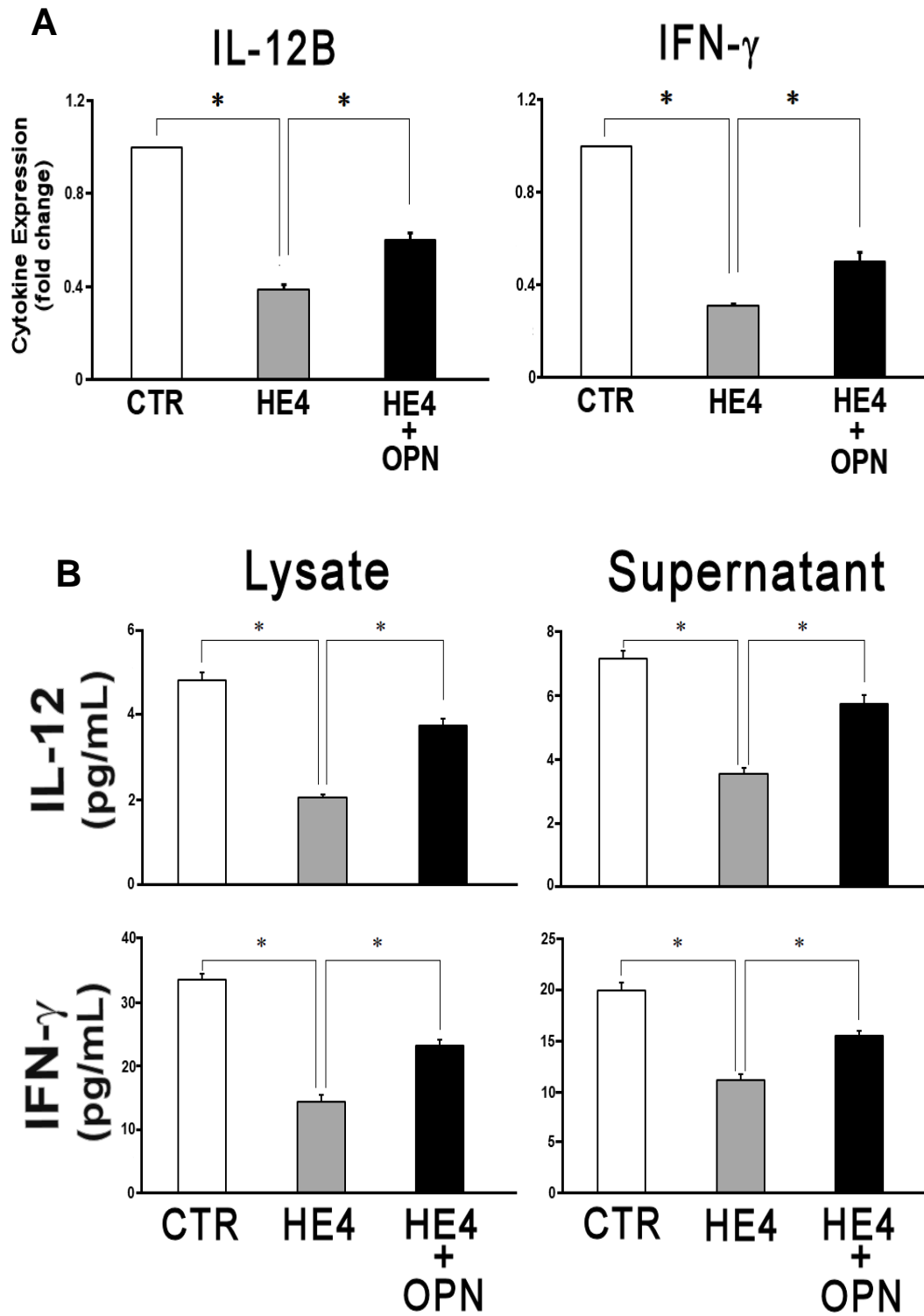
Figure I.3 Responses of SKOV3 and OVCAR8 human ovarian cancer cell lines to PBMC conditioned media.

(A) Cells were incubated with conditioned media from the PBMC culture treated with vehicle (blue line) or rHE4 (red line). The cell viabilities were assessed at 24, 48 and 72 hours after treatment (n = 10 for 0 hours, n = 8 for 24, 48 and 72 hours). (B) Cell migration activities with conditioned media were assessed at 24 hours of incubation (n = 10). (C) Ki67 immunohistochemistry staining was performed on SKOV3 / OVCAR8 cell lines incubated with the PBMC conditioned media for 24 hrs. Ki67$^+$ cells are identified with red nuclear staining (upper panel). Bar graph (lower panel) represents the percentage of Ki67$^+$ cells in total countable cells under 200x fields (n = 6). Scale bar: 50 μm. The mean is shown; error bars represent SEM (n = 10). * p < 0.05, ** p < 0.01.

84

Figure I.3

SKOV3 OVCAR8

A

B

C

Figure I.4 Flow cytometric analysis of the cytotoxicity of mononuclear cells against SKOV3 tumor cells.

Cell membranes of SKOV3 (target) cells were labeled with $DiOC18_{(3)}$ fluorescent dye and then incubated with PBMCs in the presence of propidium iodide (PI) as a marker of cell death. After washing away the non-adherent cells (PBMCs), the PI positive tumor cells were quantitated via flow cytometry (upper panel). The numbers on the histograms represent mean percentage of each bisection. The bar graph (lower panel) represents percentages of PI positive (dead / dying) cells in various culture conditions. The mean is shown; error bars represent SEM ($n > 10$). * $p < 0.01$, **$p < 0.05$.

Figure I.4
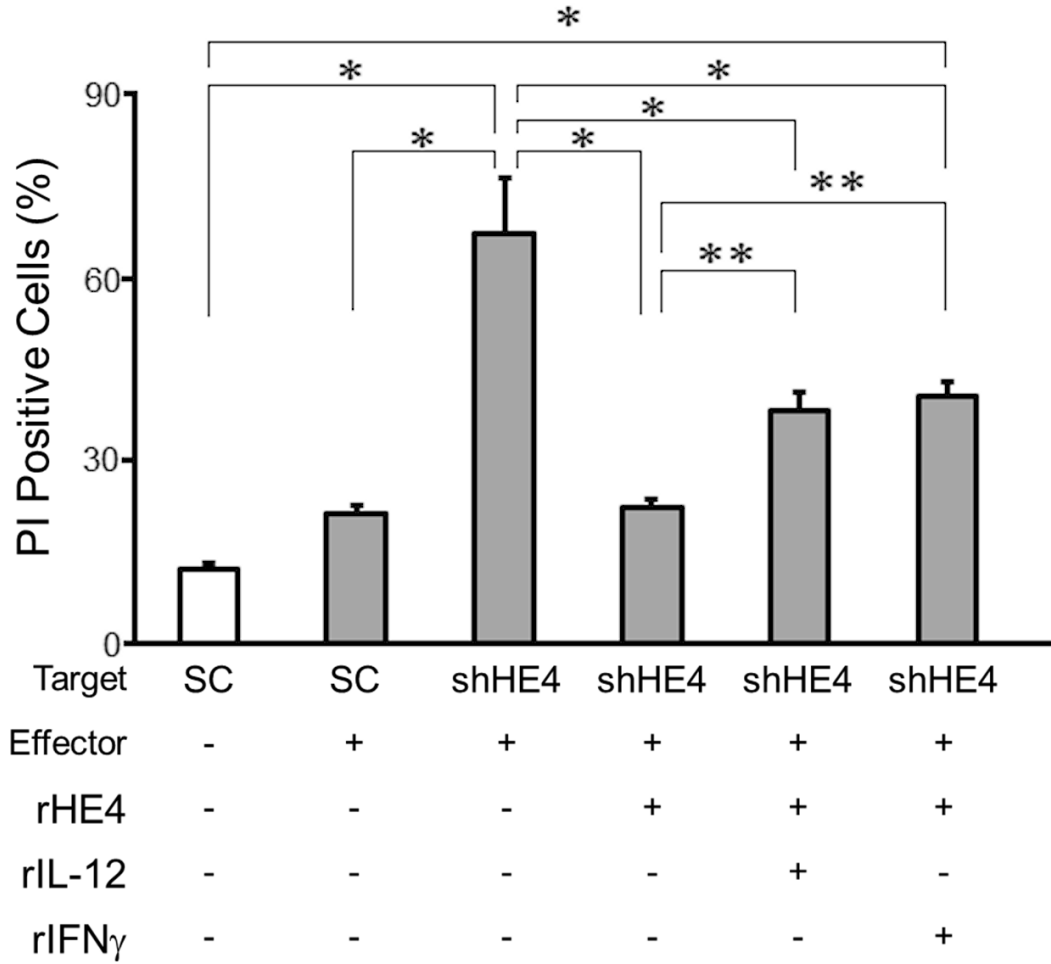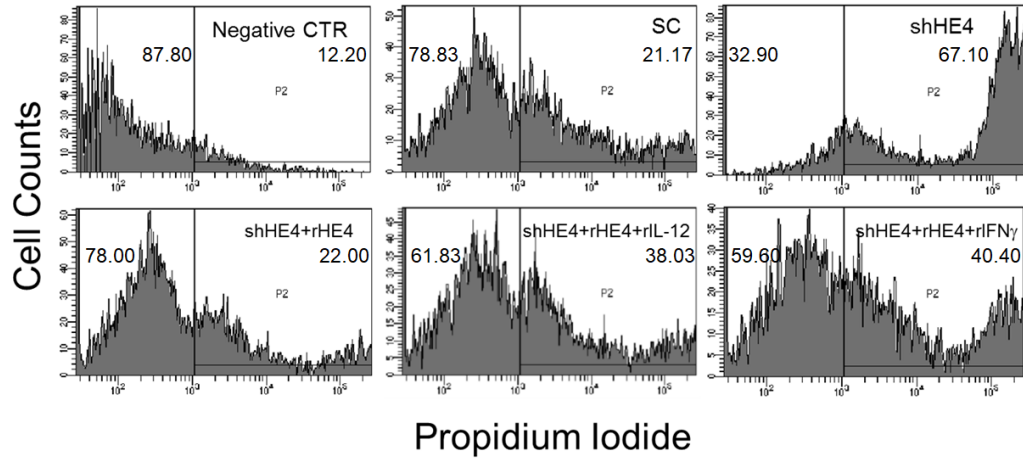
Figure I.5 Confocal immunofluorescent analysis of CD3 and OPN expression in biopsy samples.

Twenty biopsies (listed in Table 3) were evaluated. (A) Stromal and tumoral CD3+ cells and OPN+ tumor cells are indicated by arrowhead. A biopsy from a benign serous tumor (Benign) and an uninvolved section of oophorectomy (Normal) were utilized as a negative control (B). Enlarged image depicting image co-staining of stromal and tumoral CD3+/OPN+ T cells in their cytosol or the surrounding area (C, D). Graphic representations of Spearman's rank correlations between the numbers of CD3+ or OPN+ cells and clinical parameters. CR; corrected ranks.

Figure I.5

Figure I.5 a & b

Figure I.5 c & d

Table I. 1 Genes suppressed in response to HE4

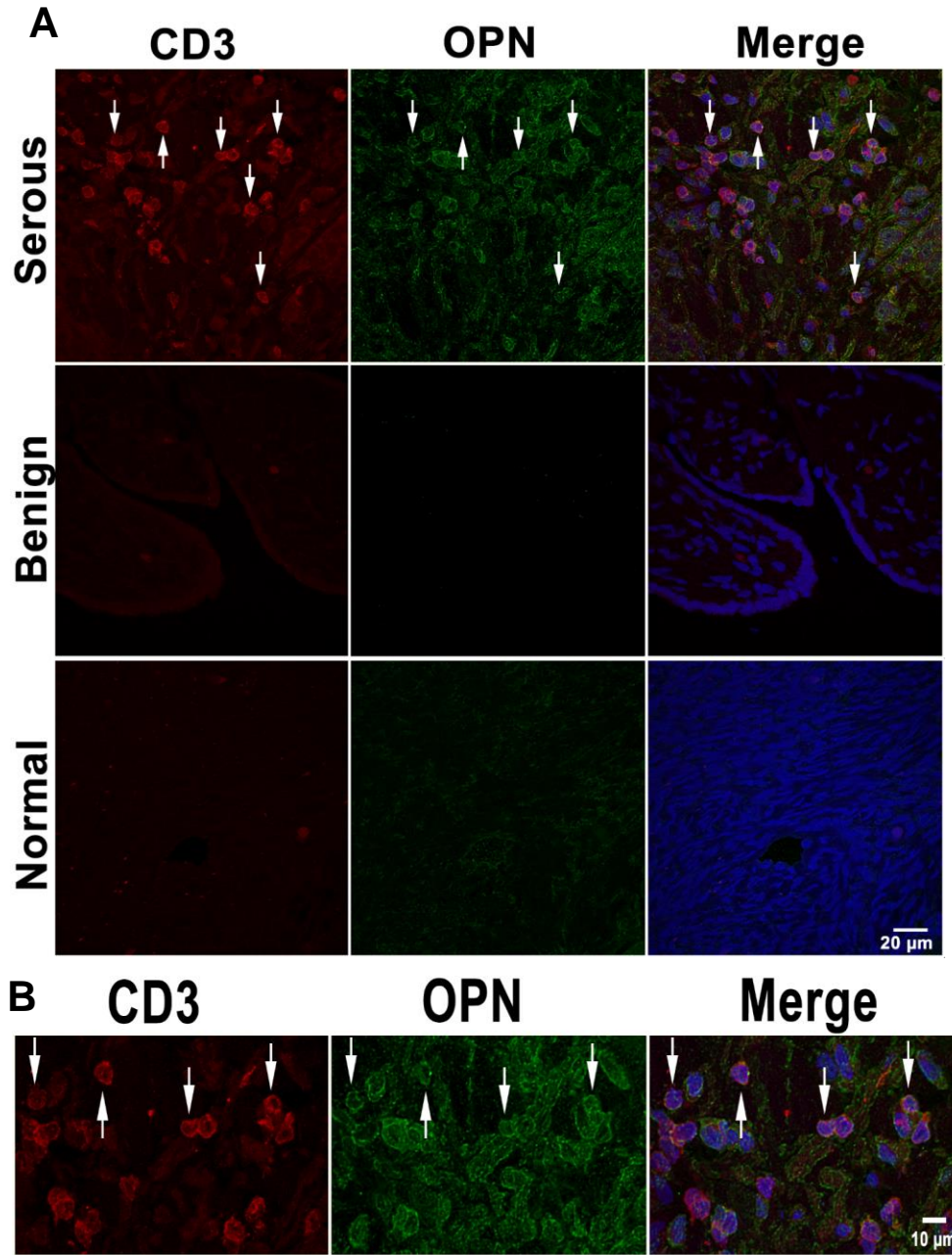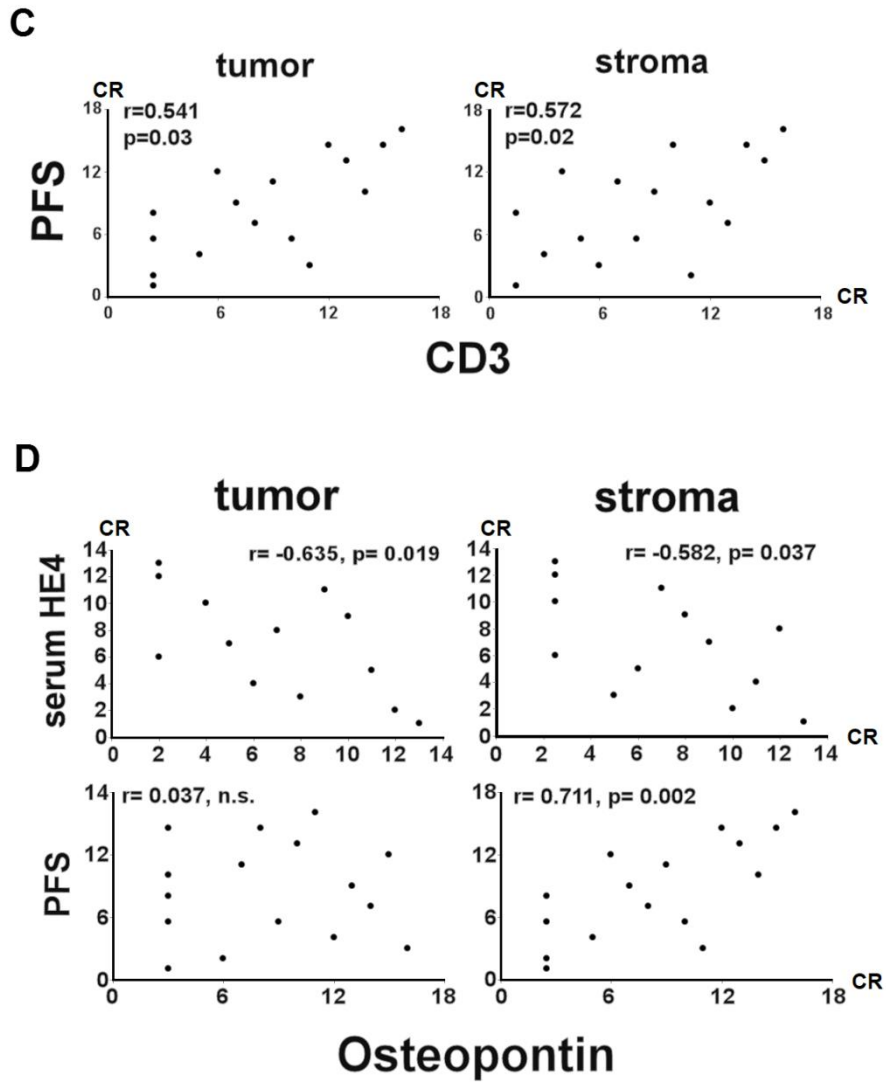| Frequency	ID	gene name
Genes suppressed in response to HE4		
Frequency	**ID**	**gene name**
15	NSS	no significant similarity
6	NM_001040058	secreted phosphoprotein 1 (SPP1), transcript variant 1
3	NM_015574	ankyrin repeat domain 17 (ANKRD17)
3	NM_001693	ATPase, H+ transporting, lysosomal 56/58kDa, V1 subunit B2 (ATP6V1B2)
3	NM_000206	interleukin 2 receptor subunit gamma (IL2RG)
3	NM_022818	microtubule-associated protein 1 light chain 3 beta (MAP1LC3B)
3	NM_001243121	phosphodiesterase 4A (PDE4A)
3	NM_080792	signal regulatory protein alpha (SIRPA)
3	NM_015131	WD repeat domain 43 (WDR43)
2	NM_001025604	arrestin domain containing 2 (ARRDC2)
2	NM_001164755	aspartate beta-hydroxylase (ASPH)
2	NM_032408	bromodomain adjacent to zinc finger domain, 1B (BAZ1B)
2	NM_002985	chemokine (C-C motif) ligand 5
2	AC132216	chromosome 11, clone RP13-786C16
2	NC_018926	chromosome 15, alternate assembly CHM1_1.1
2	NM_001291549	cyclin-dependent kinase inhibitor 1A (p21, Cip1) (CDKN1A)
2	NM_014280	DnaJ (Hsp40) homolog, subfamily C, member 8 (DNAJC8)
2	XM_011535514	eukaryotic translation elongation factor 1 alpha 1 (EEF1A1)
2	XM_011518416	family with sequence similarity 120A (FAM120A)
2	NM_020447	family with sequence similarity 219 member B (FAM219B)
2	NG_029887	golgin A3 (GOLGA3)
2	NM_002107	H3 histone, family 3A (H3F3A)
2	NM_001128619	leucine zipper protein 6 (LUZP6)
2	NM_002463	MX dynamin-like GTPase 2 (MX2)
2	NM_004687	myotubularin related protein 4 (MTMR4)
2	NM_001251855	phosphoinositide-3-kinase regulatory subunit 5 (PIK3R5)
2	NM_000437	platelet-activating factor acetylhydrolase 2, 40kDa (PAFAH2),
2	NR_049751	reticulon 3 (RTN3)
2	NM_001198719	retinoblastoma binding protein 7 (RBBP7)
2	NM_001028	ribosomal protein S25 (RPS25)
2	XM_011534644	serine/threonine kinase 10 (STK10)
2	NM_001242933	sorting nexin 1 (SNX1)
2	XR_241300	splicing factor 3b, subunit 1, 155kDa (SF3B1)
2	NM_181892	ubiquitin-conjugating enzyme E2D 3 (UBE2D3)
2	NM_006007	zinc finger, AN1-type domain 5 (ZFAND5)
1		159 genes

91

Table I. 2 Concentrations of IL-12, IFN-γ and HE4 in co-culture medium

Concentrations of IL-12, IFN-γ and HE4 in co-culture medium

Target	Effector	IL-12 (ng/mL)	INF-γ (ng/mL)	HE4 (pM)
SC	-	-	-	534.15±41.81
SC	+	14.84±0.48	177.20±1.07	639.01±50.38
shHE4	-	-	-	174.12±18.55*
shHE4	+	31.95±0.68**	417.74±3.54**	237.91±34.24**

SC; SKOV3 with scrambled oligo, shHE4; SKOV3 with
HE4 shRNA
mean ± SE is shown (n = 10)
*$p < 0.01$ vs. SC, **$p < 0.01$ vs.SC + Effector cells

Table I.3 Clinical Parameters of Donors

Table 3		
Clinical parameters of donors		
	pre-OP sHE4*	**PFS****
Sample ID	**(pmol/mL)**	**(months)**
S10-10110	174	10
S10-10726	na	16
S10-15910	na	25
S10-17790	376	12
S10-18470	529	22
S10-4387	462	31
S10-5618	na	9
S10-5842	na	na
S10-6697	150	na
S10-7183	1232	na
S11-1189	3289	8
S11-2223	550	28
S11-2493	591	37
S11-2684	3255	24
S11-3415	na	na
S11-622	na	38
S11-6675	4702	16
S11-6721	na	64
S11-7794	410	38
S11-8032	623	21
* pre-operation serum HE4		
** progression-free survival		
na; not available		

CHAPTER 4

MANUSCRIPT II

Submitted to Scandinavian Journal of Immunology, May 2018

HE4 Sabotages Cytotoxic Mononuclear Cells Inducing Dual Specificity

Phosphatase 6 Secretion

Nicole E. James[1,3*], Matthew T. Oliver[1*], Jennifer R.Ribeiro[1*], Evelyn Cantillo[1], Kim

KK[3], Rachel B. Roswell-Turner[2] Clinton O.Chichester [3], Paul A. DiSilvestro [1],Richard

G. Moore[2], Rakesh K.Singh[,2], Naohiro Yano[1**], Ting C.Zhao[4]

_____

[1] Division of Gynecologic Oncology, Program in Women's Oncology, Department of Obstetrics and Gynecology, Women and Infants Hospital, Providence, RI, United States

[2] Division of Gynecologic Oncology, Department of Obstetrics and Gynecology, Wilmot Cancer Institute, University of Rochester Medical Center, Rochester, NY 14642, United States

[3]Department of Biomedical and Pharmaceutical Sciences, University of Rhode Island, Kingston, RI, United States

[4]Department of Surgery, Roger Williams Medical Center, Boston University Medical School, Providence RI, United States

[*]N.James, M.Oliver , and J.Ribeiro contributed equally to this study

[**]Correspondence:
Naohiro Yano
naohiro.yano@CharterCARE.org

II.1 Abstract

Objective

Selective overexpression of Human epididymal secretory protein 4 (HE4) points to a role in ovarian cancer tumorigenesis but little is known about the role the HE4 gene or the gene product plays. Here we examine the role of the secretory glycoprotein HE4 in ovarian cancer immune evasion.

Methods

Through the modified subtractive hybridization analyses of human peripheral blood mononuclear cells (PBMCs), we have characterized gene targets of HE4 and established a preliminary mechanism of HE4-mediated immune failure in ovarian tumors.

Results

Dual specificity phosphatase 6 (DUSP6) emerged as the most upregulated gene in PBMCs upon *in vitro* exposure to HE4. CD8^{+} cells and CD56^{+} cells found to be sources of the upregulated DUSP6. The HE4 exposure enhanced Erk1/2 phosphorylation specifically in these cell populations and the effect was erased by co-incubation with DUSP6 inhibitor, (E)-2-benzylidene-3-(cyclohexylamino)-2,3-dihydro-1H-inden-1-one (BCI). In co-culture with PBMC, HE4-silenced SKOV3, a human ovarian carcinoma cell line, exhibited enhanced proliferation with exposure to the external HE4; this effect was partially attenuated by adding BCI to the culture. Additionally, the reversal effects of BCI were erased in the co-culture with CD8^{+} / CD56^{+} cell deprived PBMC.

95

Conclusion

Taken together, these findings show that DUSP6 is a suppressor of the cytotoxicity of the CD8$^+$ and CD56$^+$ lymphocytes and HE4 enhances tumorigenesis of ovarian cancer through the compromised cytotoxicity of the CD8$^+$ and CD56$^+$ cells by upregulation of self-produced DUSP6, which acts as an autocrine factor.

II.2 Introduction

Epithelial ovarian cancer (EOC) is the fifth leading cause of cancer death in women, and the deadliest gynecologic cancer. The American Cancer Society estimates that in 2017, there will be an estimated 22,440 new cases of EOC and 14,080 deaths in the United States [1]. Only 15% of patients are diagnosed at an early stage when the disease is fundamentally curable, keeping the 5-year survival rate at a dismal 46% [2]. Recurrence following initial treatment is common, occurring in approximately 80% of cases, and all patients with recurrent disease eventually succumb to their illness [3]. These dire statistics highlight the need for continued research into improved diagnostic and treatment options for EOC.

Despite continued efforts, there remains a lack of effective treatments for EOC. Standard first-line therapy consists of debulking surgery followed by taxane-platinum chemotherapy[3]. Other targeted therapies are also employed, including the antiangiogenic drug bevacizumab and the PARP inhibitor olaparib; however, these treatments have not led to an improvement in overall survival [4]. One promising new area of investigation lies in understanding how tumors develop immune tolerance and evade elimination by cytotoxic lymphocytes. Immune checkpoint molecules such as PD-1, CTLA4, TIM3, IDO, and others, suppress T cell activation and help tumor cells escape targeting and elimination by the immune system [5]. Nivolumab, a monoclonal antibody against PD-1, is expressed on T cells and suppresses their activation upon binding of its tumor cell associated ligands, PDL1/PDL2, has greatly improved survival for metastatic melanoma patients [6]. PD-1 has also been studied in relapsed platinum-resistant EOC; however, overall response rates for EOC do not exceed 15%

97

[7]. This inefficacy of immune checkpoint inhibitors is likely due to compensatory immune suppressive pathways [8,9], or activation of oncogenic pathways that promote immune tolerance [5]. Overall, we require a greater understanding of factors that contribute to immune evasion in EOC in order to develop treatments that reactivate the body's immune response to tumors.

Human epididymis protein-4 (HE4) is a member of the whey acidic four-disulfide core protein family [10]. It is elevated in tumor tissue and serum of EOC patients, and is used as part of the Risk of Ovarian Malignancy Algorithm (ROMA)—along with CA125 and menopausal status—for the diagnosis and management of EOC [11, 12]. ROMA shows greater sensitivity and specificity for the detection and monitoring of EOC than the Risk of Malignancy Index, which uses CA125, pelvic sonography, and menopausal status [12]. HE4 also has the advantage of presenting fewer false positives than CA125 in the case of benign gynecologic disorders [11, 13]. *In vitro* and *in vivo* studies have shown that HE4 promotes multiple aspects of ovarian cancer aggression, including growth and proliferation; invasion, migration, and adhesion; chemoresistance, and anti-estrogen resistance [14–23]. Clinically, patients with high levels of serum HE4 have greater chemoresistance and worse prognosis [22, 24–26]. We hypothesized that HE4 may also promote immune evasion in EOC. We began to test this hypothesis by determining HE4-mediated gene expression in peripheral blood mononuclear cells (PBMCs), and went on to evaluate the effect of HE4 and one of its targets, DUSP6, on immune cell function and cytotoxicity against ovarian cancer cells.

II.3 Methods

Subtractive hybridization and TA-cloning

5×10^7 PBMCs from single donor were suspended in 5 mL of serum free RPMI1640 medium (Invitrogen, 31800) and incubated with or without 0.01 μg/mL of rHE4 (Abcam, ab184603) for 6 hours. Then, total RNA was isolated using TRIzol™ Reagent (Invitrogen, 15596018). Next, mRNA was purified using Magnosphere™ UltraPure mRNA Purification Kit (Takara-Clontech, 9186). From the 5 μg of mRNA, subtractive cDNA libraries were constructed using PCR-Select™ cDNA Subtraction Kit (Takara-Clontech, 637401) following the manufacturer's protocols. PCR products of the differentially expressed genes were cloned into a pUC19-TA vector. Top 10 competent cells (Invitrogen, C404003) were transformed with the clones and were seeded on a Xgal/IPTG containing LB/ampicillin plates. The colonies of clones containing the inserts were selected by blue/white selection and were amplified by direct colony PCR using LA Taq® DNA polymerase (Takara-Clontech, RR002A) and M13 primers.

Cell culture

Primary human PBMCs were obtained under the auspices of Women & Infants Hospital IRB approval from total blood of four individual volunteer by density gradient centrifugation using Histopaque®-1077 (Sigma-Aldrich, 10771). The human ovarian tumor cell line, SKOV3, human NK cell line, NK-92MI, human T cell line, TALL-104 and H9 were obtained from ATCC (HTB-77, CRL-2408, CRL-11386 and HTB-176, respectively). RPMI1640 was used for culturing PBMC and lymphocyte

99

lines and DMEM (Invitrogen, 31600) were used for SKOV3. Conditioned media were obtained from a 24-hour PBMC culture. Residual rHE4 in the conditioned media was deprived as follows. Five mL of media was incubated with 10 μg (100 μL) of anti-human HE4 antibody (Santa Cruz Biotechnology, sc-293473) for 1 hour at 4 degrees. And then, 100 mL packed volume of protein G coated sepharose beads (GE Healthcare Life Science, 17061801) were added to the media and incubated for 4 hours at 4 degrees. After the incubation, the sepharose beads were removed by centrifugation and the supernatants were processed through sterile 0.2 μm pore syringe filter. For the cell-mediated cytotoxicity assay, 1×10^6 target cells (SKOV3) were seeded on 6-well plates, and then were incubated overnight with complete media. The next day, cells were placed in serum free media for another overnight incubation and then 5×10^6 / mL of the effector cells (PBMCs) were added to the quiescent target cells. After a 12-hour incubation, the effector cells were washed away and harvested target cells were stained with 1 μg / mL of propidium iodide with or without Alexa Fluor® 488 labeled annexin V (Invirogen, V13241). Some of the wells contained 0.01 μg/mL of rHE4 and 1 μM of DUSP6 inhibitor, (E)-2-benzylidene-3-(cyclohexylamino)-2,3-dihydro-1H-inden-1-one (BCI; Sigma-Aldrich, B4313). All experiments were performed under serum free condition.

Flow cytometry

FITC-labeled anti CD3, CD4, CD8, CD14, CD19 and CD56 antibodies were obtained from BD Biosciences (555916, 561005, 560960, 555397, 555412 and 562794, respectively). Alexa Fluor® 647-conjugated anti DUSP6 antibody was obtained from

Abcam (ab200751). Alexa Fluor® 647-conjugated anti phosphor-p44/42 MAPK antibody was obtained from Cell Signaling Technology (13148). After staining for cell surface markers (CD3, CD14, CD19 and CD56) the cell membrane was permeabilized by 0.2 % Triton X-100 and 0.2 % digitonin, and then stained for DUSP6 or phosphor-p44/42-MAPK. Flow cytometric analysis was performed with FACSCanto system and FACSDiva software (BD Biosciences).

Quantitative Real-Time PCR

RNA was isolated from cells using TRIzol (Invitrogen, A33250) according to the manufacturer's instructions. cDNA was synthesized using SuperScript III reverse transcriptase (Invitrogen, 18080093). qPCR was performed using Premix Ex-Taq^{TM} II (Clontech-Takara, 639676) probes for DUSP6. All reactions were normalized using GAPDH as an endogenous control. Amplification data were analyzed using the ΔΔCt method.

ELISA

ELISA kits for HE4 and DUSP6 were obtained from MyBioSource (MBS280223 and MBS073193, respectively). The assays were performed following the manufacturer's instruction.

Western blotting

Phosphorylation of Erk1/2 in NK-92MI, TALL-104 and H9 cell lines were assessed by western blotting. Antibodies against phosphorylated and total Erk1/2 MAPK were

101

obtained from Cell Signaling Technology (9101 and 4695). The results were visualized with SuperSignal™ West Pico chemiluminescent substrate (ThermoFisher Scientifics, 34080) and analyzed with the UN-SCAN-IT gel software for Windows (Silk Scientific Inc.).

HE4 silencing with shRNA

shRNA for human HE4 (Origene, TR318721) were transfected into SKOV3 using Lipofectamine® 2000 (Invitrogen, 11668) following the manufacture's instruction. Individual single cells were selected by culturing under the pressure of 5 μg / mL of puromycin (Research Products International, 58-58-2).

Cell viability assay

1×10^3 / well SKOV3 cells were seeded in a 96-well culture plate. After overnight incubation with serum free medium, 5×10^6 /mL of effector cells (PBMCs) were added to the quiescent cells. The cell viabilities were evaluated at 24, 48 and 72 hours using fluorescent based CEllTiter-Blue® (Promega, G8080) and Spectra Max Gemini EM fluorescent micro plate reader (Molecular Devices).

Immunohistochemistry

0.5×10^4 / chamber of SKOV3 cells were seeded in a 4-chamber slide. After overnight incubation with serum free medium, 5×10^6 /mL of effector cells (PBMCs) were added to the quiescent cells and the cells were cultured for 48 hrs. Ki67 positive cells were counted in twenty of 200x fields. A mouse anti-Ki67 monoclonal antibody was

102

purchased from BD Biosciences (550609). An alkaline phosphatase (ALP) labeled anti-mouse IgG secondary antibody and an ALP substrate kit were obtained from Vector laboratories (AP-2000, SK-5100).

Depletion of $CD8^+$ and $CD56^+$ cells from PBMCs

$CD8^+$ and $CD56^+$ cells were removed from PBMC using magnetic CD8 and CD56 MicroBeads (Miltenyi Biotec, 130-045-201 and 130-050-401) with autoMACS cell separator (Miltenyi Biotec, 130-092-545). Briefly, 5×10^7 of PBMC was suspended in 60 μL of separation buffer (PBS, pH 7.2 with 0.5 % BSA and 2 mM EDTA), and then, 20 μL each of CD8 and CD56 MicroBeads were added to it, followed by 15 minutes incubation at 4 degrees. After washing, resuspended the cells in 500 μL of the separation buffer and proceed to magnetic separation using autoMACS® Columns (Miltenyi Biotec, 130-021-101). Unlabeled cells that pass through were collected and combined with total effluent from washed column.

Statistics

Data ware expressed as average ± SEM of at least four independent experiments. An unpaired, two-tailed Student t-test was used to determine significance. Multiple treatments were analyzed by using one-way ANOVA followed by Ryan's multiple comparison test. Differences between groups were considered statistically significant when $p < 0.05$.

III.4 Results

Differential expression of PBMC genes after HE4 exposure

To identify differentially expressed genes after HE4 exposure, modified subtractive hybridization was performed. PCR products of the differentially expressed genes were cloned into pUC19-TA vectors to create a differential cDNA library. PCR products from 250 each of HE4-induced and HE4-suppressed gene colonies were sequenced resulting in the identification of 209 induced genes and 206 suppressed genes. Among the identified genes, 20 induced and 13 suppressed sequences showed no significant similarity (NSS) to known genes in available nucleotide databases. Among the 209 induced genes, dual specificity phosphatase 6 (DUSP6) emerged as one of the most frequently identified genes (3 times out of 250 sequences, 1.2%; Table 1).

HE4 induces DUSP6 expression in PBMCs

HE4-induced upregulation of DUSP6 in PBMCs was then confirmed via three modalities: quantitative PCR (qPCR), ELISA and flow cytometry. First, PBMCs were harvested after a 6-hour exposure with recombinant human HE4 (rHE4; 0.01μg/mL), revealing a 1.60 ± 0.13-fold increase ($p < 0.01$) in DUSP6 mRNA production (Figure 1A). The concentrations of DUSP6 in PBMC lysates (9.38 ± 0.62 vs 15.62 ± 0.97 ng/mL, $p < 0.01$) and culture supernatants (0.77 ± 0.10 vs 1.43 ± 0.14 ng / mL, $p < 0.01$) after a 24-hour exposure to rHE4 were also increased (Table 2). PBMCs were then cultured with rHE4 for 24 hours and collected for flow cytometry analysis. Protein expression of DUSP6 in CD3$^+$ PBMCs (T cells) was found to be significantly increased with HE4 exposure (34.4 ± 0.6 % vs 47.0 ± 3.2 % of total CD3$^+$ cells; $p <$

104

0.05; Figure 1B left panel). The DUSP6 expression in CD56$^+$ cells (NK/T cells, NK cells) was also increased to a lesser extent (34.1 $\pm$ 2.3 % vs 41.7 $\pm$ 1.7 % of total CD56$^+$ cells; $p < 0.05$; Figure 1B right panel). In order to identify a T cell subset involved in the HE4 responsive induction of DUSP6, two-color flow cytometry using anti-DUSP6 antibody and anti-CD4 (helper T cell) or CD8 (cytotoxic T cell) antibodies were performed. As shown in Figure 2, after a 24-hour exposure to rHE4, CD8$^+$ T cells (9.9 $\pm$ 0.8 % vs 1.9 $\pm$ 0.1 %; $p < 0.01$) but not CD4$^+$ T cells (15.6 $\pm$ 1.4 % vs 15.4 $\pm$ 1.5 %) showed significant DUSP6 induction. These finding suggested that the CD8$^+$ and CD56$^+$ cytotoxic mononuclear cells were responsible for the HE4 responsive DUSP6 induction.

CD8$^+$ and CD56$^+$ cytotoxic lymphocytes are targets of HE4 induced DUSP6

In order to identify effector cells for the HE4 induced DUSP6, two-color flow cytometry using antibodies against phosphor-Erk1/2 (pErk1/2) and CD4, CD8, CD14, CD19 and CD56 were performed. Significant decreases of pErk1/2$^+$ populations were observed in CD8$^+$ (30.2 $\pm$ 2.4 % vs 4.3 $\pm$ 0.2 % in total CD8$^+$ cells; $p < 0.01$) and CD56$^+$ (32.3 $\pm$ 4.0 % vs 5.4 $\pm$ 0.6 % in total CD56$^+$ cells; $p < 0.01$) cells after a 24 hours rHE4 (0.01 µg/mL) exposure, and the decreases were abrogated by co-treatment with 1 µM of DUSP6 inhibitor, (E)-2-benzylidene-3-(cyclohexylamino)-2,3-dihydro-1H-inden-1-one (BCI) in both CD8$^+$ cells and CD56$^+$ cells (23.3 $\pm$ 0.7 % and 30.5 $\pm$ 2.6 %, respectively; Figure 3A). Next, CD56$^+$ NK cell line (NK92MI), CD8$^+$ cytotoxic T cell line (TALL-104) and CD4$^+$ helper T cell line (H9) were incubated with the conditioned media from a 24- hour PBMC culture with or without rHE4 and BCI for 1

105

hour. The lysates of the cells were used for western blotting to evaluate Erk1/2 phosphorylation. As shown in Figure 3B, 1-hour incubation with the HE4 exposed PBMC conditioned media suppressed Erk1/2 phosphorylation in NK92MI cell (0.67 ± 0.07-fold vs CTR, $p < 0.01$) and TALL-104 cell (0.56 ± 0.10-fold vs CTR, $p < 0.01$) but not in H9 cell (1.01 ± 0.03-fold vs CTR). The rHE4 responsive pErk1/2 suppressions were abrogated by the PBMC conditioned media from co treatment with rHE4 and BCI in both NK92MI (0.90 ± 0.04-fold vs CTR) and TALL-104 (0.89 ± 0.06-fold vs CTR). These findings suggested that the HE4 induced DUSP6 acts as an autocrine suppressor for Erk1/2 MAPK in CD8^{+} and CD56^{+} cytotoxic lymphocytes.

HE4 attenuates ovarian cancer susceptibility to PBMC mediated cytotoxicity

In order to evaluate the impact of HE4 on PBMC cytotoxicity against cancer cells, the human ovarian tumor cell line, SKOV3, was co-cultured with PBMCs (5×10^6 / mL density). To minimize the effect of native HE4 produced by tumor cell, the SKOV3 cells were stably transfected with HE4 specific shRNA (shHE4). The effector cells (PBMCs) were washed away, and the target cells (SKOV3) were analyzed by three independent modalities: cell viability, Ki67 immunostaining, and flow cytometry for propidium iodide (PI) and annexin V. First, SKOV3 cells co-cultured with PBMC suspensions containing 0.01 μg/mL of rHE4 showed significantly higher viability than cells cultured with the rHE4 free suspensions at 24 (1222.70 ± 29.48 vs. 1517.98 ± 34.32, $p < 0.01$), 48 (2038.38 ± 55.94 vs. 3508.64 ± 164.98, $p < 0.01$) and 72 hours (1983.33 ± 100.41 vs. 2935.89 ± 116.47, $p < 0.01$), and the increased viabilities were partially abrogated by adding 1 μM of BCI to the culture (1295.68 ± 39.87, $2667.27 \pm$

106

95.13 and 2424.50 ± 105.70, at 24, 48 and 72 hours, respectively; Figure 4A). Second, immunohistochemistry using anti-Ki67 was performed to evaluate the proliferation activities of SKOV3 cells in the presence of PBMCs with or without rHE4 and BCI for 24 hours. The number of Ki67 positive tumor cells in rHE4-containing PBMC suspension was higher than the cells in rHE4-free suspension, and the increased activity was partially attenuated by adding BCI to the culture (27.6 ± 1.7 %, 68.5 ± 2.6 % and 48.9 ± 2.3 %, respectively; Figure 4B). Finally, after a 6 -hour incubation at 37 degrees, the effector cells were washed away and the target cells were analyzed by 2-color flow cytometry using PI and Alexa Fluor® 488 labeled annexin V. As shown in Figure 4C, SKOV3 / PBMC co-cultures with rHE4 led to a significant decrease in populations of PI / annexin v double positive dying cells (24.3 ± 1.2 % vs. 13.4 ± 0.8 %, $p < 0.01$), and the tolerance of the target cells was partially reversed by adding BCI to the culture (18.1 ± 0.6 %, $p < 0.01$ vs. CTR and HE4). These findings suggest that HE4 enhances tolerance of cancer cells against immunocompetent mononuclear cells via up-regulation of DUSP6 in PBMCs. In order to confirm involvement of CD8^{+} / CD56^{+} cytotoxic lymphocytes in the HE4 induced immunomodulation, the co-culture study was repeated using PBMCs deprived of CD8^{+} / CD56^{+} cells. As shown in Figure 5A-C, all the effects of BCI shown in Figure 4 were erased in the CD8^{+} / CD56^{+} cell free co-cultures, suggesting that the cytotoxic lymphocytes play a pivotal role in the immunoediting by DUSP6 up-regulation in response to exposure to HE4.

II.5 Discussion

Several studies from our laboratory and elsewhere have revealed multidimensional roles for HE4 in the pathogenesis of ovarian cancer, including the promotion of tumor growth, chemoresistance, anti-estrogen resistance, invasion, migration, and adhesion [14–23]. In this present study, we have begun to delineate another vital function of HE4 in disrupting immune cell function, which has implications for immune system targeting of tumor cells. DUSP6, which we found to be upregulated by rHE4 treatment in CD8^{+} T cells and CD56^{+} NK cell subsets of PBMCs, is likely one key mediator of this effect in these immune cell subsets.

DUSP6 is a member of the DUSP family that dephosphorylates threonine and tyrosine residues on MAPK substrates. It specifically dephosphorylates ERK, a member of the MAPK family that also includes p38 and JNK. MAPKs are activated by growth factors, cytokines, integrin ligands, and stress signals to regulate growth, survival, apoptosis, and immune response in diverse cell types. Interestingly, DUSP6 is expressed at low levels in resting cells and is actually stimulated by ERK activation, promoting a negative feedback loop on ERK activity [27]. This early response of DUSP6 to ERK activation could explain the apparently contradictory activation of ERK by HE4 in cancer cells [14, 16, 17, 23] and our results showing that HE4 upregulation of DUSP6 expression leads to suppression of ERK phosphorylation in PBMC subsets.

Several reports reveal a role for DUSP6 in development, organogenesis, and cancer [27]. However, its effect on cancer progression is highly dependent upon the type of cancer and even the stage. For example, in pancreatic cancer, it is upregulated in early

108

stages but is often completely diminished as the tumor progresses towards the invasive ductal carcinoma state [28]. In lung cancer, it has been shown to act as a tumor suppressor [29]. Conversely, it is upregulated in glioblastoma and HER2-positive breast cancer [30, 31]. One report found that its downregulation in ovarian cancer results in hyperactivation of ERK and subsequent chemoresistance [32]. These discrepancies are likely due to variable deregulation of ERK signaling and compensatory pathways that are highly context dependent [27]. In contrast to the roles of the tumor producing DUSP6 on the tumorigenesis, the functions of DUSP6 originated from immune cells have rarely been evaluated.

Even less is known regarding the role of DUSP6 in immune cell function. Other members of the DUSP family, including DUSP1, DUSP2, and DUSP10, are known to have roles in immune response [27], and a few reports suggest that DUSP6 does as well. Elevated DUSP6 was shown to cause downregulation of ERK phosphorylation in CD4$^+$ T cells in elderly individuals, who have suppressed immune responses [33]. Another report confirmed this age associated rise in CD4$^+$ T cell DUSP6 expression, and found that young immunosuppressed patients with end stage renal disease have DUSP6 levels comparable to elderly healthy individuals [34]. One study found that DUSP6 downregulates ERK activity in CD4$^+$ T cells and increases their regulatory T cell functions [35]. Together, these reports suggest that higher levels of DUSP6 contribute to immune suppression. It has also been shown that DUSP6 is downregulated in T cells upon IL-2 withdrawal [36], and IL-2 was found to upregulate DUSP6 gene expression in T cells [37]. Since IL-2 stimulates cytotoxic T cell expansion and activation as well as that of immune suppressive regulatory T cells

[38], it remains to be determined how the IL-2 responsiveness of DUSP6 plays into its apparent effect on immune suppression, and how this relates to tumor immune response.

Although much remains unknown regarding the specific effects of DUSP6 on cancer progression and tumor immunity, our findings begin to reveal some novel insights. We report for the first time that HE4-mediated upregulation of DUSP6 in CD8$^+$ T cell and CD56$^+$ NK cell subsets of PBMC cells leads to the inhibition of their cytotoxic activity against SKOV3 ovarian cancer cells. While DUSP6 has been connected to immune function of CD4$^+$ T cells, our results reveal that the subsets of lymphocytes affected by DUSP6 are context dependent. Further investigation into the inhibitory effects of DUSP6 in these different populations will be illuminating. Moreover, we have begun to establish HE4 as a critical regulator of immune cell function, which deepens our understanding of the mechanistic role HE4 plays in ovarian cancer pathogenesis.

II.6 References

1. What are the key statistics about ovarian cancer?

   https://www.cacer.org/cancer/ovarian-cancer

2. SEER Cancer Statistics Review, 1975-2014 National Cancer Institute

   https://seer.cancer.gov/csr/1975_2014/.

3. Kim A, Ueda Y, Naka T, Enomoto T. Therapeutic strategies in epithelial ovarian cancer. J Exp Clin Cancer Res. 2012, 31:14. doi: 10.1186/1756-9966-31-14.

4. Yap TA, Carden CP, Kaye SB. Beyond chemotherapy: targeted therapies in ovarian cancer. Nat Rev Cancer. 2009;9:167-81.

5. Zhao X, Subramanian S. Oncogenic pathways that affect antitumor immune response and immune checkpoint blockade therapy. Pharmacol Ther. 2018;181:76-84.

6. Volpe VO, Klufas DM, Hegde U, Grant-Kels JM. The new paradigm of systemic therapies for metastatic melanoma. J Am Acad Dermatol. 2017;77:356-68.

7. Mittica G, Genta S, Aglietta M, Valabrega G. Immune checkpoint inhibitors: A new opportunity in the treatment of ovarian cancer? Int J Mol Sci. 2016;17(7). pii: E1169. doi: 10.3390/ijms17071169.

8. Holmgaard RB, Zamarin D, Munn DH, Wolchok JD, Allison JP. Indoleamine 2,3-dioxygenase is a critical resistance mechanism in antitumor T cell immunotherapy targeting CTLA-4. J Exp Med. 2013;210:1389-402.

9. Curran MA, Montalvo W, Yagita H, Allison JP. PD-1 and CTLA-4 combination blockade expands infiltrating T cells and reduces regulatory T and myeloid cells within B16 melanoma tumors. Proc Natl Acad Sci USA. 2010;107:4275-80.

10. Bingle L, Singleton V, Bingle CD. The putative ovarian tumour marker gene HE4 (WFDC2), is expressed in normal tissues and undergoes complex alternative splicing to yield multiple protein isoforms. Oncogene. 2002;21:2768–73.

11. Heliström I, Raycraft J, Hayden-Ledbetter M, Ledbetter JA, Schummer M, McIntosh M, Drescher C, Urban N, Hellström KE. The HE4 (WFDC2) protein is a biomarker for ovarian carcinoma. Cancer Res. 2003;63:3695–700.

12. Moore RG, McMeekin DS, Brown AK, DiSilvestro P, Miller MC, Allard WJ, Gajewski W, Kurman R, Bast RC, Skates SJ. A novel multiple marker bioassay utilizing HE4 and CA125 for the prediction of ovarian cancer in patients with a pelvic mass. Gynecol Oncol. 2009;112:40-6.

13. Moore RG, Miller MC, Steinhoff MM, Skates SJ, Lu KH, Lambert-Messerlian G, Bast RC. Serum HE4 levels are less frequently elevated than CA125 in women with benign gynecologic disorders. Am J Obstet Gynecol. 2012;206:351.e1-8.

14. Lu R, Sun X, Xiao R, Zhou L, Gao X, Guo L. Human epididymis protein 4 (HE4) plays a key role in ovarian cancer cell adhesion and motility. Biochem Biophys Res Commun. 2012;419:274-80.

15. Lokich E, Singh RK, Han A, Romano N, Yano N, Kim K, Moore RG. HE4 expression is associated with hormonal elements and mediated by importin-dependent nuclear translocation. Sci Rep. 2014;4:5500. doi: 10.1038/srep05500.

16. Lee S, Choi S, Lee Y, Chung D, Hong S, Park N. Role of human epididymis protein 4 in chemoresistance and prognosis of epithelial ovarian cancer. J Obs Gynaecol Res. 2017;43:220-7.

17. Ribeiro JR, Schorl C, Yano N, Romano N, Kim KK, Singh RK, Moore RG. HE4 promotes collateral resistance to cisplatin and paclitaxel in ovarian cancer cells. J Ovarian Res. 2016;9:28.

18. Zhuang H, Hu Z, Tan M, Zhu L, Liu J, Liu D, Yan L, Lin B. Overexpression of Lewis y antigen promotes human epididymis protein 4-mediated invasion and metastasis of ovarian cancer cells. Biochimie. 2014;105:91-8.

19. Zhu L, Zhuang H, Wang H, Tan M, Schwab CL, Deng L, Gao J, Hao Y, Li X, Gao S, et al. Overexpression of HE4 (human epididymis protein 4) enhances proliferation, invasion and metastasis of ovarian cancer. Oncotarget. 2016;7:729-44.

20. Zhuang H, Gao J, Hu Z, Liu J, Liu D, Lin B. Co-Expression of Lewis y Antigen with Human Epididymis Protein 4 in Ovarian Epithelial Carcinoma. PLoS One. 2013;8(7):e68994. doi: 10.1371/journal.pone.0068994.

21. Wang H, Zhu L, Gao J, Hu Z, Lin B. Promotive role of recombinant HE4 protein in proliferation and carboplatin resistance in ovarian cancer cells. Oncol Rep. 2015;33:403-12.

22. Moore RG, Hill EK, Horan T, Yano N, Kim K, MacLaughlan S, Lambert-Messerlian G, Tseng YD, Padbury JF, Miller MC, et al. HE4 (WFDC2) gene overexpression promotes ovarian tumor growth. Sci Rep. 2014;4:3574. doi: 10.1038/srep03574.

23. Zhu YF, Gao GL, Tang S-B, Zhang Z-D, Huang Q-S. Effect of WFDC 2 silencing on the proliferation, motility and invasion of human serous ovarian cancer cells in vitro. Asian Pac J Trop Med. 2013;6:265-72.

24. Angioli R, Capriglione S, Aloisi A, Guzzo F, Luvero D, Miranda A, Damiani P, Montera R, Terranova C, Plotti F. Can HE4 predict platinum response during first-line chemotherapy in ovarian cancer? Tumor Biol. 2014;35:7009-15.

25. Chudecka-Głaz AM, Cymbaluk-Płoska AA, Menkiszak JL, Sompolska-Rzechuła AM, Tołoczko-Grabarek AI, Rzepka-Górska IA. Serum HE4, CA125, YKL-40, bcl-2, cathepsin-L and prediction optimal debulking surgery, response to chemotherapy in ovarian cancer. J Ovarian Res. 2014;7:62. doi: 10.1186/1757-2215-7-62.

26. Vallius T, Hynninen J, Auranen A, Carpén O, Matomäki J, Oksa S, Virtanen J, Grénman S. Serum HE4 and CA125 as predictors of response and outcome during neoadjuvant chemotherapy of advanced high-grade serous ovarian cancer. Tumour Biol. 2014;35:12389-95.

27. Bermudez O, Pagès G, Gimond C. The dual-specificity MAP kinase phosphatases: critical roles in development and cancer. Am J Physiol Cell Physiol. 2010;299:C189-202.

28. Furukawa T, Fujisaki R, Yoshida Y, Kanai N, Sunamura M, Abe T, Takeda K, Matsuno S, Horii A: Distinct progression pathways involving the dysfunction of DUSP6/MKP-3 in pancreatic intraepithelial neoplasia and intraductal papillary-mucinous neoplasms of the pancreas. Mod Pathol. 2005;18:1034-42.

29. Okudela K, Yazawa T, Woo T, Sakaeda M, Ishii J, Mitsui H, Shimoyamada H, Sato H, Tajiri M, Ogawa N, et al. Down-regulation of DUSP6 expression in lung cancer: its mechanism and potential role in carcinogenesis. Am J Pathol. 2009;175:867-81.

114

30. Messina S, Frati L, Leonetti C, Zuchegna C, Di Zazzo E, Calogero A, Porcellini A. Dual-specificity phosphatase DUSP6 has tumor-promoting properties in human glioblastomas. Oncogene. 2011;30:3813-20.

31. Lucci MA, Orlandi R, Triulzi T, Tagliabue E, Balsari A, Villa-Moruzzi E. Expression profile of tyrosine phosphatases in HER2 breast cancer cells and tumors. Cell Oncol. 2010;32:61-372.

32. Chan DW, Liu VW, Tsao GS, Yao KM, Furukawa T, Chan KK, Ngan HY. Loss of MKP3 mediated by oxidative stress enhances tumorigenicity and chemoresistance of ovarian cancer cells. Carcinogenesis. 2008;29:1742-50.

33. Li G, Yu M, Lee W-W, Tsang M, Krishnan E, Weyand CM, Goronzy JJ. Decline in miR-181a expression with age impairs T cell receptor sensitivity by increasing DUSP6 activity. Nat Med. 2012;18:1518-24.

34. Huang L, Litjens NH, Kannegieter NM, Klepper M, Baan CC, Betjes MG. pERK-dependent defective TCR-mediated activation of CD4+ T cells in end-stage renal disease patients. Immun Ageing. 2017;14:14. doi: 10.1186/s12979-017-0096-1.

35. Bertin S, Lozano-Ruiz B, Bachiller V, García-Martínez I, Herdman S, Zapater P, Francés R, Such J, Lee J, Raz E, et al. Dual-specificity phosphatase 6 regulates CD4+ T-cell functions and restrains spontaneous colitis in IL-10-deficient mice. Mucosal Immunol. 2015;8:505-15.

36. Chechlinska M, Siwicki JK, Gos M, Oczko-Wojciechowska M, Jarzab M, Pfeifer A, Jarzab B, Steffen J. Molecular signature of cell cycle exit induced in human T lymphoblasts by IL-2 withdrawal. BMC Genomics. 2009;10:261. doi: 10.1186/1471-2164-10-261.

115

37. Kovanen PE, Young L, Al-Shami A, Rovella V, Pise-Masison CA, Radonovich MF, Powell J, Fu J, Brady JN, Munson PJ, et al. Global analysis of IL-2 target genes: Identification of chromosomal clusters of expressed genes. Int Immunol. 2005;17:1009-21.

38. Boyman O, Sprent J. The role of interleukin-2 during homeostasis and activation of the immune system. Nat Rev Immunol. 2012;12:180-90.

Figure II.1 HE4 upregulates expression of DUSP6 in PBMCs.

(A) DUSP6 transcription in response to a 6-hour incubation with 0.01 µg/mL rHE4 (HE4) or vehicle (CTR) were evaluated by triplicated trials of real time PCR using PBMCs from four individual donors. (B) Two-color flow cytometric analysis of PBMC following 24-hr incubation with 0.01 µg/mL of rHE4 (HE4) or vehicle (CTR). 2D-scatterplots (upper panel) of DUSP6 (Alexa Fluor 647) and CD3 or CD56 (FITC) are shown. The lower panel shows bar graph from flow cytometric analyses using PBMCs from four individual donors. The mean ± SEM are shown. *p<0.05.

Fig. II.1
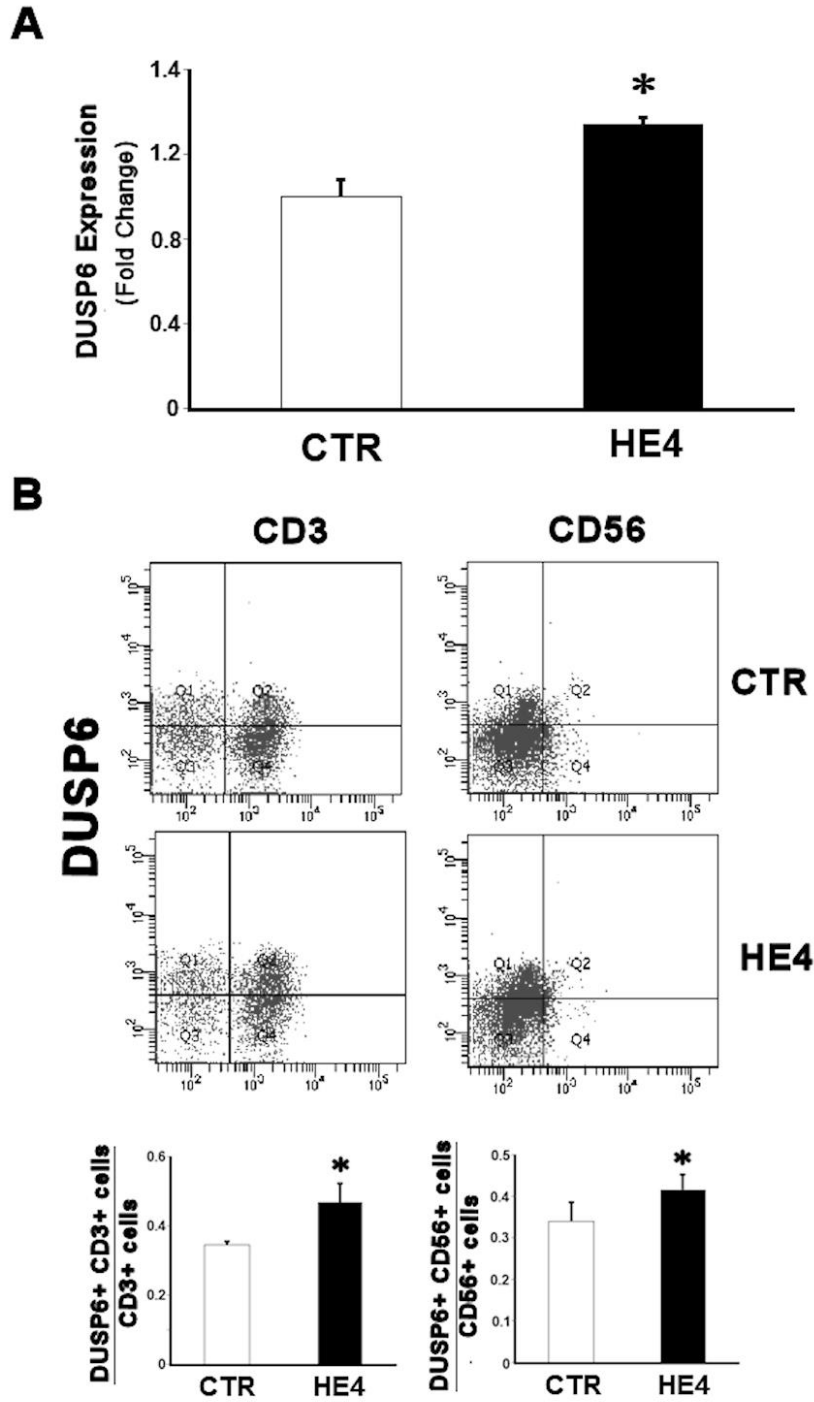
Figure II.2 HE4 upregulates expression of DUSP6 in peripheral CD8^{+} T cells.

Two-color flow cytometric analysis of PBMCs following 24-hour incubation with

0.01 µg/mL of rHE4 (HE4) or vehicle (CTR). 2D-scatterplots (upper panel) of DUSP6

(Alexa Fluor 647) and CD4 or CD8 (FITC) are shown. The lower panel shows a bar

graph from flow cytometric analyses using PBMCs from four individual donors. The
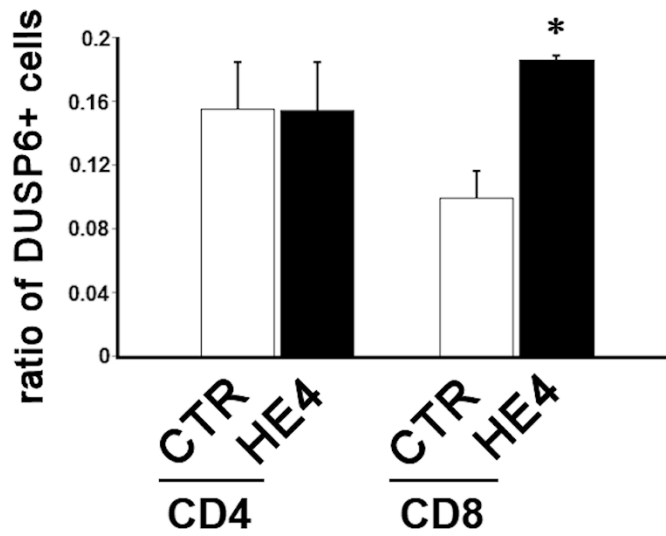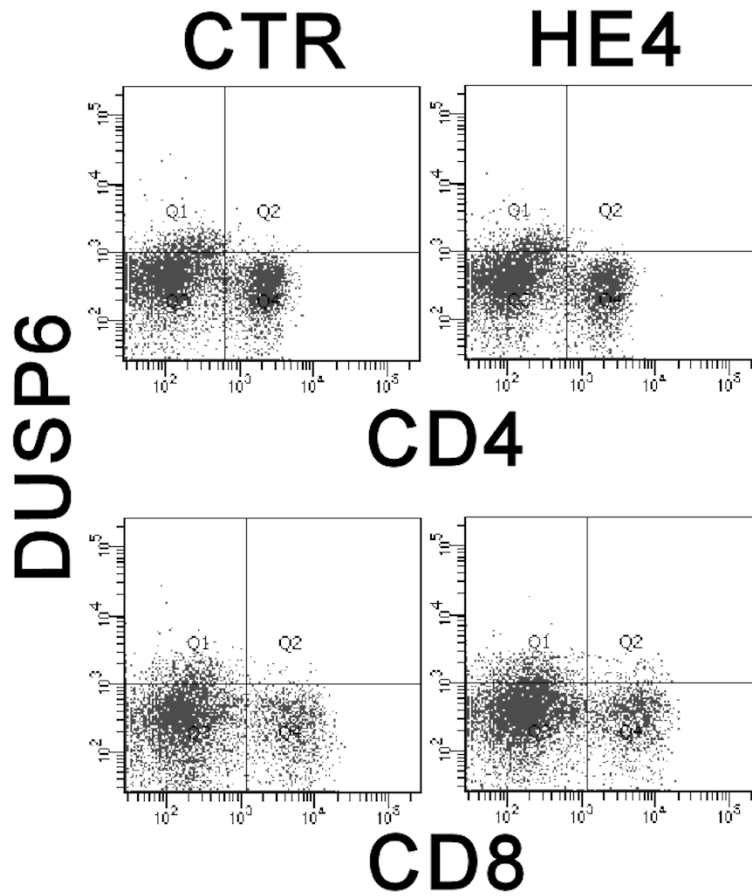
mean using ± SEM are shown. *p<0.01.

Fig. II.2

Figure II.3 HE4 suppresses Erk1/2 phosphorylation in CD8$^+$ and CD56$^+$ cells via DUSP6 induction.

 (A) Two-color flow cytometric analysis of PBMC following a 24-hour incubation with rHE4 (0.01 μg /mL) and BCI (1 μM) as indicated. 2-D scatterplots of phosphor-Erk1/2 (Alexa Fluor 647) and CD8 or CD56 (FITC) are shown. Mean ± SEM from analyses with four individual donors are shown in the bar graph. (B) Immunoblotting for phosphor-Erk1/2 in CD56$^+$ NK92MI, CD8$^+$ TALL-104 and CD4$^+$ H9 cells following a 1-hour incubation with the conditioned media from a 24-hour PBMC culture with rHE4 (0.01 μg/mL) and BCI (1 μM) in the indicated combinations. Blots of total Erk1/2 are shown as loading controls. Bar graph represents the relative band densities to controls. Mean ± SEM are shown (n=4). *p < 0.05, **p < 0.01.

121

Fig.II.3
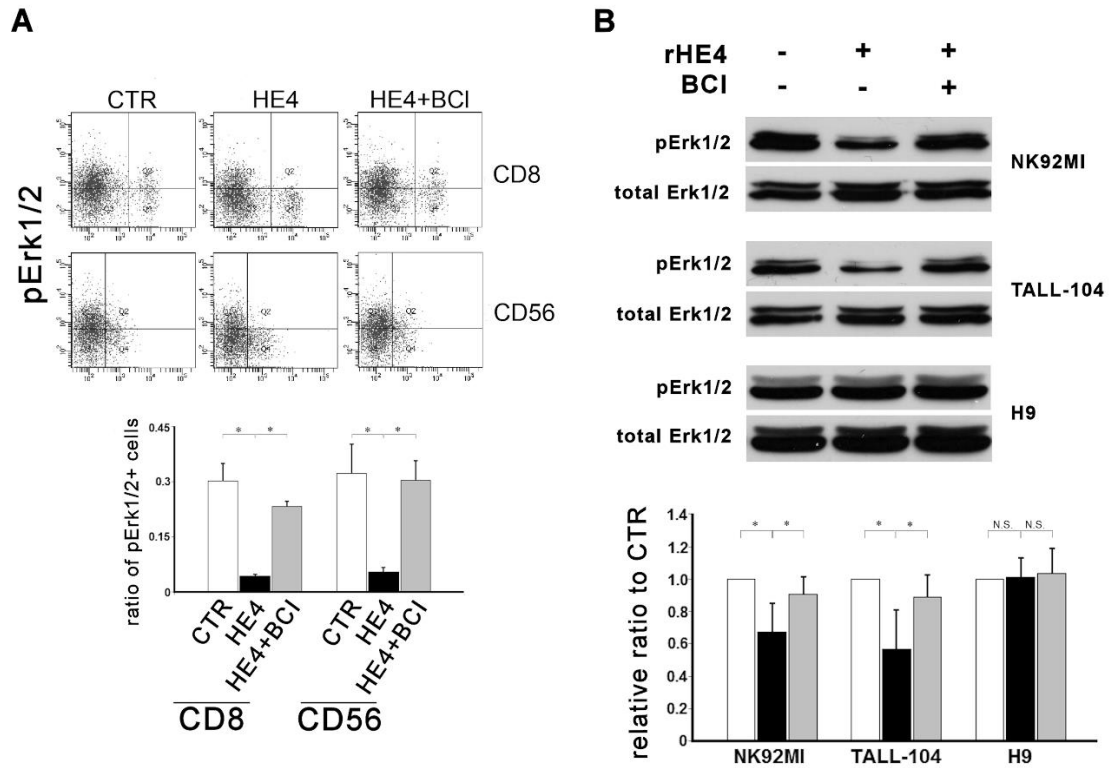
Figure II.4 Responses of SKOV3 cells to co-culture with PBMCs

(A) Cells were co-cultured with PBMC (5×10^6 / mL) with rHE4 (0.01 µg /mL) and BCI (1 µM) in indicated combinations. The cells viabilities were assessed at 24, 48 and 72 hours of the culture (n = 10). (B) Ki67 immunohistochemistry staining was performed on SKOV3 cells co-cultured with PBMC for 24 hours. Ki67^{+} cells are identified with red nuclear staining. Bar graph represents the percentage of Ki67+ cells in total countable cells under 200x fields (n = 20). (C) Two-color flow cytometric analysis of SKOV3 following 6-hour PBMC co-culture with of rHE4 (0.01 µg/mL) and BCI (1 µM) as indicated. 2D-scatterplots of propidium iodide and annexin V (Alexa Fluor® 488) are shown. Bar graph represents the percentage of propidium iodide / annexin V double positive cells in total cells (n = 4). Mean ± SEM are shown in the bar graphs. *p < 0.01.

Fig.II.4
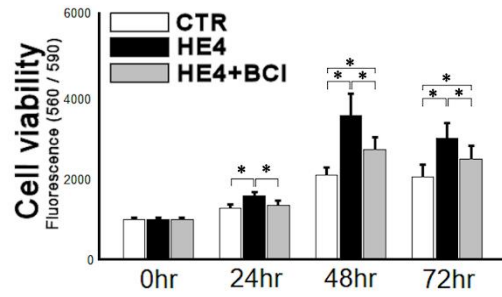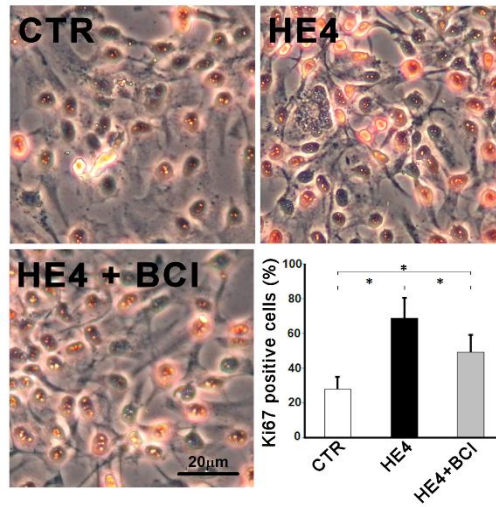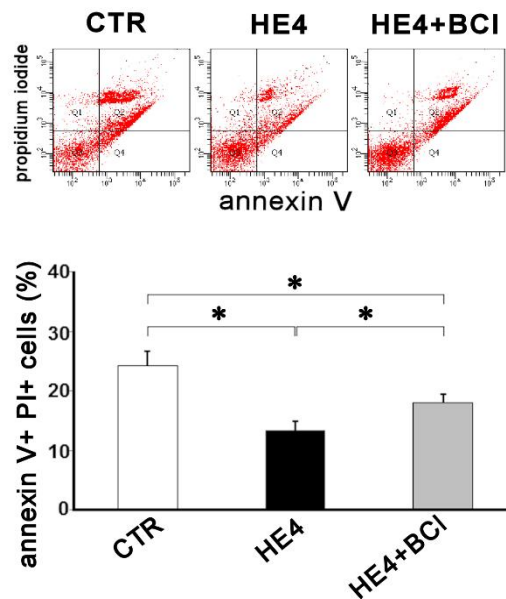
Figure II.5

Responses of SKOV3 cells to co-culture with CD8$^+$ / CD56$^+$ cell free PBMCs

(A) Cells were co-cultured with CD8$^+$ / CD56$^+$ cell-free PBMCs with rHE4 (0.01 µg /mL) and BCI (1 µM) in indicated combinations. The cells viabilities were assessed at 24, 48 and 72 hours of the culture (n = 10). (B) Ki67 immunohistochemistry staining was performed on SKOV3 cells co-cultured with CD8$^+$ / CD56$^+$ cell-free PBMCs for 24 hrs. Ki67$^+$ cells are identified with red nuclear staining. Bar graph represents the percentage of Ki67$^+$ cells in total countable cells under 200x fields (n = 20). (C) Two-color flow cytometric analysis of SKOV3 following 6 -hour CD8$^+$ / CD56$^+$ cell free PBMCs co-culture with of rHE4 (0.01 µg/mL) and BCI (1 µM) as indicated. 2D-scatterplots of propidium iodide and annexin V (Alexa Fluor$^®$ 488) are shown. Bar graph represents the percentage propidium iodide / annexin V double positive cells in total cells (n = 4). Mean ± SEM are shown in the bar graphs. *p < 0.01.
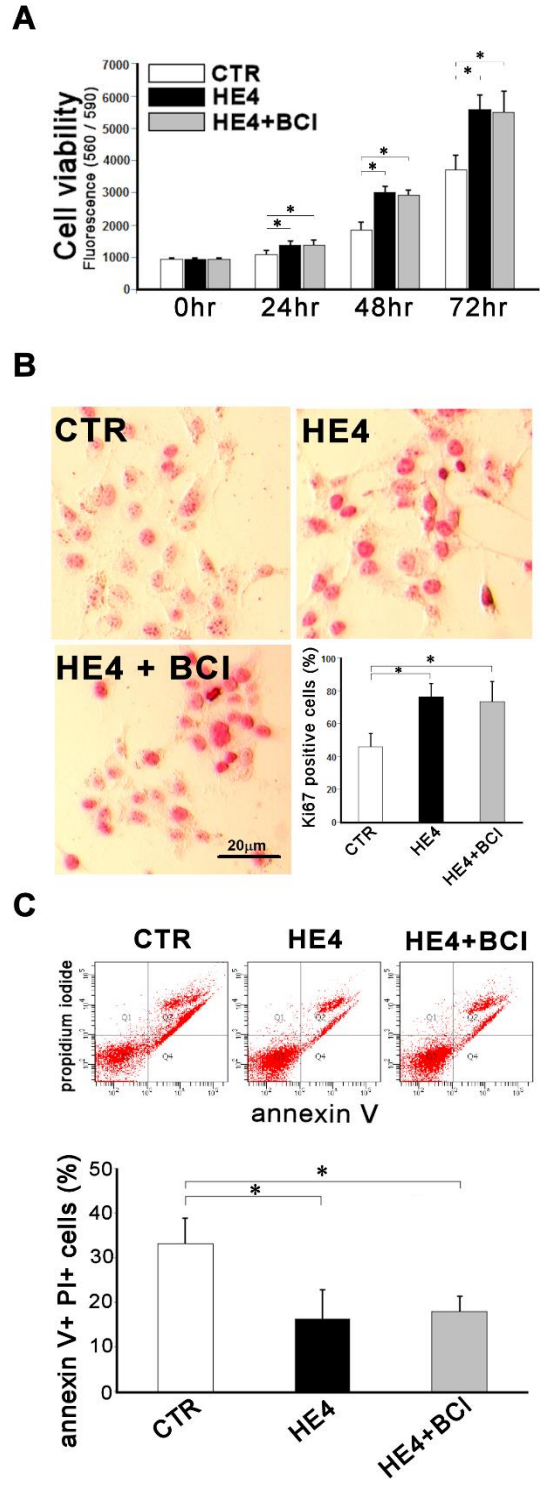
Fig.II.5

A

B

C

Table II.1 Genes induced in response to HE4

Frequency	ID	gene name
23	NSS	no significant similarity
3	NG_033915	dual specificity phosphatase 6 (DUSP6)
3	XM_017002424	capping actin protein of muscle Z line alpha sub unit 1 (CAPZA1)
3	NM_001402	eukaryotic translation elongation factor 1 alpha 1 (EEF1A1)
3	XM_017000674	FGR proto-oncogene, Src family tyrosone kinase (FGR)
3	NM_001261446.1	thioredoxin reductase 1 (TXNRD1)
3	NM_021109	thymosin beta 4, X-linked (TMSB4X)
3	BC006364	tubulin folding cofactor D
2	AK223032	beta actin variant
2	AC008397.7	chromosome 19 clone CTC-251H24
2	NM_001170330	chromosome 4 open reading frame 3 (C4orf3)
2	AY430097	DAZ associated protein 2 (DAZAP2)
2	NM_001005360	dynamin 2 (DNM2)
2	NG_002350.4	eukaryotic translation elongation factor 1 alpha 1 pseudogene 5 (EEF1A1P5)
2	NM_004468.4	four and a half LIM domains 3 (FHL3)
2	NM_001077488	GNAS complex locus (GNAS)
2	NM_001321232	histocompatibility (minor) HA-1 (HMHA1)
2	NM_000206.2	interleukin 2 receptor, gamma (IL2RG)
2	NM_001127605.2	lipase A, lysosomal acid (LIPA)
2	NM_012335.3	myosin IF (MYO1F)
2	XM_011541520	notch 2 (NOTCH2)
2	NM_001165412	nuclear factor of kappa light polypeptide gene enhancer in B-cells 1 (NFKB1)
2	NM_020820.3	phosphatidylinositol-3,4,5-trisphosphate dependent Rac exchange factor 1 (PREX1)
2	NM_001251855	phosphoinositide-3-kinase regulatory subunit 5 (PIK3R5)
2	NM_201384.2	plectin (PLEC)
2	NM_002952	ribosomal protein S2 (RPS2)
2	NM_001007.4	ribosomal protein S4, X-linked (RPS4X)
2	NM_000655	selectin L (SELL)
2	NM_004252	SLC9A3 regulator 1 (SLC9A3R1)
2	NM_022733.2	small ArfGAP2 (SMAP2)
2	NM_001278206	solute carrier family 43, member 3 (SLC43A3)
2	NM_025250.2	tweety family member 3 (TTYH3)
2	BC050652.1	zinc finger, DHHC-type containing 16
2	NM_004773	zinc finger, HIT-type containing 3 (ZNHIT3)
2	XM_011516569	zyxin (ZYX)
1		154 genes

127

Table II.2 DUSP6 concentration in cell lysates and culture media of PBMCs

Cell	lysates*	Culture	media**
CTR	HE4	CTR	HE4
9.38 ± 0.62	15.62 ± 0.97***	0.77 ± 0.10	1.43 ± 0.14***

*I 2.5 mg/mL of total protein(ng/mL)

**in 5 mL media of 5 x 10^6 PBMC culture

The mean ± are shown, n = 10 / each group, ***< 0.01 vs CTR

CHAPTER 5

MANUSCRIPT III

In Preparation for Submission to Oncotarget

Inhibition of DUSP6 Sensitizes Ovarian Cancer Cells to Chemotherapeutic

Agents Via Regulation of ERK Signaling Response Genes

Nicole E. James[1,3], Lindsey Beffa[1], Matthew T. Oliver[1], Naohiro Yano[2], Richard N.

Freiman[4], Paul A. DiSilvestro[1], Clinton O.Chichester[3], Jennifer R.Ribeiro[1*]

_____

[1] Division of Gynecologic Oncology, Program in Women's Oncology, Department of Obstetrics and Gynecology, Women and Infants Hospital, Providence, RI, United States

[2]Department of Surgery, Roger Williams Medical Center, Boston University Medical School, Providence RI, United States

[3]Department of Biomedical and Pharmaceutical Sciences, University of Rhode Island, Kingston, RI, United States

[4] Department of Cellular and Molecular Biology and Biochemistry, Brown University, Providence, RI

[*]Correspondence:
Jennifer R. Ribeiro
jrribeiro@wihri.org

III.1 Abstract

Dual Specificity phosphatase 6 (DUSP6) is a phosphatase that deactivates extracellular-signal-regulated kinase (ERK). Since the ovarian cancer clinical biomarker human epididymis protein 4 (HE4) has been shown to interact with the ERK pathway, the objective of this study was to determine the relationship between DUSP6 and HE4 and begin to elucidate the role of DUSP6 in epithelial ovarian cancer (EOC). Western blot and quantitative PCR following knockdowns showed that HE4 and DUSP6 levels were reduced with knockdown of the other protein in SKOV3 and OVCAR8 ovarian cancer cells. Furthermore, DUSP6 levels were upregulated in cells overexpressing HE4. Since HE4 has been shown to promote chemoresistance in EOC, the effect of DUSP6 on chemotherapeutic response was evaluated. MTS assay revealed a significant decrease in cell viability with pharmacological inhibition of DUSP6 using BCI in cells treated with carboplatin or paclitaxel, compared to treatment with single-agent chemotherapy alone. Quantitative PCR was used to evaluate gene expression responses to BCI, recombinant HE4 (rHE4), carboplatin, paclitaxel, and combinatorial treatments. DUSP6 inhibition with BCI altered expression of ERK pathway response genes, including early growth response protein 1 (EGR1) and c-Jun. Expression of EGR1, a strong promotor of apoptosis, was higher in ovarian cancer cells co-treated with BCI and paclitaxel or carboplatin than in cells treated with chemotherapeutic agent alone. Alternatively, the expression of c-Jun, a proto-oncogene, decreased with co-treatment of BCI and paclitaxel or carboplatin. The effect of BCI on the expression of these two genes opposed the effect of rHE4 on their expression. Finally, expression levels of DUSP6 in EOC tissue were evaluated by

immunohistochemical staining and quantification of mean and maximum intensity or integrated optical density (IOD). Levels of DUSP6 were noted to be significantly upregulated in serous EOC tissue compared to adjacent normal tissue, and a positive correlation between HE4 and DUSP6 levels was observed by Spearman Rank correlation. Unpaired 2-tailed student t-test was employed to determine statistical significance of results. In conclusion, DUSP6 inhibition sensitizes ovarian cancer cells to chemotherapeutic agents and alters gene expression of ERK response genes. The ability to detect HE4 levels in EOC patients coupled with the established co-dependence of DUSP6 with HE4, indicates that DUSP6 could plausibly function as a novel therapeutic target in EOC.

III.2 Introduction

Epithelial ovarian cancer (EOC) remains the most common and deadly gynecologic cancer, responsible for 240,000 diagnoses and 152,000 deaths worldwide each year [1]. The 5-year survival rate remains at 35% [2], which is largely due to difficulty with early diagnosis, coupled with the frequency of chemoresistant recurrences [3]. Although a majority of EOC is initially responsive to chemotherapy, once the disease recurs, chemoresistance inevitably develops and the patient eventually will succumb to their illness [4]. Therefore, there is a need for improved diagnostic approaches, as well as novel treatment targets to combat chemoresistance.

Human epididymis protein 4 (HE4) has been established as a novel clinical biomarker for EOC. Inclusion of preoperative levels of HE4 into the diagnostic Risk of Ovarian Malignancy Algorithm (ROMA) results in demonstrably improved specificity and sensitivity in detection and monitoring of the disease over Cancer Antigen 125 (CA 125), pelvic sonography, and menopausal status [5]. Research has also shown its mechanistic involvement in promoting EOC pathogenesis, including the promotion of proliferation, chemoresistance, anti-estrogen resistance, adhesion, invasion, and migration [6–16]. One oncogenic pathway that has been shown to interact with HE4 in several studies is the extracellular signal regulated kinase (ERK) pathway. Several reports indicate that ERK activation is enhanced with HE4 treatment or overexpression, while ERK activation is reduced with HE4 knockdown [8, 14, 15]. Our lab has revealed a more complicated response of ERK to recombinant HE4 treatment; specifically, we have observed downregulation of ERK phosphorylation at early time points, and upregulation at later time points [8]. Although the exact

132

mechanism of HE4 interaction with the ERK pathway is not clarified, it is well established that HE4 mediates ERK activation in EOC.

Dual specificity phosphatase 6 (DUSP6) is a key negative regulator of ERK signaling via dephosphorylation of ERK at serine/tyrosine residues. ERK activation upregulates gene expression of DUSP6, which promotes a negative feedback loop on ERK activation [17]. DUSP6 has been shown to have differing effects on tumor progression depending on the tumor type. In pancreatic cancer, it is initially upregulated, but diminished at later stages, and is considered a tumor suppressor [18]. It is also considered a tumor suppressor in lung cancer [19]. However, in glioblastoma and HER-2 positive breast cancer, it has been shown to be upregulated [20, 21]. In gastric cancer, DUSP6 inhibition can overcome chemoresistance [22], and it has also been characterized as a therapeutic target in acute lymphoblastic leukemia [23]. One study in ovarian cancer suggested that it may act as a tumor suppressor [24]. The goal of the present study was to determine the relationship between HE4 and DUSP6 in EOC and begin to elucidate the role of DUSP6 in EOC.

III.3 Methods

Cell Culture, Treatments, and siRNA Knockdowns

SKOV3 and OVCAR8 cells were obtained from ATCC and cultured in Dulbecco Modified Eagle Medium (DMEM) with 10% fetal bovine serum and 1% penicillin/streptomycin, in a humidified incubator at 37°C/5% CO_2. Cells were plated at sub-confluent density the day before treatments. Cells were treated with 3.75 μM BCI (Sigma, B4313), 20 nM recombinant HE4 (My BioSource, MBS355616), 100-

133

500 µM carboplatin (Sigma Aldrich, C2538), 10 nM paclitaxel (Sigma Aldrich, T7402), or control treatments (.037% DMSO and/or H_2O) for indicated time points. Knockdowns were performed using siRNA directed against DUSP6 (Santa Cruz, sc-39000), HE4 LNA GapmeRs (Exiqon, 300600 Design ID 414262-1), control non-targeting siRNA (Santa Cruz, sc-37007) or Negative Control GapmeRs (Exiqon, 300610). Five µL lipofectamine 2000 (Invitrogen, 52887) was incubated at room temperature in 100 µL serum/antibiotic free DMEM. Meanwhile, siRNA was incubated separately in 100 µL serum/antibiotic free medium at a concentration of 2 µM for 5 minutes. The tubes were combined and incubated at room temperature for 20 minutes. The complex was added to cells cultured in DMEM with serum but no antibiotic to a final concentration of 100 nM. Cells were collected or underwent additional treatments after 48 hours.

Western Blot

Western blot was performed as previously described [9]. GAPDH was used as a loading control. Antibodies and dilutions used are as follows:

DUSP6 (MyBioSource, MBS8516662, 1:500)

HE4 (Santa Cruz, sc-293-473, 1:200)

GAPDH (Cell Signaling, 2118, 1:2000)

Phospho-ERK (Cell Signaling, 1:2000)

ERK (Cell Signaling, 1:2000)

Densitometry

Image J "analyze gel" function was used to perform densitometry analysis of western blot images in 8-bit TIFF format. Band densities were normalized to GAPDH, and the lowest value was set to 1 for plotted graphs.

Quantitative RT-PCR

Quantitative RT-PCR was performed as previously described [9]. Validated primers for *DUSP6*, *EGR1*, and c-*JUN* were purchased from realtimeprimers.com. Custom primer sequences (Invitrogen) are as follows:

18s rRNA (F) – CCG CGG TTC TAT TTT GTT GG

18s rRNA (R) – GGC GCT CCC TCT TAA TCA TG

Cell Viability Assay

Cells were seeded at 2 000 cells/well in 96-well plates and treated as described above. After 48 h, cell viability assays were performed by adding 10 µl/well of CellTiter 96® Aqueous One Solution Cell Proliferation MTS Assay (Promega, G3580), incubating at 37°C/5% CO^2 for 2 h, and reading absorbance at 492 nm. Results are displayed as percent survival of vehicle treated cells.

Immunohistochemistry

Immunohistochemical staining of an ovarian cancer microarray (US Biomax, OV802a) and patient tissues from the Women & Infants Pathology Department was performed as previously described [35], using antibodies for HE4 (Santa Cruz, sc-

135

293473), DUSP6 (MyBioSource, MBS8516662). Confocal microscopy was performed by an independent imaging technician at the Rhode Island Hospital Digital Imaging Core Facility with a Nikon C1si confocal (Nikon Inc. Mellville, NY, USA). Two to three fields/sample were randomly selected based on DAPI staining, and minimum, mean, and maximum gray values were determined for each field. For the tumor microarray, normal adjacent tissues were used to set the threshold for positive staining. Integrated optical density (IOD) was calculated in serous samples using the mean values multiplied by the total area.

Statistics

Where statistics are shown, n≥3 biological replicates. Error bars represent standard deviation (STDEV) for quantitative PCR and MTS results, and standard error of the mean (SEM) for immunohistochemistry results. P-values were determined by unpaired, 2-tailed Student t-test. For correlation analysis, Spearman rank test was used to determine R value. Differences were considered statistically significant when $p < 0.05$.

III.4 Results

HE4 and DUSP6 Levels Are Co-Dependent in Ovarian Cancer Cell Lines

We first confirmed the upregulation of DUSP6 by HE4 by examining mRNA and protein levels in SKOV3 and OVCAR8 ovarian cancer cells stably overexpressing HE4 (clone 1 and clone 5, respectively) or their null vector (NV) counterparts. DUSP6 mRNA was upregulated by HE4 overexpression (1.2)-fold (p<0.05) and (3.9)-fold

136

(p<0.05), in SKOV3 and OVCAR8 cells, respectively (Figure 1A-B). To determine the reciprocity of the relationship between HE4 and DUSP6, we performed transient siRNA knockdown of DUSP6 and LNA GapmeR knockdown of HE4. We observed that knockdown of HE4 protein resulted in a corresponding downregulation of DUSP6, and knockdown of DUSP6 resulted in a corresponding downregulation of HE4 (Figure 1C-F).

Inhibition of DUSP6 Sensitizes Ovarian Cancer Cells to Chemotherapeutic Drugs

Next, we wanted to begin to determine the function of DUSP6 in ovarian cancer cells. Since one well-known role of HE4 in EOC is the promotion of chemoresistance, we treated SKOV3 and OVCAR8 cells with a DUSP6 inhibitor (BCI) alone or in combination with paclitaxel or carboplatin, the standard of care chemotherapeutic agents in EOC. Treatment of cells with BCI alone resulted in a small but significant reduction in cell viability as determined by MTS assay – 86.3% and 84.7% in OVCAR8 and SKOV3, respectively. In both cell lines, co-treatment with BCI and carboplatin resulted in a synergistic effect on cytotoxicity compared to either treatment alone. Carboplatin alone treatment resulted in 89.8% and 86.8% survival in OVCAR8 and SKOV3 cells, respectively, while BCI with carboplatin resulted in 33.9% and 50.2% survival in OVCAR8 and SKOV3 cells, respectively. In OVCAR8 cells, a synergistic effect was noted with BCI and paclitaxel treatment as well, with survival reducing from 51.4% with paclitaxel alone to 25.3% with BCI and paclitaxel (Figure 2A-B).

DUSP6 Inhibition Alters Expression of ERK Pathway Responsive Genes

In order to determine how regulation of ERK signaling by BCI versus rHE4 might affect downstream gene expression, we treated cells with BCI alone or in combination with rHE4, paclitaxel, or carboplatin, and examined expression of the ERK pathway response genes EGR1 and c-Jun. EGR1 is a transcription factor involved in promoting apoptosis in many cancers [25–28], and has been shown to be involved in cisplatin resistance in esophageal and ovarian cancers [29, 25]. We have previously shown that HE4 suppresses EGR1 gene upregulation in response to cisplatin treatment of SKOV3 cells [8]. On the other hand, c-Jun is an AP-1 transcription factor involved in promoting cell survival and growth [30, 31]. Treatment with BCI modestly upregulated EGR1 expression in both cell lines, while treatment with rHE4 downregulated EGR1 expression—a result that is in agreement with our previous study showing HE4 suppresses cisplatin-mediated upregulation of EGR1. The effect of BCI on EGR1 expression was more apparent with rHE4 co-treatment, where it reversed the downregulation of EGR1 by rHE4. Furthermore, co-treatment with BCI and either paclitaxel or carboplatin upregulated expression of EGR1 compared to treatment with either chemo drug alone. These results show that BCI opposes the effects of HE4 on EGR1 expression and promotes EGR1 expression while suppressing c-Jun expression in cells exposed to chemotherapy drugs (Figure 3A-D).

DUSP6 Levels Are Upregulated in EOC Tissue Compared to Adjacent Normal Tissue, and Correlate with HE4 Tissue Levels

To verify the clinical relevance of our findings, we performed immunohistochemistry of DUSP6 in an EOC tumor microarray and compared levels in serous adenocarcinoma samples (n=40) to levels in normal adjacent tissue (NAT; n=7). Mean intensity of DUSP6 was 545 (+/- 24.5) in EOC samples, and 432 (+/-19.6) in NAT (p=0.005). Moreover, maximal intensity was significantly greater in serous EOC samples than NAT. Maximum intensity was 1653 (+/-75.3) for EOC and 900 (+/- 110.3) for NAT (p=0.016), indicating that some areas of EOC exhibited particularly strong staining for DUSP6 (Figure 4A). Representative images are shown in Figure 4B.

In order to determine if a correlation exists between HE4 levels and DUSP6 levels in EOC, we co-stained for both proteins in the ovarian tissue microarray, and calculated correlations for mean intensity values and integrated optical density (IOD). Spearman Rank correlation test revealed a positive correlation between DUSP6 and HE4 mean intensities (R=0.45, p=0.0038) and IOD values (R=0.64, p=0.00001) (Figure 4C-D). Together, these results suggest that DUSP6 may be involved in promoting tumorigenesis in EOC, and corroborate our results indicating a relationship between HE4 and DUSP6.

III.5 Discussion

In this study, we have determined that HE4 and DUSP6 levels are co-dependent in ovarian cancer cells, and that these two proteins interact and are correlated in patient

139

tissue. Future studies are needed to elucidate the exact mechanistic relationship between DUSP6 and HE4. Studies by us and others have confirmed that HE4 activates ERK in ovarian cancer cells [8, 14, 15], while DUSP6 is a known negative regulator of ERK signaling [17]. Interestingly, despite the fact that HE4 and DUSP6 have opposing roles on ERK activation, they appear to produce similar effects on biological function of tumor cells. Our results show that activation of ERK by the DUSP6 inhibitor BCI as opposed to HE4 produces very different effects on gene expression and cellular functions such as chemotherapy response.

The two ERK responsive genes we have characterized show opposite expression patterns with BCI treatment. EGR1 is activated by ERK via the transcription factor ELK-1, and EGR1 is itself a transcription factor that activates expression of pro-apoptotic genes [32]. A previous study by our lab showed that HE4 overexpression in SKOV3 cells suppresses cisplatin-mediated upregulation of EGR1 [8]. Here, we observe that HE4 downregulates EGR1 expression, which is consistent with these previous results. Conversely, BCI treatment opposes the effect of rHE4 on EGR1 expression, indicating differing effects downstream of ERK activation by these two treatments. C-Jun, which is also an ERK responsive gene, is regulated oppositely as EGR1. rHE4 treatment upregulates expression of c-Jun, which is consistent with its role as a promoter of tumor growth and proliferation [6, 12, 13, 33, 34]. Meanwhile, BCI again opposes this effect in BCI and rHE4 co-treated cells. Furthermore, BCI suppresses chemotherapy-mediated increases in c-Jun levels. The effects of BCI on EGR1 and c-Jun together may contribute to the overall increased efficacy of BCI and chemotherapy treatment over chemotherapy alone.

140

The role of DUSP6 in EOC is not well studied. One report showed that DUSP6 appears to function as a tumor suppressor in EOC [24], but our results suggest the opposite effect. Therefore, further study is needed to fully elucidate the role of DUSP6 and determine if its function is context dependent. In general, DUSP6 remains an interesting protein, in that it has opposing roles in different tumor types. In some cancers, it appears to act as a tumor suppressor, while in others it acts to promote tumorigenesis and aggressive behavior [19–24]. Our results are consistent with a recent study by Wu et al. (2018) showing its involvement in cisplatin resistance in gastric cancer [22]. The authors observed an increase in phospho-ERK with BCI treatment, but a downregulation of the ERK-response genes RPS6KA1, EGR1, MMP2, MMP9, MYC, and ELK3. Furthermore, they found that BCI treatment enhanced cisplatin sensitivity in gastric cancer cells and in vivo xenografts. In our study, we observed different effects of DUSP6 inhibition on ERK-response genes depending upon gene function—namely, upregulation of the tumor suppressor EGR1 and downregulation of the proto-oncogene c-Jun. Collectively, our study and the one by Wu et al. illustrate that the relationship between ERK activation and downstream gene activation is not straightforward and appears to be highly context-dependent. Therefore, although BCI serves to increase ERK activation, it has different effects on ERK response genes, which serve to enhance chemotherapy efficacy.

In conclusion, this study highlights a novel function of DUSP6 in EOC and reveals that it may be involved in regulating chemoresponse. Targeting HE4 and/or DUSP6 in EOC may be an effective method of reversing chemoresistance and improving long-term response rates in select patient populations.

141

III.6 References

1. Van Zyl B, Tang D, Bowden NA: Biomarkers of platinum resistance in ovarian cancer: what can we use to improve treatment. *Endocr Relat Cancer* 2018, 25:R303–R318.

2. Morgan RD, Clamp AR, Evans DGR, Edmondson RJ, Jayson GC: PARP inhibitors in platinum-sensitive high-grade serous ovarian cancer. *Cancer Chemother Pharmacol* 2018, 81:647–658.

3. Foley OW, Rauh-Hain JA, del Carmen MG: Recurrent epithelial ovarian cancer: an update on treatment. *Oncology (Williston Park)* 2013, 27:288–94, 298.

4. Kim A, Ueda Y, Naka T, Enomoto T: Therapeutic strategies in epithelial ovarian cancer. *J Exp Clin Cancer Res* 2012, 31:14.

5. Moore RG, McMeekin DS, Brown AK, DiSilvestro P, Miller MC, Allard WJ, Gajewski W, Kurman R, Bast RC, Skates SJ: A novel multiple marker bioassay utilizing HE4 and CA125 for the prediction of ovarian cancer in patients with a pelvic mass. *Gynecol Oncol* 2009, 112:40–46.

6. Lu R, Sun X, Xiao R, Zhou L, Gao X, Guo L: Human epididymis protein 4 (HE4) plays a key role in ovarian cancer cell adhesion and motility. *Biochem Biophys Res Commun* 2012, 419:274–280.

7. Lokich E, Singh RK, Han A, Romano N, Yano N, Kim K, Moore RG: HE4 expression is associated with hormonal elements and mediated by importin-dependent nuclear translocation. *Sci Rep* 2014, 4:5500.

8. Ribeiro JR, Schorl C, Yano N, Romano N, Kim KK, Singh RK, Moore RG: HE4 promotes collateral resistance to cisplatin and paclitaxel in ovarian cancer cells. *J*

Ovarian Res 2016, 9:28.

9. Ribeiro JR, Gaudet HM, Khan M, Schorl C, James NE, Oliver MT, DiSilvestro PA, Moore RG, Yano N: Human Epididymis Protein 4 Promotes Events Associated with Metastatic Ovarian Cancer via Regulation of the Extracelluar Matrix. *Front Oncol* 2018, 7:332.

10. Zhuang H, Tan M, Liu J, Hu Z, Liu D, Gao J, Zhu L, Lin B: Human epididymis protein 4 in association with Annexin II promotes invasion and metastasis of ovarian cancer cells. *Mol Cancer* 2014, 13:243.

11. Zhuang H, Gao J, Hu Z, Liu J, Liu D, Lin B: Co-Expression of Lewis y Antigen with Human Epididymis Protein 4 in Ovarian Epithelial Carcinoma. *PLoS One* 2013, 8.

12. Wang H, Zhu L, Gao J, Hu Z, Lin B: Promotive role of recombinant HE4 protein in proliferation and carboplatin resistance in ovarian cancer cells. *Oncol Rep* 2015, 33:403–12.

13. Moore RG, Hill EK, Horan T, Yano N, Kim K, MacLaughlan S, Lambert-Messerlian G, Tseng YD, Padbury JF, Miller MC, Lange TS, Singh RK: HE4 (WFDC2) gene overexpression promotes ovarian tumor growth. *Sci Rep* 2014, 4:3574.

14. Lee S, Choi S, Lee Y, Chung D, Hong S, Park N: Role of human epididymis protein 4 in chemoresistance and prognosis of epithelial ovarian cancer. *J Obs Gynaecol Res* 2017, 43:220–227.

15. Zhu YF, Gao GL, Tang S-B, Zhang Z-D, Huang Q-S: Effect of WFDC 2 silencing on the proliferation, motility and invasion of human serous ovarian cancer cells in

143

vitro. *Asian Pac J Trop Med* 2013, 6:265–72.

16. Zhu L, Guo Q, Jin S, Feng H, Zhuang H, Liu C, Tan M, Liu J, Lin B: Analysis of the gene expression profile in response to human epididymis protein 4 in epithelial ovarian cancer cells. *Oncol Rep* 2016, 36:1592–604.

17. Bermudez O, Pagès G, Gimond C: The dual-specificity MAP kinase phosphatases: critical roles in development and cancer Bermudez O, Pagès G, Gimond C. The dual-specificity MAP kinase phosphatases: critical roles in development and cancer. *Am J Physiol Cell Physiol* 2010, 299:189–202.

18. Furukawa T, Fujisaki R, Yoshida Y, Kanai N, Sunamura M, Abe T, Takeda K, Matsuno S, Horii A: Distinct progression pathways involving the dysfunction of DUSP6/MKP-3 in pancreatic intraepithelial neoplasia and intraductal papillary-mucinous neoplasms of the pancreas. *Mod Pathol* 2005, 18:1034–42.

19. Okudela K, Yazawa T, Woo T, Sakaeda M, Ishii J, Mitsui H, Shimoyamada H, Sato H, Tajiri M, Ogawa N, Masuda M, Takahashi T, Sugimura H, Kitamura H: Down-regulation of DUSP6 expression in lung cancer: its mechanism and potential role in carcinogenesis. *Am J Pathol* 2009, 175:867–881.

20. Messina S, Frati L, Leonetti C, Zuchegna C, Di Zazzo E, Calogero A, Porcellini A: Dual-specificity phosphatase DUSP6 has tumor-promoting properties in human glioblastomas. *Oncogene* 2011, 30:3813–20.

21. Lucci MA, Orlandi R, Triulzi T, Tagliabue E, Balsari A, Villa-Moruzzi E: Expression profile of tyrosine phosphatases in HER2 breast cancer cells and tumors. *Cell Oncol* 2010, 32:361–72.

22. Wu QN, Liao YF, Lu YX, Wang Y, Lu JH, Zeng ZL, Huang QT, Sheng H, Yun

JP, Xie D, Ju HQ, Xu RH: Pharmacological inhibition of DUSP6 suppresses gastric cancer growth and metastasis and overcomes cisplatin resistance. *Cancer Lett* 2018, 412:243–255.

23. Shojaee S, Caeser R, Buchner M, Park E, Swaminathan S, Hurtz C, Geng H, Chan LN, Klemm L, Hofmann WK, Qiu YH, Zhang N, Coombes KR, Paietta E, Molkentin J, Koeffler HP, Willman CL, Hunger SP, Melnick A, Kornblau SM, Müschen M: Erk Negative Feedback Control Enables Pre-B Cell Transformation and Represents a Therapeutic Target in Acute Lymphoblastic Leukemia. *Cancer Cell* 2015, 28:114–128.

24. Chan DW, Liu VWS, Tsao GSW, Yao KM, Furukawa T, Chan KKL, Ngan HYS: Loss of MKP3 mediated by oxidative stress enhances tumorigenicity and chemoresistance of ovarian cancer cells. *Carcinogenesis* 2008, 29:1742–1750.

25. He J, Yu J-J, Xu Q, Wang L, Zheng JZ, Liu L-Z, Jiang B-H: Downregulation of ATG14 by EGR1-MIR152 sensitizes ovarian cancer cells to cisplatin-induced apoptosis by inhibiting cyto-protective autophagy. *Autophagy* 2015, 11(May):373–384.

26. Dong Q, Zhang J, Hendricks DT, Zhao X: GRO?? and its downstream effector EGR1 regulate cisplatin-induced apoptosis in WHCO1 cells. *Oncol Rep* 2011, 25:1031–1037.

27. Mohamad T, Kazim N, Adhikari A, Davie JK: EGR1 interacts with TBX2 and functions as a tumor suppressor in rhabdomyosarcoma. *Oncotarget* 2018, 9:18084–18098.
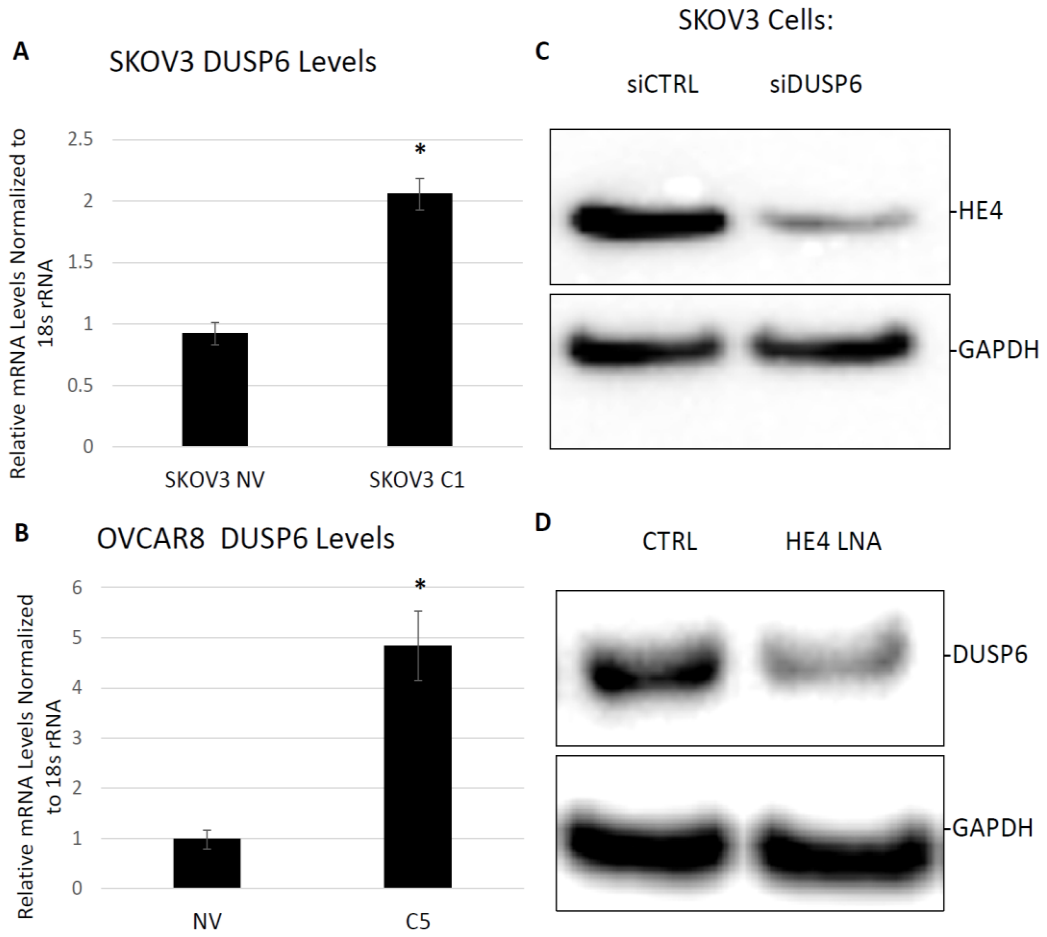
28. Maifrede S, Magimaidas A, Sha X, Mukherjee K, Liebermann DA, Hoffman B: Loss of Egr1, a human del5q gene, accelerates BCR-ABL driven chronic myelogenous leukemia. *Oncotarget* 2017, 8.

29. Dong Q, Zhang J, Hendricks DT, Zhao X: GROβ and its downstream effector EGR1 regulate cisplatin-induced apoptosis in WHCO1 cells. *Oncol Rep* 2011, 25:1031–7.

30. Wisdom R, Johnson RS, Moore C: c-Jun regulates cell cycle progression and apoptosis by distinct mechanisms. *Embo J* 1999, 18:188–197.

31. Vogt PK: Fortuitous convergences: the beginnings of JUN. *Nat Rev Cancer* 2002, 2:465–469.

32. Manente AG, Pinton G, Tavian D, Lopez-Rodas G, Brunelli E, Moro L: Coordinated sumoylation and ubiquitination modulate EGF induced EGR1 expression and stability. *PLoS One* 2011, 6:e25676.

33. Zhu L, Zhuang H, Wang H, Tan M, Schwab CL, Deng L, Gao J, Hao Y, Li X, Gao S, Liu J, Lin B: Overexpression of HE4 (human epididymis protein 4) enhances proliferation, invasion and metastasis of ovarian cancer. *Oncotarget* 2015:729–744.

34. Zhu YF, Gao GL, Tang SB, Zhang ZD, Huang QS: Effect of WFDC 2 silencing on the proliferation, motility and invasion of human serous ovarian cancer cells in vitro. *Asian Pac J Trop Med* 2013, 6:265–272.

35. James NE, Cantillo E, Oliver MT, Roswell-Turner RB, Ribeiro JR, Kim K, Chichester III CO, DiSilvestro PA, Moore RG, Singh RK, Yano N, Zhao TC: HE4 suppresses the expression of osteopontin in mononuclear cells and compromises their cytotoxicity against ovarian cancer cells. *Clin Exp Immunol* 2018:[Epub ahead of print].

Figure III.1 HE4 and DUSP6 Levels are Co-Dependent in Ovarian Cancer Cell Lines

DUSP6 mRNA levels are higher in SKOV3-C1 (A) and OVCAR8-C5 (B) cells

overexpressing HE4 than in null vector (NV) cells. *p<.05 (C) HE4 protein levels are

reduced in cells with DUSP6 knockdown. (D) DUSP6 protein levels are reduced with

HE4 knockdown.

148

Fig.III.1

A — SKOV3 DUSP6 Levels

Relative mRNA Levels Normalized to 18s rRNA

SKOV3 NV   SKOV3 C1

B — OVCAR8 DUSP6 Levels

Relative mRNA Levels Normalized to 18s rRNA

NV   C5

C — SKOV3 Cells:

siCTRL   siDUSP6

HE4

GAPDH

D — CTRL   HE4 LNA

DUSP6

GAPDH

Figure III.2 Inhibition of DUSP6 Sensitizes Ovarian Cancer Cells to Chemotherapeutic Drugs.

(A) SKOV3 cells exhibited reduced viability when co-treated with the DUSP6 inhibitor BCI and either paclitaxel or carboplatin compared to either chemotherapeutic agent alone. (B) SKOV3 cells exhibited reduced viability when co-treated with the DUSP6 inhibitor BCI and either paclitaxel or carboplatin compared to either chemotherapeutic agent alone. Error bars represent standard deviation of 3 biological replicates in a single experiment. *p<0.05, ***p<.0005, ****p<.00005

Fig.III.2

A   OVCAR8 - 24 h MTS Assay

B   SKOV3 - 24 h MTS Assay
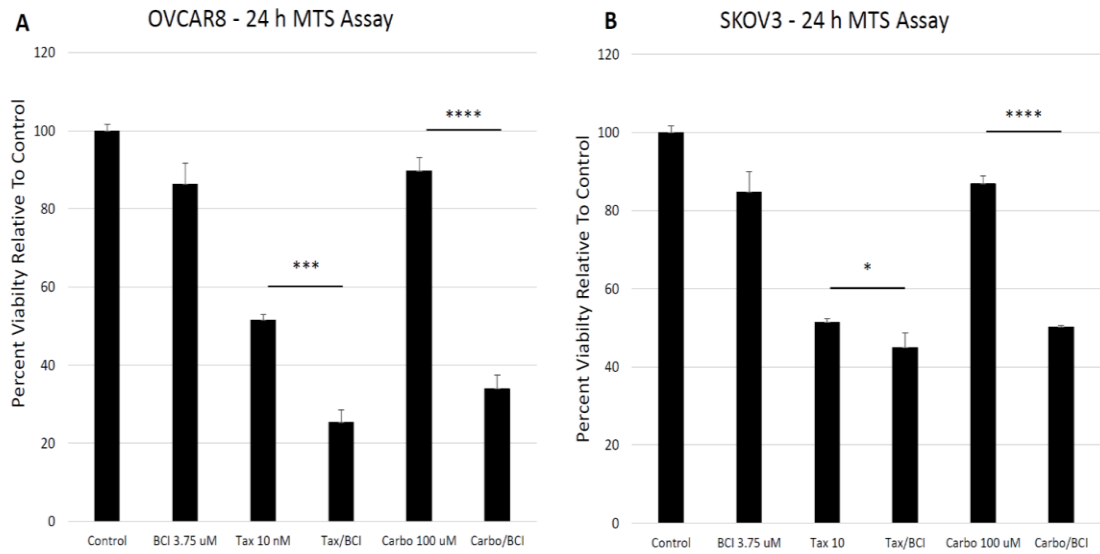
Figure III.3 DUSP6 Inhibition Alters Expression of ERK Pathway Responsive Genes. (A-B) BCI opposes the effect of rHE4 on EGR1 levels in OVCAR8 and SKOV3 cells. EGR1 mRNA levels are higher in cells co-treated with BCI and chemotherapeutic drugs than in cells treated with chemotherapy alone. (C-D) BCI opposes the effect of rHE4 on EGR1 levels in OVCAR8 and SKOV3 cells. JUN mRNA levels are lower in cells co-treated with BCI and chemotherapeutic drugs than in cells treated with chemotherapy alone. n=2-3 independent experiments.

Fig.III.3

A — OVCAR8-EGR1

B — SKOV3-EGR1

C — OVCAR8-JUN

D — SKOV3-JUN
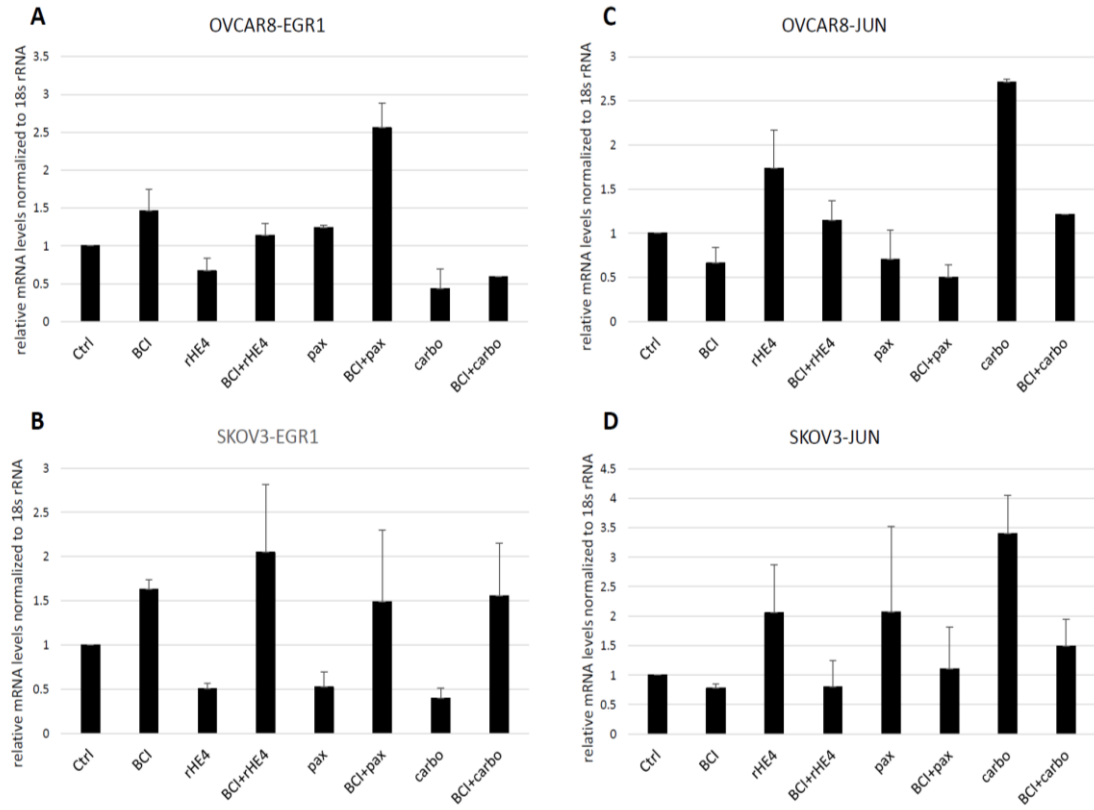
Figure III.4

Figure 4. DUSP6 Levels are Higher in EOC Tissue than Normal Adjacent Tissue, and Correlate with HE4 Tissue Levels.

(A) DUSP6 mean and maximum intensity staining is higher in serous EOC tissue (n=40) than in normal adjacent tissue (NAT) (n=7). Error bars represent deviation. *p<0.05 (B) Representative images of NAT and serous EOC DUSP6 staining. (C) Correlation of DUSP6 and HE4 mean intensity. (D) Correlation of DUSP6 and HE4 integrated optical density (IOD). Graph excludes one outlier data point for clarity (data is included in Spearman Rank Correlation calculation).

Fig.III.4
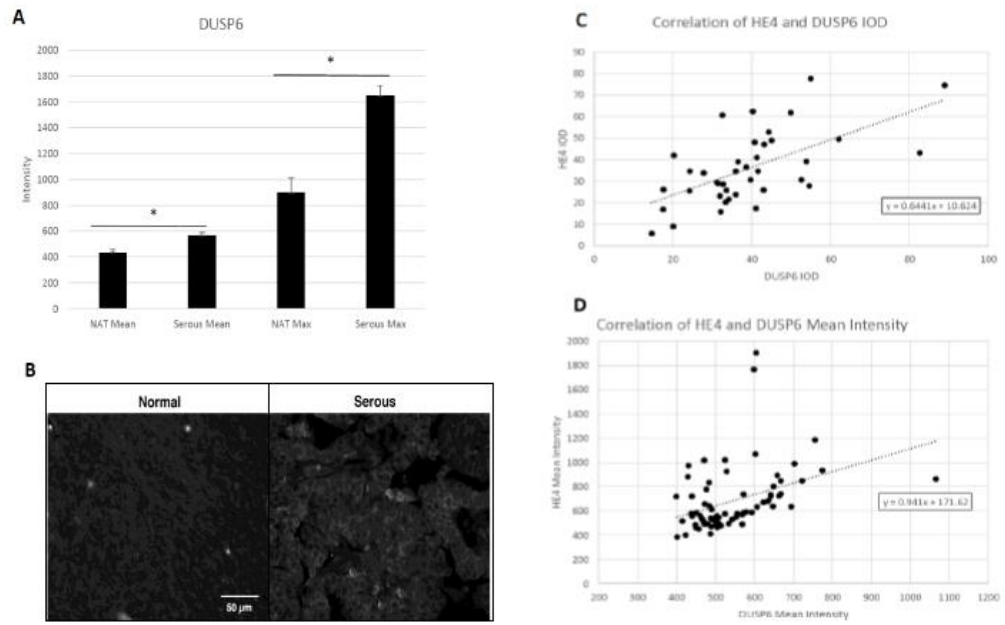
CHAPTER 6

MANUSCRIPT IV

Submitted to Scientific Reports, July 2018

Septin-2 is Overexpressed in Epithelial Ovarian Cancer and Mediates

Proliferation via Regulation of Cellular Metabolism Proteins

Nicole E. James[1,2], Evelyn Cantillo[1], Clinton O.Chichester[2], Naohiro Yano[2],

Kyukwang K.Kim [4], Paul A. DiSilvestro[1] ,Clinton O.Chichester[3],R.Shyama Prasad

Rao[5], Jennifer R.Ribeiro[1], Richard G Moore[4], Nagib Ahsan[6,7*], Rakesh K.Singh[4*]

_____

[1] Division of Gynecologic Oncology, Program in Women's Oncology, Department of Obstetrics and Gynecology, Women and Infants Hospital, Providence, RI, United States

[2] Department of Biomedical and Pharmaceutical Sciences, University of Rhode Island, Kingston, RI, United States

[3] Department of Surgery, Roger Williams Medical Center, Boston University Medical School, Providence RI, United States

[4] Wilmot Cancer Institute, Division of Gynecologic Oncology, Department of Obstetrics and Gynecology, University of Rochester Medical Center, Rochester, NY, United States

[5] Biostatistics and Bioinformatics Division, Yenepoya Research Center, Yenepoya University, Mangalore 575018, India

[6] Center for Cancer Research Development, Proteomics Core Facility, Rhode Island Hospital, Providence, RI, USA

[7]Division of Biology and Medicine, Alpert Medical School, Brown University, Providence, RI 02903, USA

[*]Correspondence:

Nagib Ahsan
nagib_ahsan@brown.edu

Rakesh K Singh
rakesh_singh@urmc.rochester.org

IV.I Abstract

Epithelial Ovarian Cancer (EOC) is associated with dismal survival rates due to the fact that patients are frequently diagnosed at an advanced stage and eventually become resistant to traditional chemotherapeutics. Hence, there is a crucial need for new and innovative therapies. Septin-2, a member of the septin family of GTP binding proteins, has been characterized in EOC for the first time and represents a potential future target. Septin-2 was found to be overexpressed in serous and clear cell human patient tissue compared to benign disease. Stable septin-2 knockout clones developed in an ovarian cancer cell line exhibited a significant decrease in proliferation rates. Comparative label-free proteomic analysis of septin-2 knockout cells revealed differential protein expression of pathways associated with the TCA cycle, acetyl CoA, proteasome and spliceosome. Further validation of target proteins indicated that septin-2 plays a predominant role in post-transcriptional and translational modifications as well as cellular metabolism and are the first to suggest the potential novel role of septin-2 in promoting EOC tumorigenesis through these mechanisms.

158

IV.2 Introduction

Epithelial Ovarian Cancer (EOC) is the most lethal gynecologic malignancy [1]. In 2018, there will be an estimated 22,240 new cases of EOC diagnosed and 14,070 deaths in the United States. While EOC accounts for only 2.5 % of all female cancers, it is responsible for 5% of all cancer deaths due to low disease survival rates [2]. These dire statistics are attributed to the fact that the majority of patients are diagnosed at an advanced stage. In addition, while patients generally respond well to frontline platinum-based chemotherapy, chemoresistant recurrences are common [3]. Therefore, there is a strong need for novel early detection methods and targeted therapies for EOC patients.

Septin-2 is a member of the septin family, a conserved family comprised of 13 GTP binding proteins [4]. Septins, which are structurally observed as rods and filaments, are vital to a number of cellular processes, including cytokinesis, vesicle trafficking, and exocytosis [5]. They are considered to be a fourth component of the cytoskeleton due to their association with actin, microtubules, and membranes [6]. Septins have been identified as having a role in neurodegenerative disease, since they were detected in brain tissue from patients with Alzheimer disease [7]. In addition, they have been reported to be involved in bacterial infections, Parkinson's disease, and male infertility [8].

In more recent years, emphasis has been placed on investigating the role of septins in tumorigenesis [9]. Due to their natural function in scaffolding and membrane compartmentalization, it is plausible that they could also play a role in the organization of membrane associated proteins involved in diverse tumorigenic

159

signaling pathways [6]. Septin-9 is the best studied septin family member in relationship to cancer, and its methylation status is utilized as a biomarker in colorectal cancer [10]. However, there have also been numerous studies linking septin-2 to neoplasia. Thus far, septin-2 has been specifically implicated in Hodgkin's lymphoma and biliary tract, gastric, hepatocellular, and breast cancer [11–15], but its role in EOC has not yet been investigated.

In this study, we begin to elucidate septin-2's function in EOC. As septins have been shown to have diverse roles in tumorigenesis, this is the first step in specifically defining septin-2's contribution to EOC pathogenesis. To establish the clinical relevance of septin-2 in EOC, we first sought to compare levels of septin-2 in various histological pathologies of EOC versus benign disease. Furthermore, we present for the first time a global analysis of septin-2 mediated proteomics in EOC and describe signaling pathways most affected by septin-2 depletion. The results from this study lay the framework for future mechanistic studies to determine the precise role of septin-2 in EOC.

IV.3 Methods

Cell Culture

SKOV3 wild type (SKOV3WT) and OVCAR8 wild type (OVCAR8WT) cell lines were obtained from American Type Culture Collection (ATCC) and were cultured in Dulbecco's Modified Eagle Medium supplemented with 10% fetal bovine serum and 1% penicillin/streptomycin in a humidified incubator at $37°C/5\%$ CO_2.

160

Septin-2 silencing with shRNA

shRNA for human HE4 (Santa Cruz Biotechnology, sc-40936-SH) or control shRNA

(Santa Cruz Biotechnology, sc-108066) was transfected into SKOV3WT cells using

Lipofectomine® 2000 (Invitrogen, 11668) following the manufacturer's instructions.

Individual single cells were selected by culturing under the pressure of 5 ug/mL of

puromycin (Research products International, 58-58-2), and clonal populations were

allowed to expand. Phenotypes of the clones were evaluated by western blotting using

anti Septin-2 antibody (Novus Biologicals, NBP1-85212)

Proliferation Assay

SKOV3WT, Plasmid C, KO#9, and KO#11 were plated at equal densities in

100x20mm plates. Cells were trypsinized at 72 and 96 hours, and replicates of three

were counted using a hemocytometer to compare proliferation rates. The experiment

was repeated three times and error bars represent standard deviation. Statistical

significance was determined by an unpaired, two-tailed Student *t*-test, where p<.05

was considered significant.

Immunohistochemistry and confocal immunofluorescent microscopy

Formalin-fixed paraffin embedded human ovarian tissue slides were obtained from the

Women and Infants Pathology Department. The human ovarian tissue microarray was

obtained from US Tissue Biomax (OV802a). Slides obtained from Women and Infants

were baked at 65 °C for two hours, and the microarray for 20 minutes. All slides were

subsequently washed in xylene, 100% ethanol, 95% ethanol, 70% ethanol,

161

deoxygenated water, and FTA Hemagglutination Buffer. Antigen retrieval was then performed using DAKO antigen retrieval solution (10x) (Agilent, S1699), heated to 95 °C for 20 minutes. Slides were then blocked with 5% horse serum in FTA Hemagglutination Buffer and incubated overnight in primary Septin-2 antibody (Santa Cruz, sc-20408) at 4 °C. Secondary antibody, Alexa Fluora 488 (Thermo Fisher Scientific, A-11055) was then added to slides following incubation in the dark for one hour at room temperature. Slides were washed in between steps with FTA Hemagglutination Buffer and were cover-slipped with DAPI containing mounting medium (Vector Laboratories, H-1200). Images were acquired using a Nikon E800 microscope (Nikon Inc. Mellville, NY, USA) and an RT3 SPOT camera (Diagnostic Istruments, Sterling Heights, MI, USA). Random sampling of ten fields was based on DAPI staining. Mean intensity or integrated optical density (IOD), expressed as area*mean/1E+07, was acquired using a 40X objective. Statistical significance was determined by an unpaired, two-tailed Student t-test, where $p<.05$ was considered significant.

Western Blot

Protein was extracted from cell pellets in Cell Lysis Buffer (Cell Signaling, 9803) with 1 mM of PMSF, according to the manufacturer's protocol. The concentration of extracted proteins was determined by DC Protein Assay (Bio-Rad Laboratories, 5000116). Western blot analysis was performed by loading equal amounts of protein boiled at 70 °C with Novex Sample Reducing Agent (Life Technologies, NP009) and NuPAGE LDS sample buffer (ThermoFisher Scientific, NP0007) into a 4–12 %

162

gradient NuPAGE Novex Bis-Tris gel [Life Technologies, NP0321BOX (mini), WG1402BX10 (midi)]. The gel was then transferred using a semi-dry transfer to methanol-activated 0.2 μm PVDF membranes (Bio-Rad, 162-0177) at 0.12-0.24A for 1 h 20 m. Membranes were blocked in 5 % milk in phosphate-buffered saline with 0.05 % Tween 20 (PBS-T) for 30 m at room temperature. Finally, membranes were incubated in primary antibody diluted in 5 % milk in PBS-T overnight at 4 °C, and then in secondary antibody diluted in 5 % milk in PBS-T for 1 h at room temperature, with PBS-T washes in between. Amersham ECL Prime Western Blot Detection System (GE Healthcare, RPN2232) was employed for detection of the HRP-tagged secondary antibodies. The Biorad Chemidoc MP Imaging System was used to image all blots. GAPDH was used as a loading control. Antibodies and respective dilutions used are as follows:

GAPDH (cell signaling, 2118, [1:2000])

Septin-2(novus biologicals, NBP1-85212, [1:500])

LDHA(cell signaling, 3582S, [1:1000])

FASN (cell signaling, 3180S, [1:1000])

Enolase (santa cruz biotechnology, sc-100812 [1:500])

Transketolase (santa cruz biotechnology, sc-390179) [1:500])

Quantitative PCR

RNA was extracted from cells by Trizol /LiCl precipitation. Total RNA (1000 ng) was then reverse transcribed into cDNA using the iScript cDNA Synthesis Kit (Bio-Rad, 1708890), following the manufacturer's protocol. Quantitative PCR was performed in

triplicate by loading 1 μl cDNA reaction, 1 μM forward and reverse validated Septin-2 primers (Origene HP232247), 10 μl SYBR Green (Applied Biosciences [ABI], 4367659) and 5 μl RNAse-free water to each well. Samples were run using the ABI 7500 Fast Real-Time PCR System. Data was then analyzed using the ΔΔCt method. All gene expression levels were normalized to 18 s rRNA.

Densitometry

Densitometry analysis of western blots was performed using image J. Blot images were analyzed in 8-bit JPEG format, using the "analyze gel" function. Relative band densities were normalized to GAPDH loading control.

Sample preparation for LC-MS/MS analysis

Cell pellets were subjected in lysis buffer (8 M urea, 1 mM sodium orthovanadate, 20 mM HEPES, 2.5 mM sodium pyrophosphate, 1 mM β-glycerophosphate, pH 8.0, 20 min, 4°C), sonicated and cleared by centrifugation (14 000 × g, 15 min, 4°C). Protein concentration was measured (Pierce BCA Protein Assay, Thermo Fisher Scientific, IL, USA) and a total of 100 μg of protein per sample was subjected for trypsin digestion. Typtic peptides were desalted using C18 Sep-Pak plus cartridges (Waters, Milford, MA) and were lyophilized for 48 hours to dryness. The dried eluted peptides were reconstituted in buffer A (0.1 M acetic acid) at a concentration of 1 μg/μl and 5 μl was injected for each analysis.

The LC-MS/MS was performed on a fully automated proteomic technology platform [16,17] that includes an Agilent 1200 Series Quaternary HPLC system (Agilent

164

Technologies, Santa Clara, CA) connected to a Q Exactive Plus mass spectrometer (Thermo Fisher Scientific, Waltham, MA). The LC-MS/MS set up was used as described earlier [18]. Briefly, the peptides were separated through a linear reversed-phase 90 min gradient from 0% to 40% buffer B (0.1 M acetic acid in acetonitrile) at a flow rate of 3 µl /min through a 3 µm 20 cm C18 column. The electrospray voltage of 2.0 kV was applied in a split flow configuration, and spectra were collected using a top-9 data-dependent method. Survey full scan MS spectra (m/z 400-1800) were acquired at a resolution of 70,000 with an AGC target value of 3×10^6 ions or a maximum ion injection time of 200 ms. The peptide fragmentation was performed via higher-energy collision dissociation with the energy set at 28 NCE. The MS/MS spectra were acquired at a resolution of 17,500, with a targeted value of 2×10^4 ions or a maximum integration time of 200 ms. The ion selection abundance threshold was set at 8.0×10^2 with charge state exclusion of unassigned and z =1, or 6-8 ions and dynamic exclusion time of 30 seconds.

Bioinformatics analysis

Peptide spectrum matching of MS/MS spectra of each file was searched against a species-specific databases (UniProt; downloaded 2/1/2015) using MASCOT v. 2.4 (Matrix Science, Ltd, London, UK). A concatenated database containing "target" and "decoy" sequences was employed to estimate the false discovery rate (FDR) [19]. Msconvert from ProteoWizard (v. 3.0.5047), using default parameters and with the MS2Deisotope filter on, was employed to create peak lists for Mascot. The Mascot database search was performed with the following parameters: trypsin enzyme cleavage specificity, 2 possible missed cleavages, 10 ppm mass tolerance for precursor

165

ions, 20 mmu mass tolerance for fragment ions. Search parameters permitted variable modification of methionine oxidation (+15.9949 Da) and static modification of carbamidomethylation (+57.0215 Da) on cysteine. The resulting peptide spectrum matches (PSMs) were reduced to sets of unique PSMs by eliminating lower scoring duplicates. To provide high confidence, the Mascot results were filtered for Mowse Score (>20). Peptide assignments from the database search were filtered down to a 1% FDR by a logistic spectral score as previously described [19,20].

Relative quantitation of the identified peptides

Relative quantification of peptide abundance was performed via calculation of selected ion chromatograms (SIC) peak areas. Retention time alignment of individual replicate analyses was performed as previously described [21]. Peak areas were calculated by inspection of SICs using in-house software programmed in R 3.0 based on the Scripps Center for Metabolomics' XCMS package (version 1.40.0). This approach performed multiple passes through XCMS' central wavelet transformation algorithm (implemented in the centWave function) over increasingly narrower ranges of peak widths and used the following parameters: mass window of 10 ppm, minimum peak widths ranging from 2 to 20 seconds, maximum peak width of 80 seconds, signal to noise threshold of 10 and detection of peak limits via descent on the non-transformed data enabled. SIC peak areas were determined for every peptide that was identified by MS/MS. In the case of a missing MS/MS for a particular peptide, in a particular replicate, the SIC peak area was calculated according to the peptide's isolated mass and the retention time calculated from retention time alignment. A minimum SIC peak area equivalent to the typical spectral noise level of 1000 was

166

required of all data reported for label-free quantitation. Individual SIC peak areas were normalized to the peak area of the standard synthetic peptide DRVYHPF that was exogenously spiked prior to reversed-phase elution into the mass spectrometer. Quantitative analysis was applied to replicate experiments. To select peptides that show a statistically significant change in abundance between control vs treatment cells, q-values for multiple hypothesis tests were calculated based on p-values from two-tailed unpaired Student's t tests using the R package QVALUE as previously described [22,23].

IV.4 Results

Septin-2 is overexpressed in EOC

A preliminary proteomic study determined interacting partners of the clinical EOC biomarker HE4. It was noted that septin-2 was the most upregulated HE4-interacting protein (13-fold) in SKOV3 ovarian cancer cells overexpressing HE4 compared to null vector cells (data not shown). This finding prompted us to begin to characterize septin-2's role in EOC, as it had not been previously documented in the literature. To establish the clinical relevance of septin-2 in EOC, we evaluated its levels in EOC samples of a variety of histopathologies and compared these to levels in benign controls. Immunohistochemical analysis of septin-2 levels in a human ovarian tissue microarray comprising normal, serous, mucinous, clear cell, and dysgerminoma histopathologies revealed that mean intensity of the septin-2 staining was statistically significantly greater in serous EOC (703.3889 pixels) than in adjacent normal tissue (539 pixels) *(p=0.0037)* (Fig.1a). While all other histopatholgies exhibited higher

167

mean intensity levels of septin-2—mucinous (603 pixels), clear cell (821 pixels), and dysgerminoma (744 pixels)—compared to the normal adjacent tissue, none where considered statistically significant possibly due to low numbers of samples available. To further investigate expression levels of septin-2 in patient samples, immunohistochemistry of septin-2 was performed in EOC and benign tissue from our institution. Integrated optical density (IOD) was calculated for each sample, which revealed statistically significant higher levels in serous (721 area*mean/1E+06, *p=0.04)* (Fig 1b. and 1c.) and clear cell (31 area*mean/1E+06, *p=0.009)* histopathologies (Fig.1d. and 1e.) compared to respective benign controls (239 area*mean/1E+06) and (6 area*mean/1E+06).

Stable knockdown of septin-2 influences cell proliferation

In order to study septin-2's function in EOC, stable septin-2 knockout shRNA clones were generated in human serous ovarian SKOV3 wild type (WT) cells. Two clonal populations were employed for these studies—knockout 9 (KO9) and knockout 11 (KO11)—based on confirmation of successful septin-2 downregulation. A stable line was also generated by clonal expansion of cells transfected with control shRNA, designated Plasmid C. To confirm the efficacy of knockdowns at the genomic level, qPCR was employed. Septin-2 levels in KO9 were 1.93- and 4.16-fold lower than WT and Plasmid C cells, respectively. Septin-2 levels in KO11 were 1.67- and 3.88-fold lower than WT and Plasmid C cells, respectively (Fig 2a).

To further validate successful knockdown of septin-2, protein levels were detected by western blot. We observed substantial decreases septin-2 levels in KO9 and KO11 compared to the WT and Plasmid C controls (Fig 2b). Septin-2 levels in KO9 were decreased by 72% compared to WT and by 62.3% compared to Plasmid C. Septin-2 levels in KO11 were reduced by 76.4% and 67.7% compared to WT and Plasmid C, respectively (Fig.2c).

To begin to determine the consequence of septin-2 knockdown in SKOV3 cells, proliferation of the shRNA clones was evaluated. WT, Plasmid C, KO9, and KO11 cells were seeded at equal cell densities and allowed to expand. The cells were trypsinized at 72 and 96 hours, and numbers of live cells in each clonal population were quantified (Fig 2d). At 72 hours, KO9 clones exhibited a 67.5% decrease in cell proliferation compared to WT, and a 60.4% decrease compared to Plasmid C. KO11 clones demonstrated a 66.4% and 59.1% decrease in proliferation from respective WT and Plasmid C cell numbers. The 96-hour timepoint revealed a 51.1% reduction in KO9 cells compared to WT and a 39.3% reduction compared to Plasmid C. KO11 cells showed a 62.6% and 53.6% decrease compared to WT and Plasmid C cells, respectively. All decreases in cell counts displayed by KO9 and KO11 at both timepoints were determined to be statistically significant ($p<0.02$). This finding strongly suggests that the downregulation of septin-2 has a profound impact on cell proliferation in EOC cells.

Proteomic analysis of septin-2 knockdown in EOC cells

A comparative label-free proteomic analysis was performed to examine global protein expression level differences resulting from the knockdown of septin-2. Interestingly,

169

significant differences in protein-peptide levels between control cells and septin-2

knockouts was observed only in KO11 populations, even though our proliferation

results demonstrated that KO9's phenotype was similar to that of KO11. We

concluded that it was possible that the knockdown resulted in less significant effects

on protein levels, but still enough to affect proliferation, or that spontaneous loss of

the knockdown had occurred during cell culture. Therefore, we proceeded with

analysis using KO11 cells. As expected, a principal component analysis of three

biological replicates of WT, Plasmid C, and KO11 revealed separate clusters when

comparing principal component 1 and principal component 2 scores (Fig.3). In

contrast, for KO9 sample, the 3 biological replicates were very scattered (Data not

shown). Therefore, for any further analysis or validation process KO9 was not

included.

Mass spectrometry of the control and knockdown cells identified 19976 unique

peptides corresponding to 3565 unique proteins. Of those, only one peptide/protein in

Plasmid C exhibited an absolute fold change greater than 1 with a q-value < 0.05

compared to WT (Fig 4a). This result allowed us to conclude that there was no

significant difference between both control cell populations. Conversely, 5% of all

peptides in KO11 cells revealed relative fold change greater than 1 (q<0.05) compared

to WT cells. In addition, 93.5% of those peptides identified as exhibiting substantial

expression differences displayed a lower peak area in KO11 than WT, indicating a

majority of peptides was downregulated (Fig 4b). Representative examples of peak-

area of four peptide sequences from the proteins galetin-3 binding protein

(LFALS3BP), transketolase (TKT), poly(A) binding protein (PABPC4), and enolase-

1(ENO1) show differential expression between control and knockdown cells. KO11/WT peak area ratios were calculated for LFALS3BP (0.051, q=0.012), TKT (0.081, q=0.0012), PABPC4 (0.50, q=0.011), and ENO1 (632.7, q=0.30) (Fig 4c). It is interesting to note that, all four of these proteins have previously been shown to play a role in tumorigenesis [24–27]. Heat maps were constructed to illustrate the clustering of the 231 differentially expressed proteins in each of the three replicates of WT, Plasmid C, and KO11 (Fig 5a) and representative peptides in the most differentially expressed proteins (Fig 5b). Comparison of both heat maps reveals an overall similar pattern of peak-area quantitation, with many of the proteins and peptide sequences within KO11 exhibiting downregulation compared to WT and Plasmid C controls.

Finally, gene ontology (GO) analysis with differentially expressed proteins showed enrichment of for, proteasomal/ubiquitin in the biological process category and RNA binding in the molecular function category (Fig 6). Enrichment was also noted for terms related to the ribonucleoprotein complex and cytosol in the cellular component category. KEGG pathway analysis revealed citric acid cycle (TCA cycle) and spliceosome enrichment among differentially expressed proteins (Fig 6). Representative proteins related to these pathways were further validated by immunoblot analysis. Enolase, LDHA, Transketolase, and FASN expression in WT and KO11 was examined via western blot. (Fig 7a.) Band density normalized to GAPDH revealed a 7.8% increase in Enolase expression from WT to KO11. A corresponding 24.2%, 52.6%, and 64.9% decrease was observed comparing WT and KO11 in LDHA, Transketolase and FASN levels respectively. (Fig 7b.)

IV.5 Discussion

For the first time, we have characterized septin-2 function in EOC and examined its proteomic effects on a global level. Several biological pathways were found to be differentially regulated in septin-2 knockout ovarian cancer cells, exemplified by representative proteins from (Fig 4c.) Galectin-3 is a member of the β-galactoside binding protein family that is involved in diverse functions inherent to cancer, such as metastasis, immune surveillance, inflammation, apoptosis, molecular trafficking, and mRNA splicing [28]. Transketolase is a pentose phosphate pathway enzyme essential for cancer growth due to its ability to control NADPH production and counteract oxidative stress [26]. Poly(A) binding protein is a highly conserved protein that plays an important role in mRNA stabilization and translation [29], which controls cell growth, proliferation, and differentiation [30]. Enloase1, found to be differentially expressed in cancer, is a key glycolytic enzyme that catalyzes 2-phosphogylgerate to phosphoenolpyruvate in the last steps of the glycolytic catabolic pathway [31].

Of these pathways identified, it was most expected that autophosphorylation and proteasomal/ubiquitin protein functions were affected by septin-2 knockdown. It has been previously established that proper control of septins' phosphorylation status is required for the completion of cytokinesis [32]. In fungus, Meseroll et. al (2013) discovered that changes in specific phosphorylation sites on septins (Cdc3p and Cdc11p) leads to the disruption of higher order septin structures, indicating septin phosphorylation is also a vital regulator of their own structure formation [33].

Similar to phosphorylation, ubiquitination represents another important septin post-translational modification. Septins have an established role interacting with proteins

172

involved in degradation pathways, such as ubiquitin ligases and de-ubiquitylating enzymes, which modulates protein turnover [12,34,35]. Recently, it has also been reported that SUMOylation of human septins is a critical process contributing to proper septin filament bundling and cytokinesis [36]. Unlike ubiquitin, SUMO (small ubiquitin-like modifiers) modification does not always lead to protein degradation, as SUMOylation can also modulate localization, interaction, and activity of the target protein [37]. Ribet et.al (2017) reported that septin-7 is constitutively SUMOylated throughout the cell cycle, and septin variants that are unable to be SUMOylated halt septin bundle formation and lead to defects in cytokinesis, highlighting its crucial role in septin filament bundling and cell division [36].

GO analysis revealed that septin-2 is also involved in post-transcriptional modifications, as the spliceosome pathway was found to be enriched among septin-2 regulated proteins (Fig 6). This result suggests that septin-2 plays a major role in the editing of both precursor messenger RNA (pre-mRNA) and proteins. The spliceosome, a large molecular complex involved in the removal of non-coding introns from pre-mRNA, represents a potential oncogenic target as evidence has shown that tumors rely on normal spliceosome function for cell survival [38,39]. In addition, Poly(A) binding protein, which we reported as an example of a differentially expressed protein (Fig. 4c), is a translation initiation factor that binds to the mRNA 3'poly(A) tail [30] and also influences cell growth and survival. Since we have shown that the knockdown of septin-2 promotes irregular expression of a multitude of pathways related to mRNA and protein modifications, it seems reasonable that its downregulation would also affect tumor cell growth.

173

As the depletion of septins can lead to cytokinesis failures, it is logical that cellular proliferation would subsequently be affected. [36] In this study, we observed a reduction in proliferation with septin-2 knockdown. (Fig.2d) Corroborating results from our study in EOC, Zhang et. al (2016) treated breast cancer cells with the broad septin inhibitor forchlorfenuron(FCF) and also observed a decrease in cell proliferation [15], which they attributed to the suppression of MEK and ERK1/2 (extracellular signal-regulated kinase 1/2) signaling [15]. Another study showed that septin-8 interacts with MAPK5 (mitogen activated protein kinase 5), further suggesting that septins play a role in the MAPK/ERK pathway [40]. Septin-9 has also been implicated in cell proliferation, as a septin-9 variant SEPT9_i1 binds to c-Jun-N terminal kinase (JNK), preventing its degradation and therefore promoting tumor cell proliferation [4]. In addition, another septin-9 variant SEPT9_i3 has been found to be phosphorylated by cell-cycle-dependent kinase 1 (CDK1), controlling entry into mitosis and promoting cell survival and proliferation [41]. These investigations highlight that septin-2, and septins in general, play an important role in cellular proliferation and potentially promote tumor growth.

Interestingly, the most novel conclusion drawn from this investigation was the robust enrichment seen in cellular metabolism and energy dynamics in proteins affected by septin-2 downregulation. This novel finding regarding septin-2 is in agreement with previous studies reporting on septin functions related to energy metabolism. One study identified that fungal septins FaCdc3 and FaCdc12 are required for lipid metabolism [42]. In addition, septin-9 was found to induce lipid droplet growth through binding to phosphatidylinositol-5-phosphate(PtdIns5P), a phospholipid with a well-established

174

role in dynamics and intracellular membrane trafficking [43]. PtdIns5P binding in turn controls septin-9 filament formation and its interaction with microtubules [44]. Furthermore, septin-11 was found to be expressed in human adipocytes and upregulated in obese individuals. SEPT11 mRNA was positively correlated with markers of insulin resistance in adipose tissue, and silencing of septin-11 muted insulin signaling and insulin-induced lipid accumulation in adipocytes [45].

Our findings, however, represent the first time a septin family member has been implicated in cellular metabolism as it relates to tumorigenesis. Acetyl-CoA, one of the pathways most differentially expressed by septin-2, is a key metabolic player that links glycolysis, fatty acid oxidation, ketogenesis, amino acid metabolism, the TCA cycle, and lipid synthesis [46]. In normoxic conditions, acetyl-CoA is derived from glucose. However, under hypoxic conditions like in cancer, acetyl-CoA has been to found to derive from acetate, suggesting that targeting the acetyl-CoA pathway in cancer could represent a viable treatment option [47]. The TCA cycle, another important metabolic pathway, was also deregulated in the septin-2 knockdown clones. While previous dogma stated that tumor cells do not utilize the TCA cycle for energy, it has now been found that some cancer cells with deregulated oncogenes and tumor suppressor genes actually do rely on the TCA cycle [48]. In addition, the metabolic proteins transketolase and enolase, which are involved in glycolysis and the pentose phosphate pathway, respectively, were found to be differentially expressed by septin-2 inhibition (Fig 4c), demonstrating that septin-2 is involved in various facets of cellular metabolism within EOC. Pathways related to metabolism and energy production have previously been found to contribute to EOC tumorigenesis, as it has been shown that

glycolysis drives chemoresistance in EOC and that high levels of fatty acid synthase (FASN) contribute to tumor cell growth through the promotion of human epidermal growth factor [49,50]. Therefore, it can be hypothesized that the inhibition of septin-2 would exhibit a therapeutic effect in EOC via suppression of tumor metabolic pathways.

Overall, our study demonstrates the novel finding that septin-2 is involved in EOC pathogenesis. This investigation represents a springboard for future studies to determine the efficacy of septin-2 inhibition, in addition to more clearly elucidating its diverse mechanistic pathways in EOC tumorigenesis. While our proteomics study was performed in a serous ovarian cancer cell line, it would be interesting to repeat the stable knockdown experiment in a clear cell EOC line, since septin-2 was also found to be overexpressed in this histopathology. Additionally, both in vitro and in vivo studies could be performed to confirm that inhibition of septin-2 affects cell viability and tumor growth in order to determine if targeting of septin-2 synergizes with platinum-based chemotherapeutics.

IV.6 References

1. Dos Santos Guimarães I, Ladislau-Magescky T, Tessarollo NG, dos Santos DZ, Gimba E, Sternberg C, et al. Chemosensitizing effects of metformin on cisplatin and paclitaxel resistant ovarian cancer cell lines. Pharmacol Reports [Internet]. 2017; Available from: https://www.sciencedirect.com/science/article/pii/S1734114017304188

2. Cancer Facts and Figures. Am Cancer Soc. 2018;1–77.

3. Westin SN, Herzog TJ, Coleman RL. Investigational agents in development for the treatment of ovarian cancer. Invest New Drugs [Internet]. 2013;31:213–29. Available from: http://www.ncbi.nlm.nih.gov/pubmed/22661305

4. Angelis D, Spiliotis ET. Septin Mutations in Human Cancers. Front Cell Dev Biol [Internet]. 2016;4. Available from: http://journal.frontiersin.org/article/10.3389/fcell.2016.00122/full

5. Schmidt K, Nichols BJ. Functional interdependence between septin and actin cytoskeleton. BMC Cell Biol. 2004;5.

6. Poüs C, Klipfel L, Baillet A. Cancer-related functions and subcellular localizations of septins. Front Cell Dev Biol. 2016;4:126.

7. Kinoshita A, Kinoshita M, Akiyama H, Tomimoto H, Akiguchi I, Kumar S, et al. Identification of septins in neurofibrillary tangles in Alzheimer's disease. Am J Pathol. 1998;153:1551–60.

177

8. Saarikangas J, Barral Y. The emerging functions of septins in metazoans. EMBO Rep. 2011. p. 1118–26.

9. Russell SEH, Hall PA. Do septins have a role in cancer? Br. J. Cancer. 2005. p. 499–503.

10. Zhang M, He Y, Zhang X, Zhang M, Kong L. A pooled analysis of the diagnostic efficacy of plasmic methylated septin-9 as a novel biomarker for colorectal cancer. Biomed Reports [Internet]. 2017; Available from: http://www.spandidos-publications.com/10.3892/br.2017.970

11. Yu J, Zhang W, Tang H, Qian H, Yang J, Zhu Z, et al. Septin 2 accelerates the progression of biliary tract cancer and is negatively regulated by mir-140-5p. Gene. 2016;589:20–6.

12. Marcus EA, Tokhtaeva E, Turdikulova S, Capri J, Whitelegge JP, Scott DR, et al. Septin oligomerization regulates persistent expression of ErbB2/HER2 in gastric cancer cells. Biochem J [Internet]. 2016;473:1703–18. Available from: http://biochemj.org/cgi/doi/10.1042/BCJ20160203

13. Jian W, Zhong L, Wen J, Tang Y, Qiu B, Wu Z, et al. SEPTIN2 and STATHMIN regulate CD99-mediated cellular differentiation in Hodgkin's lymphoma. PLoS One. 2015;10.

14. Cao L, Shao Z, Liang H, Zhang D, Yang X, Jiang X, et al. Activation of peroxisome proliferator-activated receptor-γ (PPARγ) inhibits hepatoma cell growth via downregulation of SEPT2 expression. Cancer Lett [Internet]. 2015;359:127–35. Available from:

178

http://linkinghub.elsevier.com/retrieve/pii/S0304383515000257

15. Zhang, N., Liu, L., Fan, N., Zhang, Q., Wang,W., Zheng, M., Ma, L., Li, Y., and Shi L. The requirement of SEPT2 and SEPT7 for migration and invasion in human breast cancer via MEK/ERK activation. Oncotarget. 2016;7:61587–600.

16. Yu K, Salomon AR. HTAPP: High-throughput autonomous proteomic pipeline. Proteomics. 2010;10:2113–22.

17. Yu K, Salomon AR. PeptideDepot: Flexible relational database for visual analysis of quantitative proteomic data and integration of existing protein information. Proteomics. 2009;9:5350–8.

18. Ahsan N., Belmont J, CHez Z, Clifton JG and SA. Highly reproducible improved label-free quantitative analysis of cellular phosphoproteome by optimization of LC-MS/MS gradient and analytical column construction. J Proteomics. 2017;165:69–74.

19. Elias JE, Gygi SP. Target-decoy search strategy for increased confidence in large-scale protein identifications by mass spectrometry. Nat Methods. 2007;4:207–14.

20. Yu K, Sabelli A, DeKeukelaere L, Park R, Sindi S, Gatsonis CA, et al. Integrated platform for manual and high-throughput statistical validation of tandem mass spectra. Proteomics. 2009;9:3115–25.

21. Demirkan G, Yu K, Boylan JM, Salomon AR, Gruppuso PA. Phosphoproteomic profiling of in vivo signaling in liver by the mammalian target of rapamycin complex 1 (mTORC1). PLoS One. 2011;6.

22. Storey JD. The positive false discovery rate: A Bayesian interpretation and the q-value. Ann Stat. 2003;31:2013–35.

23. Storey JD, Tibshirani R. Statistical significance for genomewide studies. Proc Natl Acad Sci [Internet]. 2003;100:9440–5. Available from: http://www.pnas.org/cgi/doi/10.1073/pnas.1530509100

24. Song L, Tang J wu, Owusu L, Sun MZ, Wu J, Zhang J. Galectin-3 in cancer. Clin. Chim. Acta. 2014. p. 185–91.

25. Liu D, Yin B, Wang Q, Ju W, Chen Y, Qiu H, et al. Cytoplasmic poly(A) binding protein 4 is highly expressed in human colorectal cancer and correlates with better prognosis. J Genet Genomics [Internet]. 2012;39:369–74. Available from: http://www.ncbi.nlm.nih.gov/pubmed/22884093

26. Xu IM-J, Lai RK-H, Lin S-H, Tse AP-W, Chiu DK-C, Koh H-Y, et al. Transketolase counteracts oxidative stress to drive cancer development. Proc Natl Acad Sci [Internet]. 2016;113:E725–34. Available from: http://www.pnas.org/lookup/doi/10.1073/pnas.1508779113

27. Qian X, Xu W, Xu J, Shi Q, Li J, Weng Y, et al. Enolase 1 stimulates glycolysis to promote chemoresistance in gastric cancer. Oncotarget [Internet]. 2017;8:47691–708. Available from: http://www.oncotarget.com/fulltext/17868%0Ahttp://www.ncbi.nlm.nih.gov/pubmed/28548950%0Ahttp://www.pubmedcentral.nih.gov/articlerender.fcgi?artid=PMC5564598

28. Ruvolo PP. Galectin 3 as a guardian of the tumor microenvironment. Biochim. Biophys. Acta - Mol. Cell Res. 2016. p. 427–37.

29. Dizin, E., Gressier, C., Magnard C., Ray, H/ , Didier, D. , Ohlmann, T., and Dalla Venezia D. BRCA1 Interacts with Poly(A)-binding Protein IMPLICATION OF BRCA1 IN TRANSLATION REGULATION. J Biol Chem. 2006;281:24236–46.

30. Yoshida M, Yoshida K, Kozlov G, Lim NS, De Crescenzo G, Pang Z, et al. Poly(A) binding protein (PABP) homeostasis is mediated by the stability of its inhibitor, Paip2. EMBO J. 2006;25:1934–44.

31. Díaz-Ramos À, Roig-Borrellas A, García-Melero A, López-Alemany R. α-enolase, a multifunctional protein: Its role on pathophysiological situations. J. Biomed. Biotechnol. 2012.

32. Dobbelaere J, Gentry MS, Hallberg RL, Barral Y. Phosphorylation-dependent regulation of septin dynamics during the cell cycle. Dev Cell. 2003;4:345–57.

33. Meseroll RA, Occhipinti P, Gladfelter AS. Septin phosphorylation and coiled-coil domains function in cell and septin ring morphology in the filamentous fungus Ashbya gossypii. Eukaryot Cell. 2013;12:182–93.

34. Nakahira M, Macedo JNA, Seraphim TV, Cavalcante N, Souza TACB, Damalio JCP, et al. A Draft of the Human Septin Interactome. PLoS One. 2010;5.

35. Diesenberg K, Beerbaum M, Fink U, Schmieder P, Krauss M. SEPT9 negatively regulates ubiquitin-dependent downregulation of EGFR. J Cell Sci [Internet]. 2015;128:397–407. Available from:

http://www.ncbi.nlm.nih.gov/pubmed/25472714

36. Ribet D, Boscaini S, Cauvin C, Siguier M, Mostowy S, Echard A, et al. SUMOylation of human septins is critical for septin filament bundling and cytokinesis. J Cell Biol. 2017;216:4041–52.

37. Westerbeck JW, Pasupala N, Guillotte M, Szymanski E, Matson BC, Esteban C, et al. A SUMO-targeted ubiquitin ligase is involved in the degradation of the nuclear pool of the SUMO E3 ligase Siz1. Mol Biol Cell [Internet]. 2014;25:1–16. Available from: http://www.molbiolcell.org/cgi/doi/10.1091/mbc.E13-05-0291

38. van Alphen RJ, Wiemer EA, Burger H, Eskens FA. The spliceosome as target for anticancer treatment. Br J Cancer [Internet]. 2009;100:228–32. Available from: http://www.ncbi.nlm.nih.gov/pmc/articles/PMC2634708/pdf/6604801a.pdf

39. Lee SCW, Abdel-Wahab O. Therapeutic targeting of splicing in cancer. Nat. Med. 2016. p. 976–86.

40. Shiryaev A, Kostenko S, Dumitriu G, Moens U. Septin 8 is an interaction partner and in vitro substrate of MK5. World J Biol Chem [Internet]. 2012;3:98–109. Available from: http://www.pubmedcentral.nih.gov/articlerender.fcgi?artid=3362842&tool=pmcentrez&rendertype=abstract

41. Liu P, Kao TP, Huang H. CDK1 promotes cell proliferation and survival via phosphorylation and inhibition of FOXO1 transcription factor. Oncogene. 2008;27:4733–44.

42. Zhang, Y., Gao, T., Shao, W.,Zheng, Z., Zhou,M. and CC. The septins FaCdc3 and FaCdc12 are required for cytokinesis and affect asexual and sexual development, lipid metabolism and virulence in Fusarium asiaticum. Mol Plant Pathol. 2017;18:1282–94.

43. Di Paolo G, De Camilli P. Phosphoinositides in cell regulation and membrane dynamics. Nature. 2006. p. 651–7.

44. Akil A, Peng J, Omrane M, Gondeau C, Desterke C, Marin M, et al. Septin 9 induces lipid droplets growth by a phosphatidylinositol-5-phosphate and microtubule-dependent mechanism hijacked by HCV. Nat Commun. 2016;7.

45. Moreno-Castellanos N, Rodríguez A, Rabanal-Ruiz Y, Fernández-Vega A, López-Miranda J, Vázquez-Martínez R, et al. The cytoskeletal protein septin 11 is associated with human obesity and is involved in adipocyte lipid storage and metabolism. Diabetologia. 2017;60:324–35.

46. Lee J V., Shah SA, Wellen KE. Obesity, cancer and acetyl-CoA metabolism. Drug Discov. Today Dis. Mech. 2013.

47. Kamphorst JJ, Chung MK, Fan J, Rabinowitz JD. Quantitative analysis of acetyl-CoA production in hypoxic cancer cells reveals substantial contribution from acetate. Cancer Metab [Internet]. 2014;2:23. Available from: http://www.cancerandmetabolism.com/content/2/1/23

48. Anderson NM, Mucka P, Kern JG, Feng H. The emerging role and targetability of the TCA cycle in cancer metabolism. Protein Cell. 2018. p. 216–37.

49. Chakraborty PK, Mustafi SB, Xiong X, Dwivedi SKD, Nesin V, Saha S, et al. MICU1 drives glycolysis and chemoresistance in ovarian cancer. Nat Commun. 2017;8.

50. Tania M, Khan MA, Song Y. Association of lipid metabolism with ovarian cancer. Curr. Oncol. 2010. p. 6–11.

Figure IV. 1 Septin-2 is overexpressed in EOC

(a.) Tissue Microarray analysis reveals that septin-2 is overexpressed significantly($p=.0037)$ in serous EOC compared to adjacent normal control. Mucinous, clear cell, and dysgerminoma all exhibited a non-significant increase in septin-2 expression (mean intensity) (b.) Staining of human EOC tissue showed a statistically significant higher($p=0.04$) septin-2 expression in serous compared to benign serous. (c.) Representative images of Serous EOC staining (left panel) vs benign (right panel). (b.) Staining of human EOC tissue showed a statistically significant higher($p=0.009$) septin-2 expression in clear cell compared to benign tissue. (e.) Representative images of clear cell EOC staining (left panel) vs benign (right panel).

185
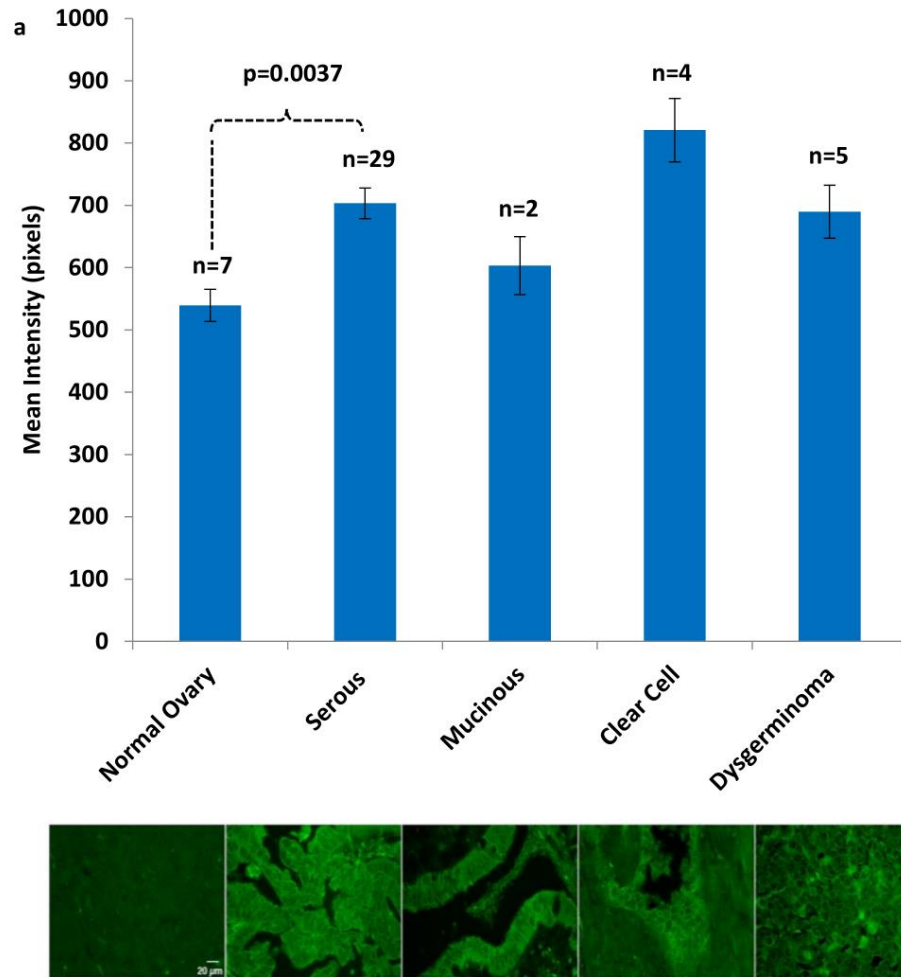
**Fig.IV.1(a)**

Fig IV.1(b-e)
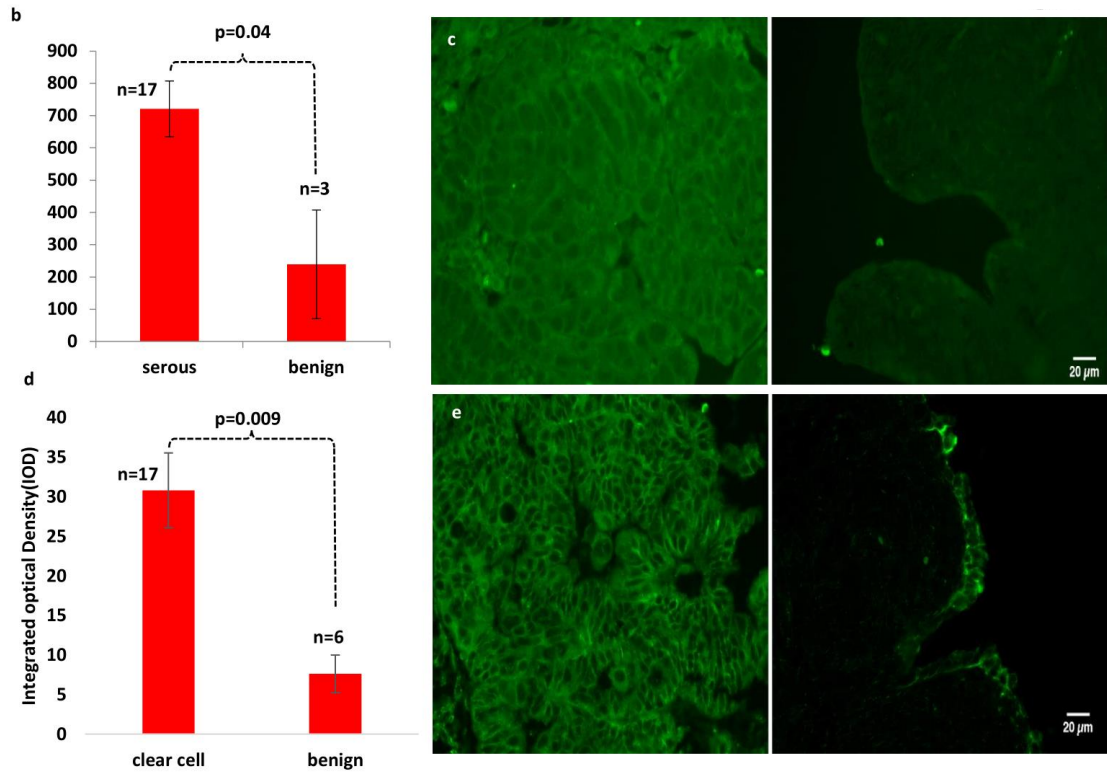
Figure IV.2 Stable septin-2 knockdown shows a decrease in proliferation

(A.) Gene expression levels of septin-2 in KO9 and KO11 where significantly

decreased ($p<0.01$) compared to WT and plasmid c control levels. (B.) Septin-2 is

decreased in KO9 and KO11 at the protein level. (C.) Relative band density of (B.).

(D.) Proliferation rates of KO9 and KO11 were significantly lower ($p<0.02$) at both 72
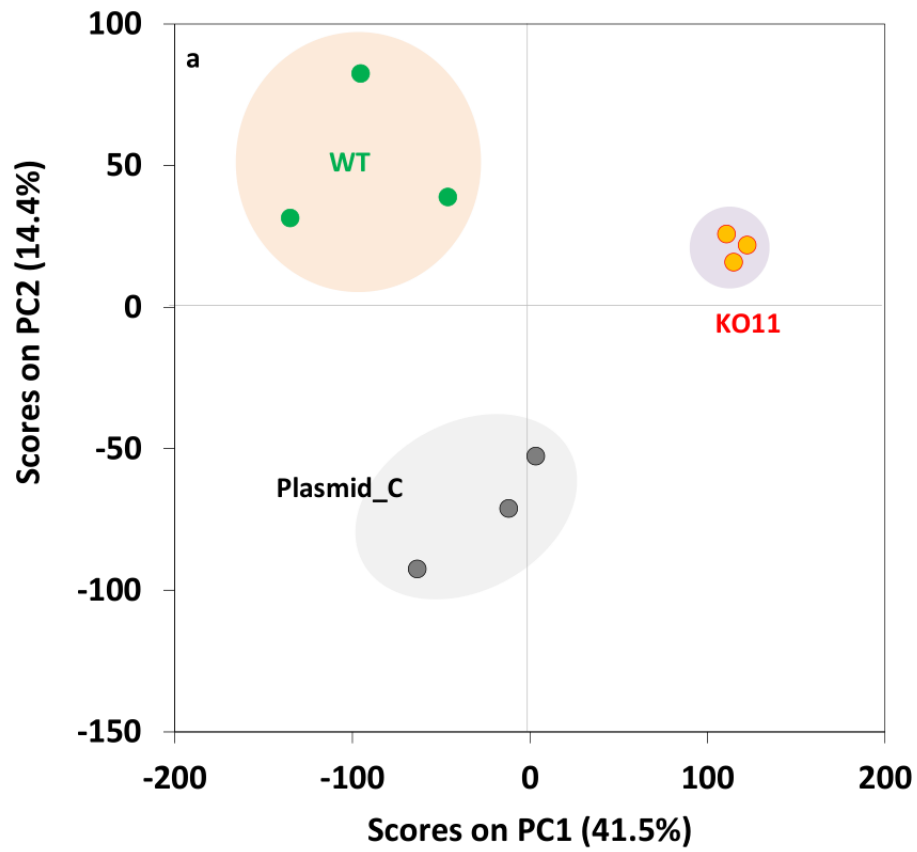
and 96 hours compared to control WT and plasmid c.

Fig.IV.2
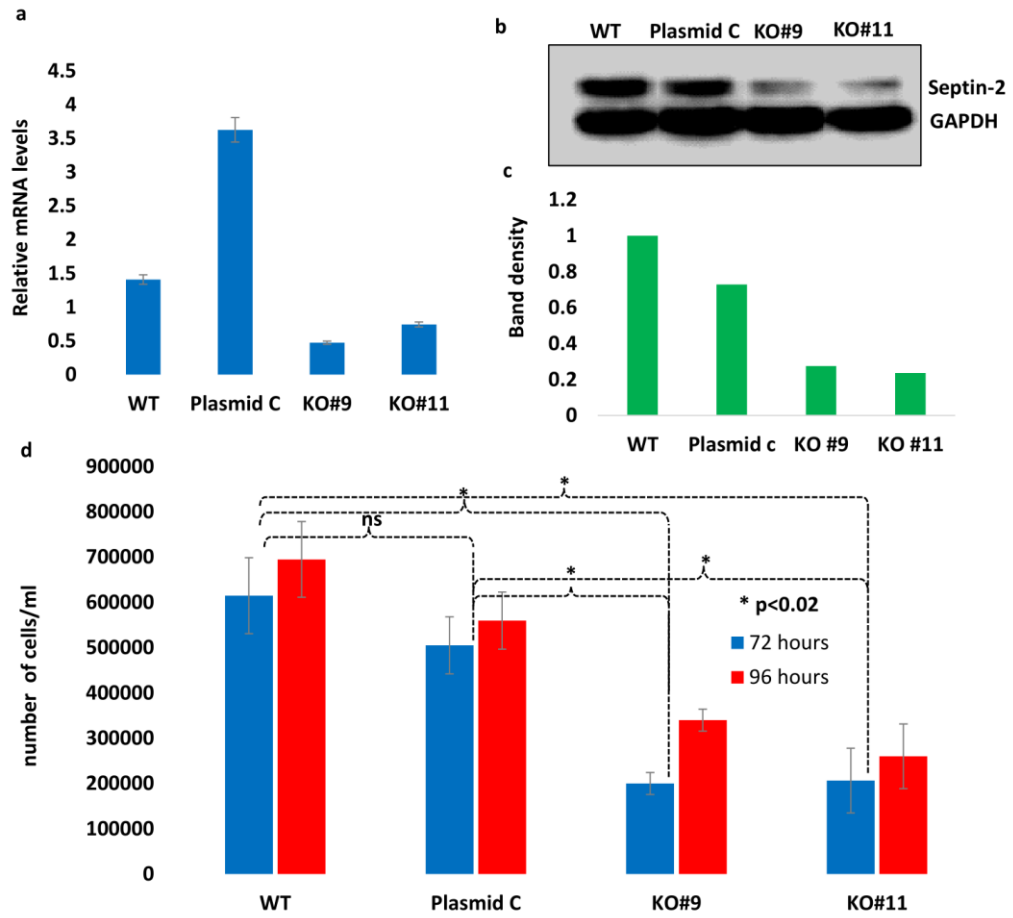
Figure IV.3 Principal Component Analysis of CO

WT, Plasmid C, and KO11 samples show clustering based on grouping. However, WT

is more dispersed and shows overlap with Plasmid C. Visualization of principal

component 1(PC1) versus principal component 2 (PC2).

190

Fig IV.3

Figure IV.4 Volcano plot of fold change versus q-value of peak area for distinct peptides

Of the 19976 distinct peptides (3565 proteins) identified, (A) only one peptide/protein (0%, red in inset pie chart) in Plasmid C and (B) 5.0% peptides in KO11 showed large difference (absolute fold change more than 1, and q < 0.05) against WT. Nearly 93.5% peptides showed lower peak-area (down regulation) in KO11. (C) represents the examples of peak-area/expression levels in replicates for four peptides are shown: 1. Galectin-3-binding protein (LGALS3BP, K7EKQ5), 2. Transketolase (TKT, P29401), 3. Poly(A) binding protein 4 (PABPC4, Q4VC03), 4. Enolase 1 (ENO1, P06733). The peptide sequence, KO11/WT peak-area ratio and respective q-values are listed for each protein.

Fig.IV.4
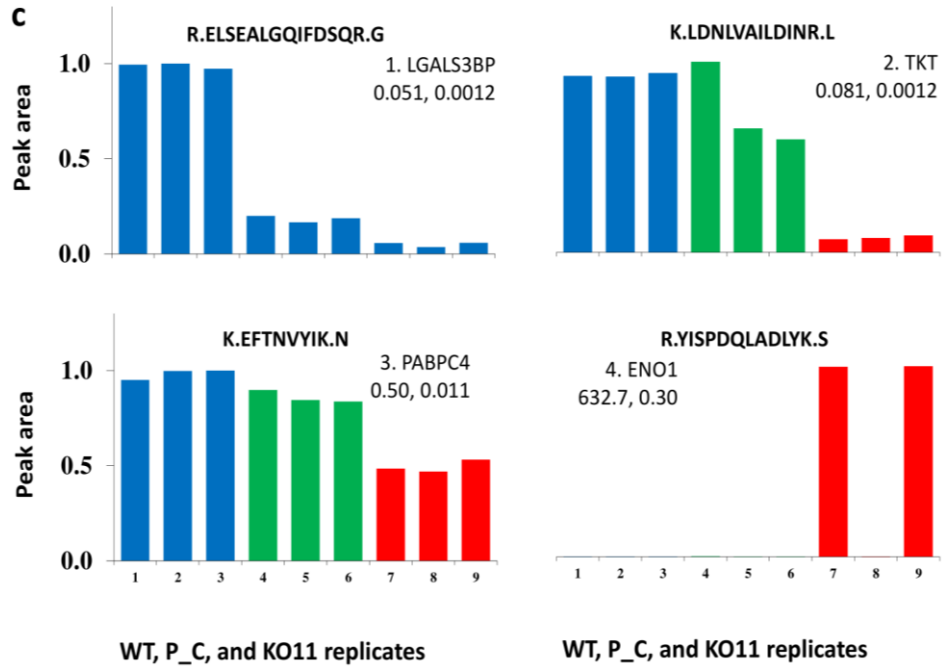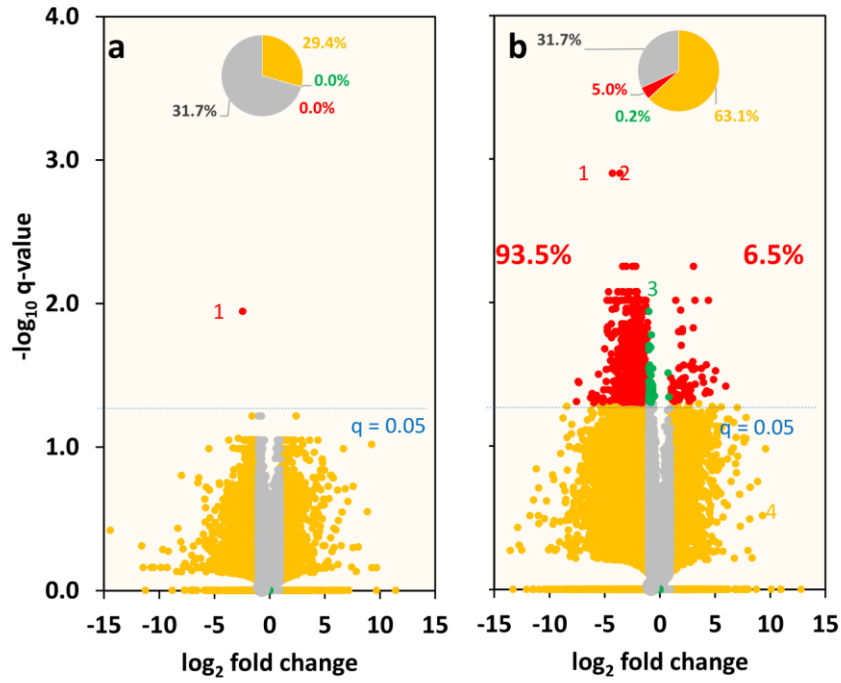
Figure IV.5 Hierarchical clustering and heat map of differentially expressed proteins and peptides

(A.) Clustering of the 231 differentially expressed proteins (B.) Peptides in most differentially expressed proteins, for example, Q9P2E9 (RRBP1, Ribosome binding protein 1) with 60 peptides, showing an overall similar pattern of peak-area quantitation.
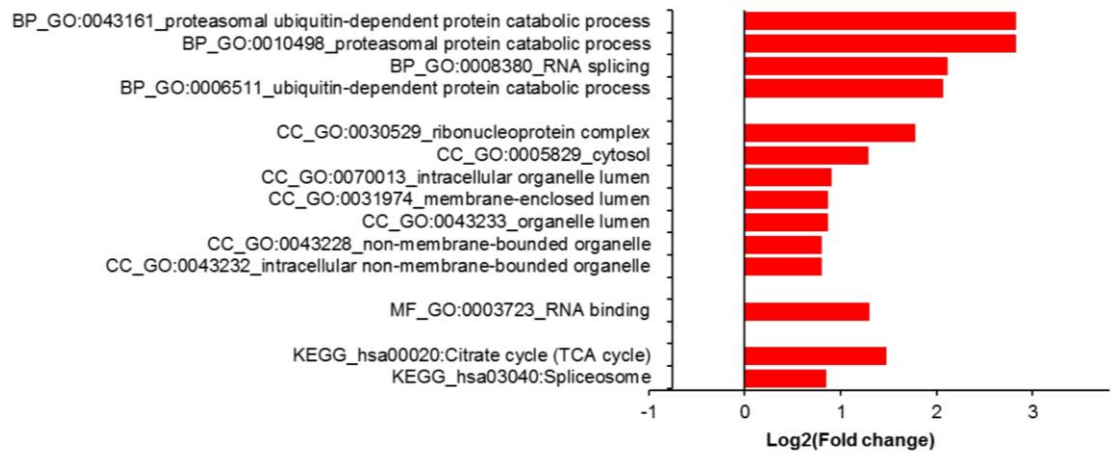
Fig.IV.5
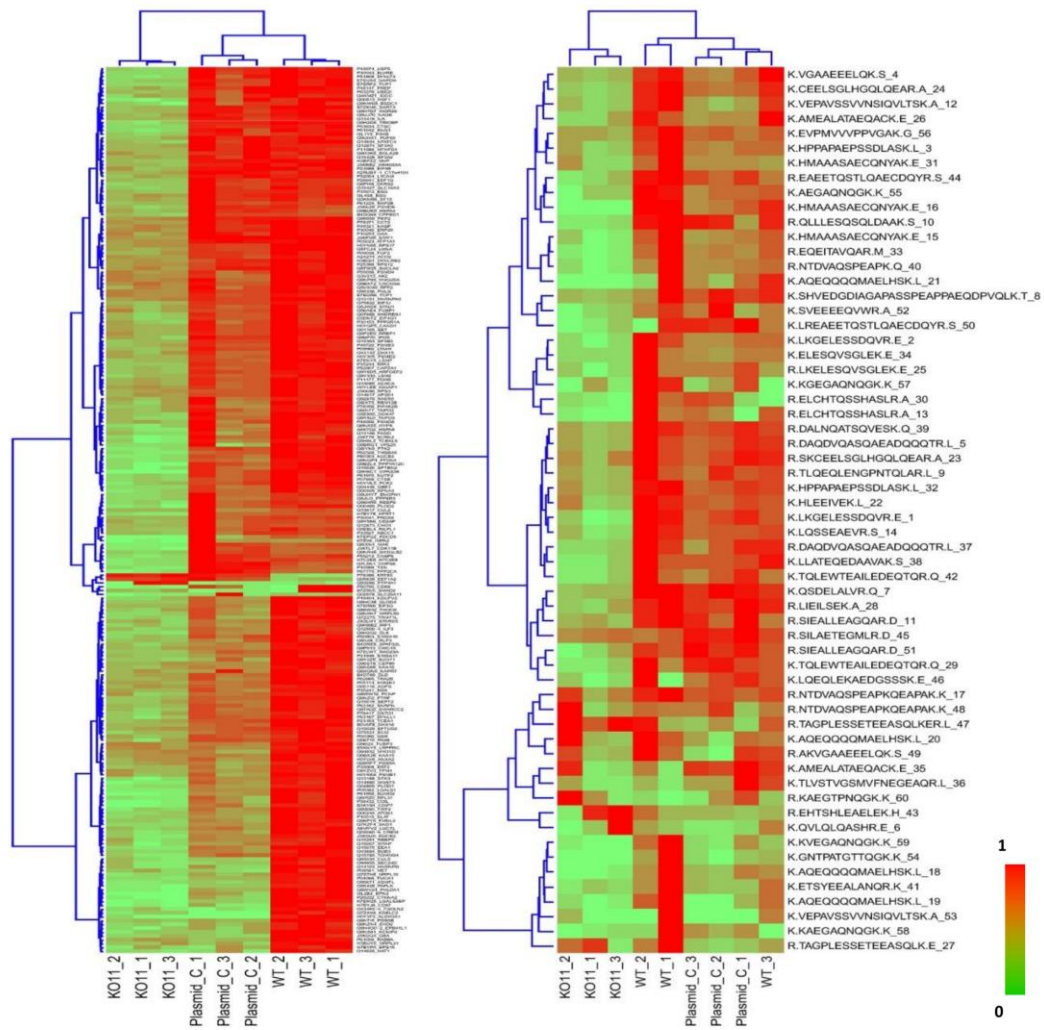
Figure IV.6 Gene ontology (GO) analysis

Gene ontology (GO) analysis using DAVID (https://david.ncifcrf.gov/). Proteins with differential expression (n = 231, q < 0.05, in KO11 versus WT is compared with proteins (n = 3334) that showed no differential expression. Former showed enrichment for proteasomal/ubiquitin related GO terms (q << 0.05, Bonferroni) in biological process (BP) category. In cellular component (CC) and molecular function (MF) categories, differentially expressed proteins showed enrichment for ribonucleoprotein and RNA related terms. No enrichment was seen in molecular function category. Differentially expressed proteins showed enrichment for KEGG pathways relating to citrate cycle/energy and spliceosome.
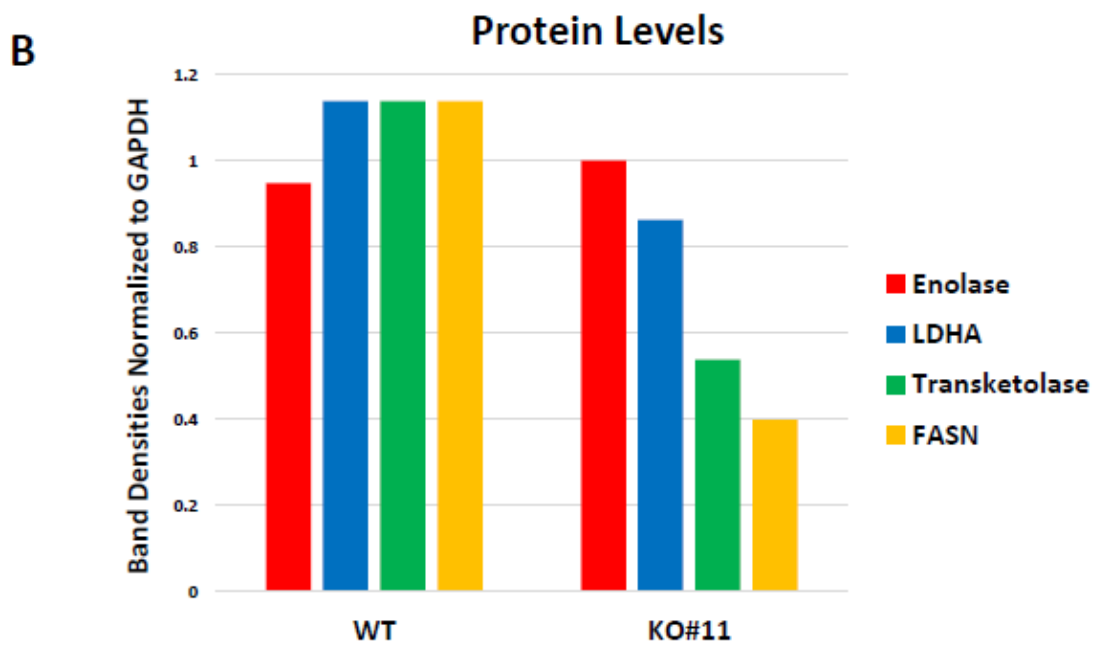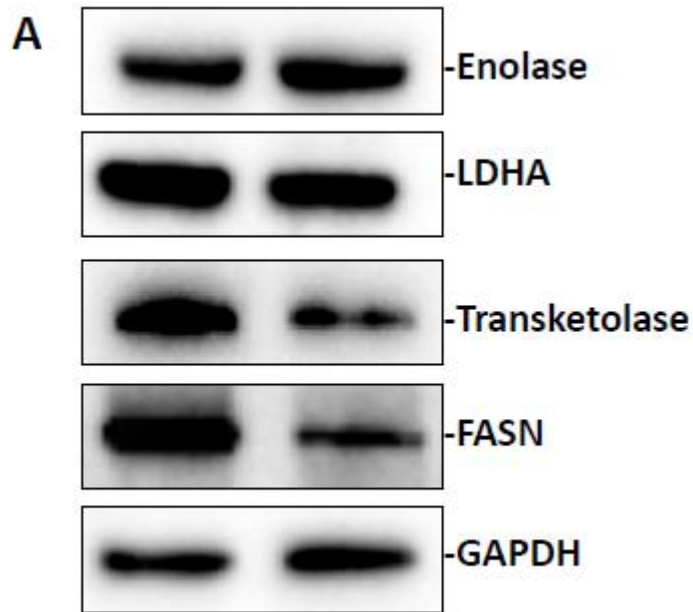
Fig.IV.6

197

Figure IV.7 Verification of Enriched Proteins Identified by Proteome Analysis

(A.) Western Blot analysis of protein expression validated in both WT and KO11 (B.)

Relative Band Densities of proteins in (A.), normalized to GAPDH.

Fig.IV.7

CHAPTER 7

CONCLUSION

Epithelial ovarian cancer (EOC) is such a deadly disease largely owing to the two major challenges of diagnosis and treatment. Ovarian cancer is detected at a late stage when tumor cells have already detached and metastasized directly into the peritoneal cavity, making it challenging for all lesions to be removed surgically [1]. Therefore, extensive disease remains in the body even after surgery. While treatment has evolved to include PARP inhibitors and anti-angiogenic therapies, prognosis remains poor. Immunotherapies for the treatment of cancer have recently garnered much attention, as it has been observed that the number of intratumoral T-cell numbers correlate to a better clinical outcome [2]. However, establishing a breakthrough immune target for ovarian cancer has been met with challenges, as the response rate remains low [3]. Therefore, a critical need for novel therapies for EOC still exists.

HE4 plays a unique role in EOC as it has been implicated in both diagnosis and prognosis of the disease. As a clinical biomarker, HE4 represents a promising early detection method. Compared to the more established biomarker CA-125, it is less frequently elevated in benign disease and is potentially able to identify patients that are at high risk for primary platinum resistance [4]. While much is known about HE4 clinically, far less is known about its biological functions in EOC. The goal of this investigation was to determine the mechanisms in which HE4 drives ovarian pathogenesis, and to ultimately provide evidence as to whether HE4 should be recommended as a therapeutic target for EOC.

As HE4 was initially suggested to have a potential role in innate immunity, [5] these studies aimed to better understand HE4's function in tumor immunity. For the first time, this investigation has shown that HE4 is involved in promoting ovarian tumor immune evasion, through influencing expression of two proteins, osteopontin (OPN) and dual specificity phosphatase 6 (DUSP6). Subtractive hybridization revealed that when peripheral blood mononuclear cells (PBMCs) were treated with recombinant HE4, OPN was the most downregulated protein, and DUSP6 was the most upregulated.

OPN is a secreted glycoprotein that has been identified as having important T helper 1 (Th1) cytokine functions. [6]Specifically, it was discovered that HE4 suppresses OPN in CD3+ T cells, while also impairing the secretion of IL-12 and IFN-γ, two important cytokines downstream of OPN that promote T-cell survival [6,7]. Furthermore, when ovarian cancer cells were cultured with media from PBMCs cultured with recombinant HE4, those cells were less susceptible to cell death, which was reversed upon silencing of HE4. Also, in human EOC patient tissue, serum HE4 levels inversely correlated to the number of OPN positive T cells in patient tumors.

The second objective in defining HE4's role in tumor immunity was to delineate the effect of HE4's upregulation of DUSP6. DUSP6 is an extracellular signal-regulated kinase (ERK) phosphatase that has been found to regulate CD4+ T cell activation and differentiation through the inhibition of T-cell receptor (TCR) dependent ERK activation [8]. Interestingly, upon testing HE4's upregulation of DUSP6 in specific subsets of cells within PBMCs, the upregulation was found to be restricted to CD8+

201

T-cells and CD56+ natural killer (NK) cells, and not CD4+ T cells. It was also discovered that HE4 promotes ERK ½ phosphorylation in these cell populations. Upon co-culture of PMBCs with ovarian tumor cells it was found that adding recombinant HE4 enhanced cell proliferation. However, this effect was attenuated by the addition of an allosteric DUSP6 inhibitor (BCI). PBMCs devoid of CD8+/CD56+ cells did not produce the same result, proving that CD8+ and CD56+ populations were solely responsible for the observed effects. This result was particularly interesting in light of HE4's hypothesize role in innate immunity, since NK cells, as part of the innate immune response, have been found to play an important role in helping tumor cells escape immune surveillance [9].

These two studies indicate that through targeting of HE4, it may be possible to restore a normal tumor immune response. To confirm this, future directions include testing the inhibition of HE4 via a neutralizing antibody in an immune competent mouse model to see how this affects tumor burden. In addition, testing HE4 inhibition in vivo in combination with platinum-based chemotherapeutics and immune checkpoint inhibitors to determine synergistic effects is important. Results from these studies will be valuable, as many successful EOC regimens are combination therapies that produce higher response rates and lower resistance rates compared with monotherapies [10]. Before HE4 can truly be recommended as a novel therapy that can remedy tumor immune evasion, results from these in vivo experiments should be obtained.

The study of DUSP6 and HE4 in immune cells lead to an additional investigation that examined DUSP6's role in epithelial ovarian cells. This was of particular interest since DUSP6 has not been well defined in cancer, and it has been published that HE4

202

interacts with the ERK signaling pathway in EOC [11–13]. This study confirmed that DUSP6 functions similarly to HE4 in EOC pathogenesis, as the inhibition of both factors promotes apoptosis in EOC cells. Furthermore, DUSP6 is overexpressed in serous EOC patient tissue and intratumoral levels of HE4 and DUSP6 correlate. Since it has been published that HE4 promotes chemoresistance in EOC [14], the effect of DUSP6 on platinum response was also evaluated. When DUSP6 was inhibited with BCI in combination with carboplatin and paclitaxel, it produced a synergistic response over single-agent chemotherapeutic. To assess downstream effects of this inhibition, it was shown that BCI altered genomic levels of the ERK related response genes early growth response protein 1 (EGR1), a strong promoter of apoptosis and proto-oncogene c-Jun [15]. EGR1 was upregulated in cells co-treated with BCI and either paclitaxel or carboplatin, compared to a single-agent treatment, while c-Jun expression was decreased upon co-treatment. This study was able to define a new role for DUSP6 within EOC, indicating that targeting this factor is important both to restore proper tumor immune function and to overcome chemoresistance in EOC cells.

Moreover, as HE4 has the ability to be detected in patient serum, it would be interesting to determine if DUSP6 could also be detected in patient blood. Additional future directions include establishing stable DUSP6 knockdown and overexpressing clones to test cancer related phenotypes. Furthermore, as HE4 overexpressing and stable knockout cell lines have been previously established, global genomic arrays could then be performed to establish similarities and differences between the overexpression and knockout populations of each factor.

203

Finally, the last part of this thesis sought to characterize the novel protein septin-2 in EOC. Septin-2 is a member of the septins protein family, which comprises 13 GTP binding proteins that play important roles in various cellular processes including cytokinesis [16,17]. Septin-2 was identified in a small proteomics study as most enriched with HE4 immunoprecipitation in HE4 overexpressing cells versus null vector cells. For the first time, this study revealed that septin-2 is overexpressed in both serous and clear cell EOC patient tissue. Establishment of stable knockout clones in an ovarian cell lines showed that proliferation was drastically decreased in septin-2 knockout clones. Global proteome analysis was employed to determine the relevant pathways in which septin-2 is involved with in EOC, revealing that down regulation of septin-2 produced differential expression of major metabolic and cellular energy pathways.

As this was a pilot study with the simple goal of defining septin-2 in EOC, more research needs to be completed in order to understand its mechanistic role in ovarian tumorigenesis. Future directions involve an in vivo study to determine if septin-2 knockout lead to a decrease in tumor growth, alike to the reduction of cell proliferation observed in vitro. Furthermore, it will also be important to elucidate the mechanistic relationship between septin-2 and HE4, in addition to determining how septin-2 and HE4 interact with metabolic and cellular energy pathways. This is an especially original finding as both proteins have not been previously found to interact with cellular metabolism and may lead to new novel therapeutic targets for EOC.

As a reputable clinical biomarker, HE4 is valuable in the diagnosis and prognosis of EOC; however, knowledge of its role in treatment of EOC is deficient in comparison.

Overall, this thesis compilation improves the understanding of HE4's diverse biological function in EOC, through highlighting its role in the promotion of tumor immune dysfunction and characterizing novel interacting proteins. As there is a dire need for innovative targeted therapies for EOC patients, this thesis presents new evidence that inhibiting HE4 represents promise not only in downregulating molecular mechanisms that promote tumorigenesis, but also in restoration of normal tumor immune function. Furthermore, global genomic and proteomics analysis of differential HE4 levels revealed its relationship to novel factors that had not previously been characterized in EOC prior to this investigation. Taken as a whole, this dissertation offers original insights that emphasize the importance of HE4's role in the pathogenesis of EOC.

References

1. Long L., Yin, M.,and Min W. 3D Co-culture System of Tumor-associated Macrophages and Ovarian Cancer Cells. Bio Protoc. 2018;8.

2. Wieser, V., Gaugg,I., Fleischer,M.,Shivalingaiah,G.,Wenzel,S.,Sprung,S.,Lax,S.,Zeiment, A., Fiegal, H., and Marth C. BRCA1/2 and TP53 mutation status associates with PD-1 and PD-L1 expression in ovarian cancer. Oncotarget. 2018;9:17501–11.

3. Bose CK. Immune Checkpoint Blockers and Ovarian Cancer. Indian J Med Paediatr Oncol [Internet]. 2017;38:182–9. Available from: http://www.ncbi.nlm.nih.gov/pubmed/28900328%0Ahttp://www.pubmedcentral.nih.gov/articlerender.fcgi?artid=PMC5582557

4. Liao JB, Yip YY, Swisher EM, Agnew K, Hellstrom KE, Hellstrom I. Detection of the HE4 protein in urine as a biomarker for ovarian neoplasms: Clinical correlates. Gynecol Oncol. 2015;137:430–5.

5. Bingle L, Cross SS, High AS, Wallace WA, Rassl D, Yuan G, et al. WFDC2 (HE4): a potential role in the innate immunity of the oral cavity and respiratory tract and the development of adenocarcinomas of the lung. Respir Res [Internet]. 2006;7:61. Available from: http://www.pubmedcentral.nih.gov/articlerender.fcgi?artid=1459147&tool=pmcentrez&rendertype=abstract

6. Renkl AC, Wussler J, Ahrens T, Thoma K, Kon S, Uede T, et al. Osteopontin functionally activates dendritic cells and induces their differentiation toward a Th1-polarizing phenotype. Blood. 2005;106:946–55.

7. Yoo, JK., Cho, JH.,Lee, SW.,and Sung Y. IL-12 Provides Proliferation and Survival Signals to Murine CD4+ T Cells Through Phosphatidylinositol 3-Kinase/Akt Signaling Pathway. J Immunol. 2002;169:3637–43.

8. Bertin S, Lozano-Ruiz B, Bachiller V, García-Martínez I, Herdman S, Zapater P, et al. Dual-specificity phosphatase 6 regulates CD4+ T-cell functions and restrains spontaneous colitis in IL-10-deficient mice. Mucosal Immunol. 2015;8:505–15.

9. Marcus A, Gowen BG, Thompson TW, Iannello A, Ardolino M, Deng W, et al. Recognition of tumors by the innate immune system and natural killer cells. Adv Immunol. 2014;122:91–128.

10. Hagan Vetter, M. and Hays J. Use of Targeted Therapeutics in Epithelial Ovarian Cancer: A Review of Current Literature and Future Directions. Clin Ther. 2018;40:361–71.

11. Wang H, Zhu L, Gao J, Hu Z, Lin B. Promotive role of recombinant HE4 protein in proliferation and carboplatin resistance in ovarian cancer cells. Oncol Rep. 2015;33:403–12.

12. Zhu YF, Gao GL, Tang SB, Zhang ZD, Huang QS. Effect of WFDC 2 silencing on the proliferation, motility and invasion of human serous ovarian cancer cells in vitro. Asian Pac J Trop Med. 2013;6:265–72.

13. Crowell J a, Steele VE, Fay JR. Targeting the AKT protein kinase for cancer chemoprevention. Mol Cancer Ther. 2007;6:2139–48.

14. Ribeiro JR, Schorl C, Yano N, Romano N, Kim KK, Singh RK, et al. HE4 promotes collateral resistance to cisplatin and paclitaxel in ovarian cancer cells. J Ovarian Res [Internet]. 2016;9:28. Available from:

http://www.ncbi.nlm.nih.gov/pubmed/27184254%5Cnhttp://www.pubmedcentral.
nih.gov/articlerender.fcgi?artid=PMC4869286

15. Gregg J, Fraizer G. Transcriptional Regulation of EGR1 by EGF and the ERK
Signaling Pathway in Prostate Cancer Cells. Genes Cancer [Internet]. 2011;2:900–
9. Available from:

http://www.ncbi.nlm.nih.gov/pubmed/22593802%5Cnhttp://www.pubmedcentral.
nih.gov/articlerender.fcgi?artid=PMC3352154

16. Angelis D, Spiliotis ET. Septin Mutations in Human Cancers. Front Cell Dev Biol
[Internet]. 2016;4. Available from:

http://journal.frontiersin.org/article/10.3389/fcell.2016.00122/full

17. Schmidt K, Nichols BJ. Functional interdependence between septin and actin
cytoskeleton. BMC Cell Biol. 2004;5.